Low Frequency Perturbations in Inhomogeneous Plasmas

By

Ali Ahmad

CIIT/FA06-PPH-004/ISB

PhD Thesis

In

Physics

COMSATS Institute of Information Technology
Islamabad-Pakistan
Spring 2013

COMSATS Institute of Information Technology

Low Frequency Perturbations in Inhomogeneous Plasmas

A Thesis Presented to

COMSATS Institute of Information Technology, Islamabad

In partial fulfillment

of the requirement for the degree of

PhD Physics

By

Ali Ahmad

CIIT/FA06-PPH-004/ISB

Spring, 2013

Low Frequency Perturbations in Inhomogeneous Plasmas

A Post Graduate Thesis submitted to the Department of Physics as partial fulfillment of the requirement for the award of Degree of PhD (Physics)

Name	Registration Number
Ali Ahmad	CIIT/FA06-PPH-004/ISB

Supervisor

Dr. Hamid Saleem
Adjunct Professor
Department of Physics
COMSATS Institute of Information Technology, Islamabad
and
Director General
National Centre for Physics, Islamabad

Final Approval

This thesis titled

Low Frequency Perturbations in Inhomogeneous Plasmas

By

Ali Ahmad

CIIT/FA06-PPH-004/ISB

Has been approved

For the COMSATS Institute of Information Technology, Islamabad

External Examiner: _____

Dr. M. Salahuddin
Pakistan Atomic Energy Commission, Islamabad

External Examiner: _____

Dr. Riaz Khan
National Tokamak Fusion Program
Pakistan Atomic Energy Commission, Islamabad

Supervisor: _____

Dr. Hamid Saleem
Adjunct Professor, Department of Physics
COMSATS Institute of Information Technology, Islamabad

HoD: _____

Prof. Dr. Arshad Saleem Bhatti
Head of Department of Physics
COMSATS Institute of Information Technology, Islamabad

Chairman: _____

Prof. Dr. Sajid Qamar
Chairman, Department of Physics
COMSATS Institute of Information Technology, Islamabad

Dean, Faculty of Sciences: _____

Prof. Dr. Arshad Saleem Bhatti
Dean, Faculty of Sciences
COMSATS Institute of Information Technology, Islamabad

Declaration

I **Ali Ahmad**, registration number **CIIT/FA06-PPH-004/ISB**, hereby declare that I have produced the work presented in this thesis, during the scheduled period of study. I also declare that I have not taken any material from any source except referred to wherever due that amount of plagiarism is within acceptable range. If a violation of HEC rules on research has occurred in this thesis, I shall be liable to punishable action under the plagiarism rules of the HEC.

Date: _____

Signature of the student:

_____

Ali Ahmad

CIIT/FA06-PPH-004/ISB

Certificate

It is certified that **Mr. Ali Ahmad**, registration number **CIIT/FA06-PPH-004/ISB**, has carried out all the work related to this thesis under my supervision at the Department of Physics, COMSATS Institute of Information Technology (CIIT), Islamabad and the work fulfills the requirement for award of PhD degree.

Date: _____

Supervisor:

_____

Dr. Hamid Saleem

Adjunct Professor
Department of Physics
COMSATS Institute of Information Technology, Islamabad

Head of Department:

_____

Prof. Dr. Arshad Saleem Bhatti

Head of Department of Physics,
COMSATS Institute of Information Technology, Islamabad

Dedicated

To

My mother, father,

brother and sisters

ACKNOWLEDGEMENTS

All Praises to Almighty Allah, the most benevolent and merciful, who enabled me to complete this research work successfully

First and foremost I would like to express my sincere gratitude to my supervisor Dr. Hamid Saleem for his invaluable guidance and supervision during the completion of this thesis. His passion and support for research was always motivational for me even during tough times in my Ph.D. pursuit. Without his encouragement, patience, and instructions, this thesis would not have been completed.

I am deeply grateful to Prof. Dr. Arshad Saleem Bhatti, Dean, Faculty of Sciences and Head of Physics Department and Prof. Dr. Sajid Qamar, Chairman of Physics Department at CIIT for their cooperation and support in all respects regarding my Ph.D. studies at the Physics Department. Special appreciation goes to Prof. (s) Dr. (s) Kamaluddin Ahmad (CIIT), Arshad Majeed Mirza (QAU), Mahnaz Haseeb (CIIT) and Dr. Farida (CIIT) for useful discussions. I am also grateful to PINSTECH and NCP authorities who allowed me to do Ph.D. research work.

My heartiest thanks to all my friends and colleagues at Theoretical Plasma Physics Division PINSTECH, for their cooperation. Special thanks go to Dr. Qamar-ul-Haque for useful discussions on vortices. I am also thankful to Dr. (s) Waqas, Mohsan, Shahzad and Shahid for discussions on various aspects of plasma physics. My thanks also due to Dr. Muhammad Sajid for his help in mathematica programming. I am also grateful to Dr. Shabbir who helped me in thesis format. My cordial thanks to my friends, Shaukat, Moosa, Asad, Faisal, Hafeez, Nasim and Kaleem for their cooperation and good company.

Finally, I would like to thank my parents and other family members, who love me so much and always pray for my success. I am thankful to my caring wife and loving children for their patience and encouragement during my research. I am also grateful to my elder brother Mian Muhammad Ahmad for his kind support and encouragement during my academic carrier.

Ali Ahmad

CIIT/FA06-PPH-004/ISB

ABSTRACT

Low Frequency Perturbations in Inhomogeneous Plasmas

The waves and instabilities produced by inhomogeneous currents $\mathbf{J}_{0z}(x)$ in plasmas along the initially constant magnetic field $\mathbf{B}_{0z}\hat{\mathbf{z}}$ are investigated. The total zero-order magnetic field is twisted and becomes space dependent $\mathbf{B}_0 = \mathbf{B}_{0z}\hat{\mathbf{z}} + \mathrm{B}_{0y}(x)\hat{\mathbf{y}}$. In heavier ion (like barium) plasmas the ion dynamics can be ignored in the presence of sheared flow of electrons. Electrostatic current-driven wave with the frequency near $\omega_r \simeq (\kappa_B/k_\perp)\omega_{ce}$ (where $\kappa_B = |d \ln B_0/dx|$, $\omega_{ce} = eB_0/m_e c$ and $k_\perp$ is the perpendicular wavenumber) can exist in such plasmas and it becomes unstable under certain conditions. The nonlinear equations for this mode have been derived and stationary solutions in the form of vortices and solitons have been obtained.

Due to sheared flow of electrons and ions in the presence of stationary dust, a low frequency electrostatic current-driven drift like wave with real frequency $\omega_r \simeq (cT_e/eB_0)\kappa_B k_\perp$ has also been proposed to exist in dusty plasmas. The nonlinear equations for this wave including the effects of density gradient have been derived. The effects of kappa distribution of electrons have also been investigated. D'Angelo's mode is modified in the presence of superthermal electrons. In the nonlinear regime the wave can give rise to dipolar vortex structures if the shear in flow is weaker and tripolar vortices if the flow has steeper gradient. The results have been applied to Saturn's magnetosphere corresponding to negatively charged dust grains.

The very low frequency wave at dust time scale can also be produced by the sheared currents if dust is assumed to be dynamic. These very low frequency waves and instabilities with small growth rates can be important in the planetary and cometary magnetospheres due to the interaction of solar wind. In the nonlinear regime these waves give rise to electrostatic structures such as vortices and solitons. A comparison of these very low frequency current-driven dust waves with the current-driven ion waves is also presented to point out analogous physical pictures with different temporal and spatial scales. The theoretical model is a general one and here it is applied to Saturn's magnetosphere for illustration.

The global drift mode is also studied in a plasma bounded in a cylinder having Gaussian density profile. The effect of magnetic shear on the wave propagation along density gradient is studied in a Cartesian geometry assuming absorbing boundary. It is found that the wave amplitude is reduced when two-ion species are present (with the same concentration) compared to pure electron-ion plasma.

Contents

List of Figures

List of Abbreviations

AGN	Active Galactic Nuclei
K	Kelvin
D	Deuterium
T	Tritium
^{235}U	Uranium 235
LH	Lower Hybrid
k	wavenumber
MHD	Magneto hydrodynamic
HM	Hasegawa-Mima
KdV	Korteweg-de Vries
ei	electron-ion

List of Publications in International Journals

[1]. **Ali Ahmad** and H. Saleem, “Current-driven electron drift solitons”, Phys. Lett. A **377**, 3128 (2013).

[2]. **Ali Ahmad** and H. Saleem, “Short scale electrostatic vortices driven by electrons sheared flow parallel to external magnetic field in heavier ion plasmas”, Phys. Plasmas **19**, 042107 (2012).

[3]. **Ali Ahmad**, S. Ali Shan, Q. Haque, and H. Saleem, “Linear and nonlinear dynamics of current-driven waves in dusty plasmas”, Phys. Plasmas **19**, 092115 (2012).

[4]. W. Masood and **Ali Ahmad**, “Coupled dispersive drift acoustic modes in inhomogeneous dusty plasmas with different nonthermal distributions for electrons and ions”, Astrophys. Space Sci. **340**, 367 (2012).

[5]. S. A. Khan, M. K. Ayub, and **Ali Ahmad**, “Low frequency electromagnetic oscillations in dense degenerate electron-positron pair plasma, with and without ions”, Phys. Plasmas **19**, 102104 (2012).

[6]. Q. Haque, S. Yamin, and **Ali Ahmad**, “Drift-Alfven Eigenmodes in inhomogeneous electron-positron-ion plasmas”, Phys. Scr. **83**, 035501 (2011).

[7]. **Ali Ahmad,** M. Sajid, and H. Saleem, “Drift mode in a bounded plasma having two ion species”, Phys. Plasmas **15**, 012105 (2008).

[8]. H. Saleem, **Ali Ahmad,** and S. A. Khan, “Low frequency electrostatic and electromagnetic modes of ultracold magnetized nonuniform dense plasmas”, Phys. Plasmas **15**, 094501 (2008).

[9]. H. Saleem, **Ali Ahmad,** and S. A. Khan, “Low frequency electrostatic and electromagnetic modes in nonuniform cold quantum plasmas”, Phys. Plasmas **15**, 014503 (2008).

[10]. **Ali Ahmad**, H. Saleem, J. Vranjes, and S. Poedts, “Stabilizing effects of positron dynamics on the local and global drift modes”, Phys. Lett. A **366**, 466 (2007).

The thesis based on the following publications

- **Ali Ahmad** and H. Saleem, “Current-driven electron drift solitons”, Phys. Lett. A **377**, 3128 (2013).
- **Ali Ahmad** and H. Saleem, “Short scale electrostatic vortices driven by electrons sheared flow parallel to external magnetic field in heavier ion plasmas”, Phys. Plasmas **19**, 042107 (2012).
- **Ali Ahmad**, S. Ali Shan, Q. Haque, and H. Saleem, “Linear and nonlinear dynamics of current-driven waves in dusty plasmas”, Phys. Plasmas **19**, 092115 (2012).
- **Ali Ahmad,** M. Sajid, and H. Saleem, “Drift mode in a bounded plasma having two ion species”, Phys. Plasmas **15**, 012105 (2008).
- **Ali Ahmad** and H. Saleem, “Solar wind-driven dust waves and instabilities in planetary magnetospheres”, to be submitted (2014).

Chapter 1

Introduction

The aim of this thesis is to investigate the linear and nonlinear waves and instabilities in flowing plasmas relevant to laboratory and space environments using multi-fluid model. In this chapter, first we provide the motivation for such investigations, followed by an introduction to waves and instabilities and then nonlinear structures in plasmas. Finally the chapter ends with the layout of the thesis.

Plasma physics is the well developed research area with major applications to fusion, space and astrophysics. The plasma state of matter can be defined as a statistical ensemble of interacting charged particles. The rigorous definition and criteria for an ionized gas to be called a plasma is well described in plasma physics books [1, 2]. A peculiar characteristic of plasmas is its collective response to external perturbations. Some examples of plasmas are:

- The sun, stars and interstellar medium
- Solar wind and interplanetary medium
- Magnetospheres of the planets, like that of Jupiter, Saturn and Earth
- Ionosphere of Earth, radiation belts and aurora
- Solar corona and sunspots
- Pulsars, quasars and active galactic nuclei (AGN)

Following from the Aston's experiment that a helium atom is less massive than four hydrogen atoms, and using Einstein's mass-energy relation, $E = mc^2$, Sir Arthur

Eddington in 1920 suggested fusion of light elements as the source of energy in the Sun and stars.

With the passage of time the use of energy resources has increased enormously, resultantly reserves of the fossil fuels are rapidly diminishing with the additional problems of pollution and earth warming. The world energy consumption is rapidly increasing during the past years. However, the reserves of the fossil fuels are estimated to be depleted within a century.

A major success to overcome the energy crisis is achieved through the nuclear fission [3]:

$$^{235}_{92}\mathrm{U} + ^{1}_{0}\mathrm{n} \longrightarrow ^{144}_{56}\mathrm{Ba} + ^{90}_{36}\mathrm{Kr} + 2\ ^{1}_{0}\mathrm{n} + 200\ \mathrm{MeV}$$

But it has its own drawbacks, such as limited supply of ^{235}U fuel, and radioactive waste handling. However, controlled nuclear fusion is believed to provide an alternative energy source that is relatively clean and safe. Most importantly, it will provide an unlimited supply of energy to overcome the growing demand of the worlds energy. The mission is to reproduce the nuclear reactions in reactors taking place on the sun and other stars to generate energy. For hydrogen isotopes, the suitable fusion reactions along with energies are given as follows [4],

$$^{2}_{1}\mathrm{D} + ^{3}_{1}\mathrm{T} \longrightarrow ^{1}_{0}\mathrm{n} + ^{4}_{2}\mathrm{He} + 17.6\ \mathrm{MeV}$$
$$^{2}_{1}\mathrm{D} + ^{2}_{1}\mathrm{D} \longrightarrow ^{1}_{0}\mathrm{n} + ^{3}_{2}\mathrm{He} + 3.27\ \mathrm{MeV}$$
$$^{2}_{1}\mathrm{D} + ^{2}_{1}\mathrm{D} \longrightarrow ^{1}_{1}\mathrm{H} + ^{3}_{1}\mathrm{T} + 4.03\ \mathrm{MeV}$$

The energy from these fusion reactions can be achieved only if plasma system is heated to high temperatures (up to 10^8 K) to overcome the Coulomb repulsive force between the charged nuclei. Since the cross-section for deuterium (D) and tritium (T) reaction is greater than other reacting nuclei at the same temperature, that is why the present experiments use D-T fuel for nuclear fusion. However, at such high temperatures confining the high density plasma for sufficient time for significant yield of energy to occur is a major problem. The modern devices, like tokamak, use strong magnetic fields for the confinement of hot plasmas. The geometric configuration of these devices has intrinsic problems of plasma confinement due to inhomogeneities. The waves and instabilities of various kinds play a crucial role in these devices, because

they may lead to particle and energy losses, thus disrupting the confinement of the plasma.

The basic dynamics of such a complex statistical system depends on the plasma species under consideration and can be studied by various models, depending upon the phenomenon of interest. On the macroscopic scale, it is characterized by density, magnetic field, and temperature, and the perturbations are calculated by using the conservation equations such as momentum, continuity and Poisson's equations along with Maxwell's equations. On the other hand treating a microscopic phenomena, requires the kinetic approach to calculate the positions and velocities of the plasma particles.

1.1 Waves and Instabilities in Plasmas

Plasmas support a wide variety of waves depending upon the complexity of the plasma itself. For example, the most simple is an unmagnetized uniform ideal plasma, that supports the electrostatic high frequency Langmuir waves and the low frequency ion acoustic waves. With the addition of magnetic field, the plasma becomes anisotropic, supporting new modes, such as the Alfven waves, upper hybrid, lower hybrid, ion cyclotron, etc., which can exist only in a magnetized plasma. The number of waves further rises by considering additional complexities, such as density, temperature or magnetic field inhomogeneities, which are essential in fusion devices as well as in space plasmas. For example, low frequency drift waves can exist in a magnetized inhomogeneous plasma.

A large number of waves exist in plasma at different temporal and spatial scales. Since electrons are much lighter than ions, therefore there are waves at electron time scales such as upper hybrid wave, plasma wave and there are waves at ion time scales like ion cyclotron wave, ion acoustic wave and drift wave. In addition to these time scales, there are hybrid time scales in between electron and ion time scales. It is well-known that the electrostatic lower hybrid (LH) waves propagate in magnetized plasmas with frequency ω such that $\omega_{ci} \ll \omega \ll \omega_{ce}$ where $\omega_{ci} = eB_0/m_i c$ and $\omega_{ce} = eB_0/m_e c$ are ion and electron gyrofrequencies, respectively. The LH waves propagate obliquely making a small angle with the external constant magnetic field and these have been

studied extensively [5–7] and references therein.

In addition to electrons and ions, a plasma may contain massive charged particles of nanometer to micrometer size. These massive particles (solid or liquid) are referred to as dust and a plasma containing such particles is called a dusty plasma [8, 9]. The charges can be negative or positive, depending on the ambient plasma environments. Dusty plasmas are ubiquitous in space, such as, in planetary rings, in cometary tails, and in interplanetary and interstellar clouds [10–12].

The presence of dust particles, not only modifies the properties of waves when considered stationary, but can also lead to the appearance of new very low frequency waves. Here, the dynamics of dust particles introduces new temporal and spatial scales. The examples of such very low frequency waves are the dust acoustic and dust drift waves.

Plasmas also exhibit various kinds of instabilities. In the presence of a source of free energy, the forces may not restore the disturbance back to equilibrium but instead helps the perturbations to grow exponentially. The plasma dynamics is then characterized with frequencies $\omega = \omega_r + i\gamma$ where ω_r and γ are real numbers in units of frequency. The wave growth or damping depends upon the sign of the imaginary part of the frequency. For some real wavenumber, k, solutions with $\gamma > 0$ are referred to as instabilities. Wave growth or damping can be interpreted as exchange of energy between the plasma and fluctuations.

Mostly the space and laboratory plasmas are not in thermodynamic equilibrium. This deviation from thermodynamic equilibrium may be interpreted as free energy stored in the plasma, leading to plasma instabilities. Two types of instabilities (macroscopic and microscopic) may arise depending upon the way a system deviates from thermodynamic equilibrium. Macroscopic instability originates due to gradients or inhomogeneity of plasma species in the coordinate space, whereas the microscopic instability originates due to anisotropy in the velocity space or due to velocity distribution shape other than the Maxwellian distribution. Examples of macroscopic instability are the Kelvin Helmholtz instability due to shear flow and drift instability due to density gradient, whereas examples of microscopic instability are two stream instability and loss cone instability.

1.2 Plasma Flows and Instabilities

A wide variety of plasma systems is characterized by spatial inhomogeneities and flows. Sheared plasma flows parallel and perpendicular to the equilibrium magnetic field direction are ubiquitous in space and laboratory [13–18], and are considered to play an important role in the generation of plasma instabilities and turbulence. Long ago [19], it was proposed that the sheared plasma flow parallel to the external magnetic field can give rise to a purely growing electrostatic instability. A year later, the experiments were performed in a Q-machine plasma, which confirmed the proposed theory of the excitation of instability due to shear flow [20]. Recently [21–23], it has been investigated that such field aligned flows cause ion acoustic and ion cyclotron instabilities in addition to the D'Angelo mode [19]. If electrons and ions have the same sheared velocity parallel to the constant external magnetic field then the zero-order current does not appear and in this case the external magnetic field remains unaffected by the plasma flow.

The two-stream instability driven by parallel electrons sheared flow in a magnetized plasma has also been studied both theoretically and by means of two-dimensional Vlasov simulations [24]. It has been shown in this work that the electrostatic waves have growing eigenfunctions in the linear case, while the localized coherent structures are formed in the nonlinear regime as seen through simulations. The electrostatic two-stream instabilities in interstellar medium have also been discussed in the presence of two types of dust particles [25].

The zero-order current can also be produced in dusty plasmas if the electrons and ions have sheared flow relative to dust particles. In this case the electron-ion flow can produce a zero-order current causing twist in the initial external magnetic field. Considering a local situation with the same electron-ion flow velocity and stationary dust, it has been shown that a low frequency drift-type wave becomes a normal mode of such plasmas even if the density is uniform [26–28].

It has been shown that the low frequency electrostatic drift waves can become unstable in the presence of sheared flows [29]. The drift waves are very important in plasmas due to their role in particle and energy transport [30]. These low frequency waves appear in the presence of density inhomogeneity and they give rise to solitary

structures in plasmas; vortices [26], solitons [31] and shocks [32].

Drift waves are low frequency (in comparison with the ion gyrofrequency) electrostatic waves in a nonuniform magnetized collisionless electron ion plasma [33]. They have importance due to their significant role in transport phenomena in magnetically confined plasmas such as tokamaks.

In the presence of collisions, the drift waves are excited due to the combined effect of the density inhomogeneity and collisions between electrons and ions. Due to collisions a phase lag is produced between the electron density perturbation and wave potential i.e., the electron response is nonadiabatic, resulting in drift wave instability taking energy from equilibrium density gradient. As a result drift dissipative instability appears in plasmas [31, 34]. Another mode between the MHD modes and drift waves is the reactive drift mode. It is considered a candidate among the most dangerous class of modes for explaining the observed transport in tokamaks [31]. This mode was first derived by Rudakov and Sagdeev during the discovery of the ion temperature gradient driven mode.

Recently [35], a theoretical model has been presented to study the excitation of low frequency electrostatic waves in a magnetized heavy ion plasma by a parallel electron velocity shear instability. The coupling of electron velocity shear instability with ion cyclotron waves has also been studied. The growth rates for a few set of parameters relevant to laboratory experiments have been examined. However, the gradient in magnetic field introduced by the current is ignored in this study. The electrostatic parallel electron velocity shear instability has also been investigated in heavier ion (like the barium plasma) including the effects of sheared magnetic field caused by the inhomogeneous background current [36]. The excitation of low-frequency electromagnetic waves by electron parallel flow has also been investigated in a collisionless magnetoplasma [37]. The interest in this area has been invoked after knowing about the potential experiments with barium plasmas in Q-machine with electrons sheared flow parallel to the external magnetic field [38]. On the other hand, if the lighter electron fluid is given a sheared flow parallel to the initially constant magnetic field in the plasma, then zero-order current will modify the field topology.

1.3 Nonlinear Structures

Equations used to describe the evolution of plasma systems are in principle nonlinear partial differential equations. The first step to study such a complex system is to linearize these equations by keeping only first order terms. Then the linear differential equations are solved by using Fourier and Laplace transforms. As a result, the set of differential equations is converted to a set of algebraic equations, giving rise to the linear dispersion relation.

However the linear theory is valid only for sufficiently small amplitude perturbations. In the presence of a source of free energy, the perturbations can become unstable. As a result, the wave amplitude becomes large and the nonlinear terms can no longer be ignored. However the plane wave solutions are only possible for linear wave equations. For nonlinear problems, the travelling wave solutions are in general very limited. Usually only particular profiles in the form of travelling wave solutions are guaranteed for some special equations.

During the last four decades, growing attention has been given to nonlinear i.e., large amplitude wave dynamics [31, 39–41] and references therein. This is due to the fact that the nonlinearities may contribute to the localization of waves resulting in various nonlinear coherent structures such as vortices, solitons, shocks etc. The shock waves arise in a nonlinear dissipative medium as a result of the balance between wave steepening and dissipation, whereas soliton formation requires a balance between wave steepening and dispersion in a nondissipative medium. The formation of different structures depends upon the type of nonlinearity. The vector nonlinearity arises through the convective part of the polarization drift and gives rise to vortices. The scalar nonlinearity gives rise to shocks and solitons. The study of nonlinear wave phenomena have received a great deal of attention to understand the basic properties of localized electrostatic perturbations in laboratory and space plasmas. We briefly describe the vortices and solitons here which will be investigated in plasmas with sheared flows and inhomogeneous currents in subsequent chapters.

1.3.1 Vortices

In recent years, there has been a tremendous interest in investigating vortex structures in plasmas and planetary atmospheres. Vortex dynamics is typically governed by nonlinear equations. Hasegawa and Mima derived a nonlinear equation for drift waves which explains the production of strong turbulence in inhomogeneous magnetized plasmas [40]. Whereas, Charney derived a nonlinear equation governing the evolution of Rossby waves for neutral fluids in planetary atmospheres [42]. Subsequently, it was shown that the Hasegawa-Mima (HM) equation has a structure identical to nonlinear Rossby wave in the inviscid limit [43]. In the linear limit, the HM and Charney equations give rise to drift waves in inhomogeneous plasmas and Rossby waves in planetary atmospheres respectively, while in the nonlinear regime both equations contain a nonlinearity in the form of two dimensional vector product or Poisson bracket. This nonlinearity is essential for the formation of dipole vortices [44]. A short introduction to vortices is given below. The HM equation is derived and is compared with Charney equation.

A vortex describes the distinct flow phenomenon in terms of vorticity, i.e., a local structure characterized by concentration of vorticity. Vorticity is a measure of the rotation or spin of the fluid. Mathematically, vorticity, $\mathbf{\Omega}$, is equal to the curl of the flow velocity $\mathbf{v}$, of a fluid, defined as,

$$\mathbf{\Omega} = \boldsymbol{\nabla} \times \mathbf{v}$$

For two-dimensional flows, vorticity is a vector in the direction perpendicular to the plane of flow.

To derive the HM equation, first we consider the electron response. For low frequency (in comparison with ion gyrofrequency) electrostatic waves in inhomogeneous plasmas, the inertialess electrons are assumed to follow the Boltzmann distribution, given as,

$$n_e = n_0 \exp\left(\frac{e\phi}{T_e}\right) \tag{1.1}$$

where ϕ is the perturbed electrostatic potential, n_0 is the equilibrium number density, T_e is the electron temperature and e is the magnitude of the electron charge. The ion

dynamics is governed by the continuity equation,

$$\frac{\partial n_i}{\partial t} + \boldsymbol{\nabla} \cdot (n_i \mathbf{v}_i) = 0 \tag{1.2}$$

and the equation of motion,

$$\frac{\partial \mathbf{v}_i}{\partial t} + (\mathbf{v}_i \cdot \boldsymbol{\nabla})\, \mathbf{v}_i = \frac{e}{m_i} \left(\mathbf{E} + \frac{\mathbf{v}_i}{c} \times \mathbf{B}_0 \right) \tag{1.3}$$

where $\mathbf{B}_0 = B_0 \hat{\mathbf{z}}$ is constant. Using the drift approximation, the ion velocity perpendicular to the ambient magnetic field becomes,

$$\mathbf{v}_{i\perp} = \frac{c}{B_0} z \times \boldsymbol{\nabla}\phi - \frac{c}{B_0 \omega_{ci}} \left(\frac{\partial}{\partial t} + \mathbf{v}_E \cdot \boldsymbol{\nabla} \right) \boldsymbol{\nabla}_\perp \phi = \mathbf{v}_E + \mathbf{v}_p \tag{1.4}$$

where the first term represents the $\mathbf{E} \times \mathbf{B}_0$ drift velocity, while the second term represents the polarization drift velocity, $\mathbf{E} = -\boldsymbol{\nabla}\phi$ and $\omega_{ci} = eB_0/m_i c$ is the ion gyrofrequency. Combining equations (1.1), (1.2) and (1.3) and ignoring nonlinear terms, we obtain a linear dispersion relation,

$$\omega = \frac{\omega_{*e}}{\left(1 + \rho_s^2 k_y^2\right)} \tag{1.5}$$

where $\omega_{*e} = v_d k_y$ is the drift wave frequency and

$$v_d = -\frac{cT_e}{eB_0} \frac{d \ln n_{io}}{dx} = \frac{\rho_s}{L_n} c_s \tag{1.6}$$

is the diamagnetic drift velocity, $L_n^{-1} = |d \ln n_{io}/dx|$ is the inverse density gradient length, $\rho_s = c_s/\omega_{ci}$ is the ion Larmor radius evaluated at the ion acoustic velocity and c_s is the ion acoustic speed. Equation (1.5), is the dispersion relation for drift waves. The term $\rho_s^2 k_y^2$ in relation (1.5) is due to the ion polarization drift and it gives rise to dispersion. The drift wave propagates with diamagnetic drift velocity v_d perpendicular to both the density gradient and ambient magnetic field. For long wavelengths the dispersion relation becomes $\omega = v_d k_y$. It represents a stable mode, called the drift mode, just a propagating plasma oscillation, where the electron density response is assumed adiabatic. Sometimes it is also called a universal mode because

of of its crucial role in magnetic confinement geometries. It is important to mention here that in a uniform plasma $v_d = 0$, hence the drift mode disappear. If the parallel ion dynamics is also considered, which was ignored while deriving HM equation under the assumption $c_s k_z \ll v_d k_y$, then the relation (1.5) gets modified, given as,

$$\omega^2 \left(1 + \rho_s^2 k_y^2\right) - \omega\omega_{*e} - c_s^2 k_z^2 = 0 \tag{1.7}$$

which is the dispersion relation for drift waves coupled with the ion acoustic waves.

The vorticity is associated with the electric field drift defined by $\Omega = \boldsymbol{\nabla} \times \mathbf{v}_E$ and is directed along z-axis. Using Eqs. (1.4) and (1.1) along with quasineutrality condition ($n_i \simeq n_e$), the ion continuity equation gives,

$$\left(1 - \rho_s^2 \nabla_\perp^2\right) \frac{\partial \phi}{\partial t} + v_d \frac{\partial \phi}{\partial y} + \mathbf{v}_E \cdot \boldsymbol{\nabla} \left(1 - \rho_s^2 \nabla_\perp^2\right) \phi = 0 \tag{1.8}$$

which can also be written as,

$$\left(1 - \rho_s^2 \nabla_\perp^2\right) \frac{\partial \phi}{\partial t} + v_d \frac{\partial \phi}{\partial y} - \frac{c}{B_0} \left\{\phi, \rho_s^2 \nabla_\perp^2 \phi\right\} = 0 \tag{1.9}$$

where,

$$\left\{\phi, \nabla_\perp^2 \phi\right\} = \left(\frac{\partial \phi}{\partial x} \frac{\partial \nabla_\perp^2 \phi}{\partial y} - \frac{\partial \phi}{\partial y} \frac{\partial \nabla_\perp^2 \phi}{\partial x}\right)$$

is the Poisson bracket. For neutral fluids, assuming $\left|\rho_s^2 \nabla_\perp^2\right| \gg 1$ and dropping the second term (containing v_d), Eq. (1.8) becomes,

$$\frac{\partial \nabla_\perp^2 \phi}{\partial t} + \left(\mathbf{v}_E \cdot \boldsymbol{\nabla}\right) \nabla_\perp^2 \phi = 0 \tag{1.10}$$

which is the two-dimensional Navier Stokes equation for the vortex flow where $\Omega = \nabla_\perp^2 \phi$ is the vorticity. For the sake of comparison, Charney equation for rotating fluids can be written as [42],

$$\left(1 - \rho_R^2 \nabla^2\right) \frac{\partial \phi}{\partial t} + v_R \frac{\partial \phi}{\partial y} - \left\{\phi, \rho_R^2 \nabla^2 \phi\right\} = 0 \tag{1.11}$$

where v_R is the Rossby velocity analogous to drift velocity v_d, ρ_R is the Rossby radius analogous to ρ_s. In neutral fluids the vorticity arises due to the geostrophic flow which

is the analog of the electric field drift.

Figure 1-1: The great red spot in the atmosphere of the Jupiter with largest vortex structure in the solar system (taken from NASA web site nssdc.gsfc.nasa.gov).

The Poisson bracket also known as vector nonlinearity helps the formation of dipole vortices as solutions of the HM and Charney equation. The stationary solution of (1.9) is obtained by transforming it to a frame $\xi = y - ut$, where u is the speed of the frame (i.e. the nonlinear structure). It can be shown that the resulting equation is satisfied by,

$$\nabla_{\perp}^{2}\phi = C_1\phi + C_2 x \tag{1.12}$$

where $\nabla_{\perp}^{2}\phi = (\partial^2\phi/\partial x^2) + \left(\partial^2\phi/\partial\xi^2\right)$ and the constants C_1 and C_2 are related by,

$$C_1 = \frac{1}{\rho_s^2}\left(1 - \frac{v_d}{u}\right) - \frac{c}{uB_0}C_2 \tag{1.13}$$

The dipolar vortex solution of (1.12) can be constructed in terms of Bessel functions by following the standard procedure [44] as is given by,

$$\begin{aligned} \phi &= \alpha^o K_1(\lambda_1 r)\cos\theta & r > r_0 \\ \phi &= \left[\alpha^i J_1(\lambda_2 r) + \frac{uB_0\left(\lambda_1^2 + \lambda_2^2\right)}{c}\right]\cos\theta & r < r_0 \end{aligned} \tag{1.14}$$

where r_0 is the radius of the vortex, α^o, α^i, λ_1, λ_2 are constants, and functions J and K are Bessel function and modified Bessel function, respectively. The solutions of the nonlinear equations in terms of vortices are discussed in detail in the subsequent chapters. The constants can be evaluated by using the continuity of ϕ, $\nabla\phi$, and $\nabla^2\phi$ at $r = r_0$.

1.3.2 Solitons

A brief description of solitons as solutions of the integrable nonlinear partial differential equations is presented here. A soliton is a special type of solitary wave. A soliton propagates over long distances at a constant speed without losing its shape. It exists due to a balance between dispersion and nonlinearity. The term soliton was used for the first time by Zabusky and Kruskal to describe particle like behavior of the localized solutions of the nonlinear equations. The story of observations of the solitary waves by John Scott Russell in 1834 is very famous and can be found in texts [45, 46]. Soliton research is also carried out in many other branches of physics including solid state physics, high energy physics and optical communications among others.

The propagation of weakly nonlinear and weakly dispersive waves can be described by the Korteweg-de Vries (KdV) equation, given as [47],

$$\frac{\partial u}{\partial t} + Au\frac{\partial u}{\partial x} + B\frac{\partial^3 u}{\partial x^3} = 0 \tag{1.15}$$

where A and B are the coefficients of the nonlinear and dispersion terms, respectively. In the absence of the dispersion term, the shape of the pulse shows that large amplitude part has large velocity and small amplitude part has small velocity resulting in wave breaking. The phenomena of wave breaking in a nondissipative and nondispersive medium is illustrated in Fig. (1-2).

The dispersion cause a spread in the group of waves. Thus a balance between nonlinearity and dispersion can form a stable pulse, the soliton. KdV equation is used in modeling of one-dimensional physical systems for the evolution of nonlinear waves. It was first derived by Korteweg and de Vries to model the long waves in shallow water [47]. Subsequently, Gardner and Morikawa derived it for waves propagating perpendicular to a magnetic field in cold plasmas [48]. Later, it was derived by Kruskal

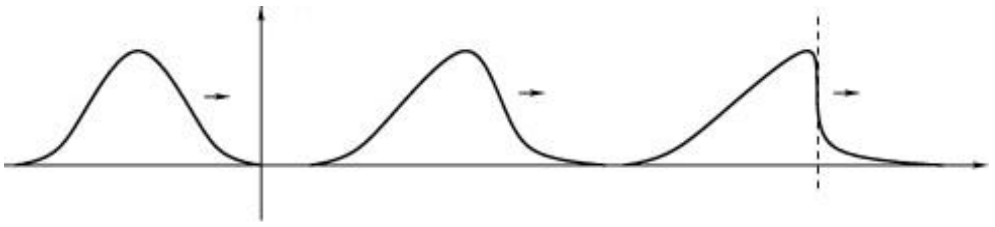

Figure 1-2: Wave steepening and breaking in a nondispersive medium.

and Zabusky for acoustic waves in anharmonic crystals [49]. Furthermore, Washimi and Taniuti used it to describe electrostatic ion acoustic waves in plasmas [50]. It is well-known that KdV equation posses a stationary solitary wave solution. The solution of Eq. (1.15) is obtained by substituting $u(\xi) = u(x - \beta t)$, such that $u \to 0$, $\frac{\partial u}{\partial \xi} \to 0$, $\frac{\partial^2 u}{\partial \xi^2} \to 0$ as $\xi \to \pm\infty$ (for localized waves) and is given by [51],

$$u(\xi) = \frac{3\beta}{A} \operatorname{sech}^2 \left[\frac{\xi}{2} \sqrt{\frac{\beta}{B}} \right] \tag{1.16}$$

This travelling wave solution is usually referred as the single-soliton solution because of some peculiar properties. The solitary structure propagates with speed β without changing its shape in contrast to dispersive wave packets. Here $3\beta/A$ is the amplitude and $2\sqrt{B/\beta}$ is the width of the soliton. For constant values of A and B, by increasing the velocity of soliton its amplitude increases whereas its width decreases. Two kinds of structures are possible depending upon the sign of the coefficient of the nonlinear term in Eq. (1.15), $0 < A$ gives compressive type soliton while for $A < 0$, one obtains refractive soliton.

1.4 Kappa Distribution Function

The observations of space plasmas have indicated the ubiquitous presence of electron and ion populations which are far away from their respective thermodynamic equilibria [52–55]. Therefore, such systems can not be characterized by the Maxwellian velocity distributions, because of high energy tails [56]. Such superthermal populations may be well described by the more general kappa (or generalized Lorentzian) distribution

function, which involve the Maxwellian core and a high-energy tail component of the power-law form. The use of the kappa-distribution function was first introduced by Vasyliunas [56] to fit OGO 1 and OGO 2 solar wind data. This is an empirical fit to the observed particle distributions. The three-dimensional isotropic kappa distribution is expressed as,

$$f_\kappa(v_j) = \frac{n_{j0}}{(\pi\kappa_j\theta_j^2)^{\frac{3}{2}}}\frac{\Gamma(\kappa_j+1)}{\Gamma(\kappa_j-1/2)}\left(1+\frac{v_j^2+2q_j\phi/m_j}{\kappa_j\theta_j^2}\right)^{-(\kappa_j+1)} \tag{1.17}$$

where j is the species, electrons ($j=e$) or ions ($j=i$), q_j is their charge, $-e$ for electrons and $+e$ for singly ionized ions, v_j and n_{j0} the electron (ion) species velocity and equilibrium number density, ϕ is the local electrostatic potential, κ is the kappa distribution power law spectral index, m_j is the particle mass and Γ is the Gamma function. Here $v^2 = v_x^2 + v_y^2 + v_z^2$ denotes the square norm of the velocity $\mathbf{v}$. The generalized thermal speed θ_j related to the true thermal speed $v_{th,j} = (2T_j/m_j)^{1/2}$ is given as,

$$\theta_j = \sqrt{\frac{2T_j}{m_j}\frac{\kappa_j-3/2}{\kappa_j}} \tag{1.18}$$

where T_j is the kinetic temperature. For large values of the spectral index, the kappa distribution approaches the Maxwellian one. Thus kappa distribution may be signified as a generalization of the Maxwellian distribution. Clearly, for a physically realistic thermal speed, one requires $\kappa > 3/2$. The kappa distribution function for various values of κ is illustrated in Fig. (1-3) [57]. In the limit $\kappa \to \infty$, kappa distribution reduces to Maxwellian distribution. Thus from (1.17) we obtain,

$$\lim_{\kappa\to\infty} f_\kappa(v) = n_0\left(\frac{m}{2\pi T}\right)^{3/2}\exp\left(-\frac{mv^2}{2T}\right) \tag{1.19}$$

The existence of such non-Maxwellian distribution functions in plasmas can significantly effect the wave propagation and transport processes. The effect of superthermal distributions on linear and nonlinear structures in plasmas has been investigated by various researchers [58–60]. Kappa distribution has also been used to study the effect of Landau damping on various plasma modes [61, 62]. Recently, the nonlinear ion acoustic solitary structures with kappa distributed electrons have also been stud-

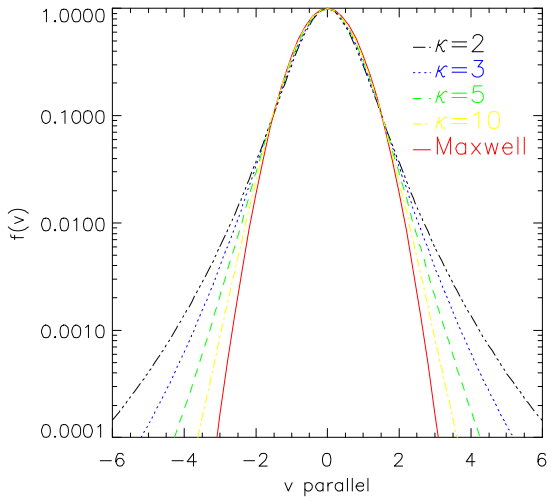

Figure 1-3: Kappa distribution function for different values of spectral index κ (taken from Ref. [57]).

ied [63]. While using kappa distribution, the effect of superthermal electrons on the oblique propagation characteristics of linear and nonlinear ion acoustic waves in an electron ion magnetized plasma has been discussed [64]. These authors have also shown that the presence of superthermal electrons has a significant effect on the nature of magnetized ion-acoustic solitons.

1.5 Layout of the Thesis

In chapter 2, we investigate the current-driven instabilities in heavier ion plasmas and the formation of solitary structures in the nonlinear regime. For this purpose, we derive the nonlinear partial differential equations governing the electron dynamics while the ions are assumed to be stationary. Then we obtain the solution in the form of dipolar vortices [65] and solitons [66].

In chapter 3, we investigate the linear and nonlinear dynamics of current-driven waves using kappa distribution for electrons and assuming the dust to be stationary. First, we derive the linear dispersion relation for electrostatic drift type waves in the presence of sheared current, which can exist in a homogeneous density plasma. Then in the nonlinear regime, we obtain the solutions under different shear flow limits [67].

In chapter 4, we investigate the dust drift waves due to zero-order current by considering the dust dynamics, whereas the electrons and ions are assumed to be inertialess. In the linear limit, the dispersion relation is derived and instability conditions are discussed. These current-driven waves and instabilities are shown to exist even if the plasma density is assumed to be homogeneous. Next, in the nonlinear regime, different type of structures such as dipolar vortices and solitons are discussed.

In chapter 5, we investigate the drift modes in a bounded plasma in several different cases. The global drift mode is studied in a cylindrical geometry having Gaussian density profile [68].

Finally in chapter 6, we present the summary and conclusions.

Chapter 2

Current-Driven Electrostatic Waves in Heavier Ion Plasmas

The current-driven waves and instabilities in magnetized plasmas have received considerable attention [28, 35, 36, 69]. Long ago [19], it was proposed that the free energy of sheared flow can give rise to a purely growing electrostatic instability in plasmas. It was shown that if both electrons and ions flow with the same sheared velocity parallel to the external constant magnetic field $\mathbf{B}_0 = B_0\hat{\mathbf{z}}$, then a purely growing electrostatic instability appears in the plasma without a zero-order current. Many years ago a few authors [35] investigated the low frequency electrostatic instabilities associated with electron velocity shear using local approximation. The electrons were assumed to flow with sheared velocity $\mathbf{v}_0 = v_0(x)\,\hat{\mathbf{z}}$ parallel to $\mathbf{B}_0$, but the effect of zero-order current was ignored.

It has been shown [36] that in the presence of zero-order current $\mathbf{J}_0 = -en_0\mathbf{v}_0$ a non-zero real frequency is associated with the electrostatic instability studied earlier [35]. The electrons sheared flow relative to stationary ions produces a zero-order current which modifies the external magnetic field and a relatively high frequency drift wave appears with real frequency $\omega_r \simeq (\kappa_B/k_\perp)\,\omega_{ce}$ where $\kappa_B = |d\ln B_0/dx|$ and $k_\perp$ is the wavevector perpendicular to the zero-order magnetic field. The wave also has a non-zero component of wavevector parallel to the magnetic field $k_\parallel$ and condition $k_\parallel < k_\perp$ holds. The short wavelength and relatively high frequency current-driven electrostatic wave can become unstable under certain conditions [36]. This drift-like wave does not

require density inhomogeneity to exist.

Many authors have investigated the effects of electron shear flow on plasma dynamics [70–72]. It has also been observed experimentally that ion cyclotron waves couple with velocity shear in the direction perpendicular to the magnetic field [73,74].

Further, it [28] has been shown that the flow of electrons and ions with the same sheared velocity along magnetic field in the presence of stationary dust produces a low frequency drift-like wave with nonzero real frequency. Therefore, the solar wind interaction with the edge regions of dusty magnetospheres of planets can give rise to an electrostatic wave. This wave can become unstable due to sheared flow and in the large amplitude regime it produces solitons in the edge of the dusty magnetosphere of planets [69]. The usual drift waves of low frequency $\omega \ll \omega_{ci}$ have been extensively studied due to their tremendous applications in electron-ion plasmas [75,76].

Aburdzhaniya *et al.* [77] studied the electron drift solitons in a magnetized plasma without zero-order flow (or current). The external magnetic field was assumed to be constant and the wave exists due to density gradient. The nonlinear structures, vortices and pulse solitons, were investigated in a pure electron plasma. It is interesting to note that the low frequency drift waves can form pulse-like solitons if electron temperature has a gradient [31]. However, the relatively high frequency electron drift wave can form soliton like structures even if electron pressure is ignored. The nonlinearity in this case appears through the convective term in electron parallel equation of motion [77]. In a stationary plasma, the electron-drift wave may not attain a large amplitude. But in the case of sheared flows the current-driven electron drift waves can become linearly unstable even if density is homogeneous [36] and in the large amplitude regime they can form solitons.

There are plans to conduct experiments with heavier ions such as barium with electrons sheared flows as mentioned in Ref. [35]. It has also been pointed out that a hybrid frequency wave is a normal mode [36] of the heavier ion ideal plasmas in the presence of sheared electrons flow along the initial constant magnetic field. It is important to investigate the dynamics of such systems in detail.

Therefore we have investigated the linear and nonlinear dynamics of this wave. It has been shown that the large amplitude electrostatic perturbations can form short scale vortex structures in such plasmas. The creation of vortex structures by electron

sheared flow-driven electrostatic waves can play an important role in plasma transport across the field lines. For the sake of physical understanding, the electrostatic perturbations are studied using Cartesian geometry.

Furthermore, we have also investigated the formation of drift wave solitons. In our case the scalar nonlinearity also appears through the convective term in parallel equation of motion similar to the case of Ref. [77]. This electron drift wave appears not due to the density inhomogeneity, but because of zero-order current which produces gradient in external magnetic field. However, for the sake of generality, we include the effects of density inhomogeneity as well.

2.1 Theoretical Model

Recently [36], the case of heavier ion plasmas has been considered and the effects of electrons sheared flow parallel to the external magnetic field have been discussed in the linear limit only. It has been shown that the shear in the external magnetic field introduces a new hybrid frequency electrostatic wave in the barium plasma. The real frequency of this wave is $\omega_r = (\kappa_B/k_\perp)\,\omega_{ce}$, where $k_\perp$ is the component of wavevector perpendicular to $\mathbf{B}_0$ and $\kappa_B = |d\ln B_0/dx| =$ constant is the inverse of the scale length of magnetic field gradient. Since in the local approximation $\kappa_B/k_\perp \ll 1$, so the frequency of the wave is smaller than electron gyrofrequency. It was also shown that in the presence of density gradients the frequency becomes $\omega_r = [(\kappa_n + \kappa_B)/k_\perp]\,\omega_{ce}$. Since in heavy ion plasmas the limit $\omega_{ci} \ll \omega_r$ is easily satisfied, the ion dynamics was also neglected. The instability conditions of this electrostatic wave have also been discussed by the authors.

Let us consider an inhomogeneous plasma containing electrons and ions immersed in an external magnetic field initially directed along z-axis $\mathbf{B}_0 = B_0\hat{\mathbf{z}}$. The initial external magnetic field is assumed constant and uniform. In equilibrium, the electrons are assumed to have sheared flow velocity parallel to the external magnetic field while ions remain stationary. The quasi neutrality condition is $n_{e0}(x) = n_{i0}(x) = n_0(x)$, where $n_{e0}(n_{i0})$ is the background number density of the electrons (ions). The equilibrium plasma density and electron velocity are assumed to have inhomogeneity in the

x-direction. The electron shear flow velocity along the magnetic field is given by,

$$\mathbf{v}_0 = v_0(x)\,\hat{\mathbf{z}}$$

while the ions remain immobile in this relatively high frequency regime. The equilibrium current due to this steady state flow of electrons parallel to the external magnetic becomes nonzero i.e.,

$$\mathbf{J}_0 = -en_0 v_0(x)\,\hat{\mathbf{z}} \neq \mathbf{0}$$

This current gives rise to sheared magnetic field satisfying Ampere's law. Thus the total magnetic field becomes inhomogeneous, and is given by [36],

$$\mathbf{B}_0 = B_{0z}\hat{\mathbf{z}} + B_{0y}(x)\hat{\mathbf{y}} = B_0\hat{\mathbf{e}}_{\|} \tag{2.1}$$

where$B_{0y} \ll B_{0z}$, $B_{0z} \equiv$ constant and $B_{0y}(x)$ is the y-component of magnetic field having gradient along x-axis. The electron shear flow is also assumed to increase in this direction. To represent the magnetic field in a simple form, the initial yz plane is rotated by a small angle. In this rotated frame z-axis is replaced by $r_{\|}$-axis and y-axis is replaced by $r_{\perp}$-axis, while x-axis remains unchanged. In this rotated frame, the magnetic field becomes $\mathbf{B}_0 = B_0\hat{\mathbf{e}}_{\|}$, where $\hat{\mathbf{e}}_{\|}$ is the unit vector along $r_{\|}$-axis, defined as,

$$\hat{\mathbf{e}}_{\|} = \frac{(\hat{\mathbf{z}} + \hat{\mathbf{y}}x/L_s)}{\sqrt{1 + x^2/L_s^2}}$$

The unit vector $\hat{\mathbf{e}}_{\perp}$ perpendicular to $\hat{\mathbf{e}}_{\|}$ becomes,

$$\hat{\mathbf{e}}_{\perp} = \frac{(\hat{\mathbf{y}} - \hat{\mathbf{z}}x/L_s)}{\sqrt{1 + x^2/L_s^2}}$$

where $L_s = \kappa_B^{-1}$ is the scale length of magnetic field gradient. The wave geometry is shown in Fig. (2-1).

The basic electrostatic drift wave like mode in hybrid frequency range does not require the plasma density inhomogeneity to exist [36]. It is driven by the electrons sheared flow parallel to the constant external magnetic field component. For the sake of generality we also take into account the effects of density inhomogeneity assuming

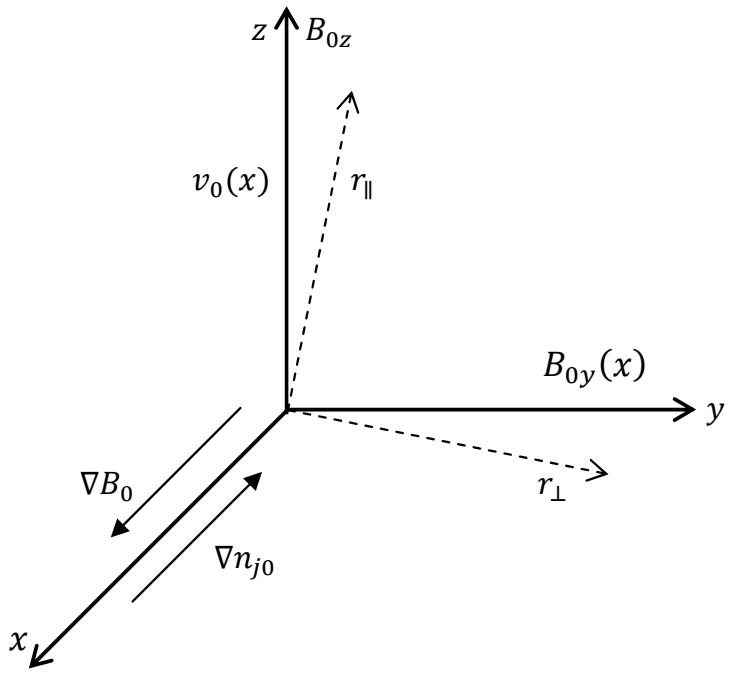

Figure 2-1: The wave geometry indicating the shear flow directed along external magnetic field.

$\boldsymbol{\nabla} n_{j0} = -\hat{\mathbf{x}}\,|dn_{j0}/dx|$ and $\kappa_{nj} = |1/n_{j0}\; dn_{j0}/dx| \equiv$ constant.

2.2 Linear Dispersion Relation

In this section, we first linearize the partial differential equations governing the electron dynamics and then Fourier transform the resulting equations to obtain the dispersion relation. The electron dynamics is governed by the continuity equation,

$$\frac{\partial n_e}{\partial t} + \boldsymbol{\nabla} \cdot (n_e \mathbf{v}_e) = 0 \tag{2.2}$$

and the momentum balance equation,

$$m_e n_e \left[\frac{\partial \mathbf{v}_e}{\partial t} + (\mathbf{v}_e \cdot \boldsymbol{\nabla})\,\mathbf{v}_e\right] = -e n_e \left[\mathbf{E} + \frac{1}{c}\mathbf{v}_e \times \mathbf{B}_0\right] - \boldsymbol{\nabla} p_e \tag{2.3}$$

where m_e is the electron mass, n_e is the electron number density, $\mathbf{v}_e$ is the electron fluid velocity, e is the magnitude of the electron charge, p_e is the electron thermal pressure

and c is the speed of light in vacuum. We consider only electrostatic perturbations here for which we use $\mathbf{E} = -\boldsymbol{\nabla}\phi$ where ϕ is the perturbed electrostatic potential. The Poisson's equation is given by,

$$\nabla^2\phi = 4\pi e\left(n_e - n_i\right) \tag{2.4}$$

Following the model presented by Saleem and Eliasson [36], a study of the low frequency (compared to the electron gyro-frequency) electrostatic perturbations is presented. For small perturbations, letting $n_e = n_0 + n_{e1}(\mathbf{r},t)$, $\mathbf{v}_e = \mathbf{v}_0 + \mathbf{v}_{e1}(\mathbf{r},t)$ with $|n_{e1}| \ll |n_0|$, etc., from Eqs. (2.2) and (2.3), the perturbed continuity and momentum equations can be written, respectively as,

$$\left(\partial_t + \mathbf{v}_0\cdot\boldsymbol{\nabla} + \mathbf{v}_{e1}\cdot\boldsymbol{\nabla}\right)n_{e1} + \boldsymbol{\nabla}\cdot\left(n_0\mathbf{v}_{e1}\right) = 0 \tag{2.5}$$

$$\left(\partial_t + \mathbf{v}_0\cdot\boldsymbol{\nabla} + \mathbf{v}_{e1}\cdot\boldsymbol{\nabla}\right)\mathbf{v}_{e1} + \left(\mathbf{v}_{e1}\cdot\boldsymbol{\nabla}\right)\mathbf{v}_0 = -\frac{e}{m_e}(\mathbf{E}_1 + \frac{1}{c}\mathbf{v}_{e1}\times\mathbf{B}_0) - \frac{T_e}{m_e n_0}\boldsymbol{\nabla}n_{e1} \tag{2.6}$$

The quantities with the subscript naught (0) denote the equilibrium quantities and the subscript (1) represent the perturbed quantities. In subsequent calculations the subscript (1) on perturbed quantities is dropped. The perpendicular velocity component is obtained by taking the cross product of the perturbed momentum equation (2.6) with $\hat{\mathbf{e}}_\parallel$, which yields,

$$\mathbf{v}_{e\perp} = \frac{c}{B_0}\hat{\mathbf{e}}_\parallel\times\boldsymbol{\nabla}_\perp\phi + \frac{cT_e}{eB_0 n_0}\boldsymbol{\nabla}n_e\times\hat{\mathbf{e}}_\parallel + \frac{1}{\omega_{ce}}\left(\partial_t + \mathbf{v}_0\cdot\boldsymbol{\nabla} + \mathbf{v}_e\cdot\boldsymbol{\nabla}\right)\mathbf{v}_e\times\hat{\mathbf{e}}_\parallel \tag{2.7}$$

while in deriving the above equation, it is assumed that the second term of (2.6) is approximately equal to $\left(\mathbf{v}_e\cdot\boldsymbol{\nabla}\right)v_0\left(x\right)\hat{\mathbf{e}}_\parallel$. For low frequencies, keeping the small terms up to the second order, the electron perpendicular velocity becomes,

$$\begin{aligned}\mathbf{v}_{e\perp} &= \frac{c}{B_0}\hat{\mathbf{e}}_\parallel\times\boldsymbol{\nabla}_\perp\phi + \frac{cT_e}{eB_0}\frac{\boldsymbol{\nabla}n_e}{n_0}\times\hat{\mathbf{e}}_\parallel \\ &\quad + \frac{1}{\omega_{ce}}\left(\partial_t + \mathbf{v}_0\cdot\boldsymbol{\nabla} + \mathbf{v}_e\cdot\boldsymbol{\nabla}\right)\left[\frac{c}{B_0}\boldsymbol{\nabla}_\perp\phi - \frac{cT_e}{eB_0}\frac{\boldsymbol{\nabla}_\perp n_e}{n_0}\right] \\ &= \mathbf{v}_E + \mathbf{v}_D + \mathbf{v}_p\end{aligned} \tag{2.8}$$

where $\mathbf{v}_E = \frac{c}{B_0}\hat{\mathbf{e}}_\parallel \times \boldsymbol{\nabla}_\perp \phi$ is the electric drift velocity, $\mathbf{v}_D = \frac{cT_e}{eB_0 n_0}\boldsymbol{\nabla} n_e \times \hat{\mathbf{e}}_\parallel$ is the diamagnetic drift velocity and $\mathbf{v}_p = \frac{1}{\omega_{ce}}\left(\partial_t + \mathbf{v}_0 \cdot \boldsymbol{\nabla} + \mathbf{v}_e \cdot \boldsymbol{\nabla}\right)\left[\frac{c}{B_0}\boldsymbol{\nabla}_\perp \phi - \frac{cT_e}{eB_0 n_0}\boldsymbol{\nabla}_\perp n_e\right]$ is the polarization drift velocity. The parallel component of the electron fluid velocity is obtained by taking the dot product of (2.6) with $\hat{\mathbf{e}}_\parallel$, which gives,

$$\left(\partial_t + \mathbf{v}_0 \cdot \boldsymbol{\nabla} + \mathbf{v}_e \cdot \boldsymbol{\nabla}\right) v_{e\parallel} + \left(\mathbf{v}_e \cdot \boldsymbol{\nabla}\right) v_0 = \frac{e}{m_e}\partial_\parallel \phi - \frac{T_e}{m_e n_0}\partial_\parallel n_e \tag{2.9}$$

The second term on the left hand side in above equation is simplified by replacing $\mathbf{v}_e$ with the corresponding components from (2.8) and thus can be written as,

$$\left(\partial_t + \mathbf{v}_0 \cdot \boldsymbol{\nabla} + \mathbf{v}_e \cdot \boldsymbol{\nabla}\right) v_{e\parallel} = \frac{e}{m_e}\partial_\parallel \phi - \frac{T_e}{m_e n_0}\partial_\parallel n_e + \frac{c}{B_0}\partial_\perp \phi \frac{dv_0}{dx} - \frac{v_{Te}^2}{\omega_{ce} n_0}\partial_\perp n_e \frac{dv_0}{dx} \tag{2.10}$$

The Poisson's equation can be written as,

$$\nabla^2 \phi = 4\pi e n_e \tag{2.11}$$

Equation (2.5) can be written as,

$$\left(\partial_t + \mathbf{v}_0 \cdot \boldsymbol{\nabla} + \mathbf{v}_e \cdot \boldsymbol{\nabla}\right) n_e + \mathbf{v}_E \cdot \boldsymbol{\nabla} n_0 + n_0 \boldsymbol{\nabla} \cdot \mathbf{v}_E + \mathbf{v}_p \cdot \boldsymbol{\nabla} n_0 + n_0 \boldsymbol{\nabla} \cdot \mathbf{v}_p + n_0 \partial_\parallel v_{e\parallel} = 0 \tag{2.12}$$

while in deriving the above equation it is assumed that $\boldsymbol{\nabla} \cdot (n_0 \mathbf{v}_D) \to 0$. Using Eqs. (2.8) and (2.11) in Eq. (2.12) we obtain,

$$\begin{aligned} &\frac{1}{4\pi e}\left(\partial_t + \mathbf{v}_0 \cdot \boldsymbol{\nabla} + \mathbf{v}_e \cdot \boldsymbol{\nabla}\right) \nabla^2 \phi - \frac{c n_0}{B_0}\left(\frac{d \ln n_0}{dx} - \frac{d \ln B_0}{dx}\right)\partial_\perp \phi + \\ &\frac{n_0}{\omega_{ce}}\left(\partial_t + \mathbf{v}_0 \cdot \boldsymbol{\nabla} + \mathbf{v}_e \cdot \boldsymbol{\nabla}\right)\left[\frac{c}{B_0}\nabla_\perp^2 \phi - \frac{c}{B_0}\lambda_{De}^2 \nabla_\perp^2 \nabla^2 \phi\right] + n_0 \partial_\parallel v_{e\parallel} = 0 \end{aligned} \tag{2.13}$$

where $\lambda_{De} = \left(T_e / 4\pi e^2 n_0\right)^{1/2}$ is the plasma Debye length. Similarly using Eq. (2.11) in Eq. (2.10), we obtain,

$$\left(\partial_t + \mathbf{v}_0 \cdot \boldsymbol{\nabla} + \mathbf{v}_e \cdot \boldsymbol{\nabla}\right) v_{e\parallel} = \frac{e}{m_e}\left(\partial_\parallel \phi + A \partial_\perp \phi\right) - \frac{e v_{Te}^2 \lambda_{De}^2}{T_e}\left(\partial_\parallel \nabla^2 \phi + A \partial_\perp \nabla^2 \phi\right) \tag{2.14}$$

where $v_{Te} = (T_e/m_e)^{1/2}$ is the electron thermal speed, and A is the normalized electron velocity shear, defined as,

$$A = \frac{1}{\omega_{ce}} \left| \frac{dv_0}{dx} \right| \tag{2.15}$$

Eqs. (2.13) and (2.14) are coupled nonlinear partial differential equations.

In order to obtain the linear dispersion relation, only the first order terms are retained in the nonlinear equations. Then assuming the electrostatic perturbations of the form $\exp\left[i\left(\mathbf{k}\cdot\mathbf{r} - \omega t\right)\right]$, the resulting linearized equations give the quadratic dispersion relation as,

$$\Omega_0^2 \left[\left(1 + \lambda_{De}^2 k_\perp^2\right) + \frac{k^2 \omega_{ce}^2}{k_\perp^2 \omega_{pe}^2} \right] + \Omega_0 \frac{\left(\kappa_n + \kappa_B\right)\omega_{ce}}{k_\perp} - \left(1 + \lambda_{De}^2 k_\perp^2\right)\omega_{ce}^2 \left(\frac{k_\parallel^2}{k_\perp^2} + \frac{k_\parallel}{k_\perp} A \right) = 0 \tag{2.16}$$

where $\Omega_0 = \omega - \omega_0$ is the Doppler shifted wave frequency with $\omega_0 = v_0 k_\parallel$ and $\omega_{pe} = (4\pi n_0 e^2/m_e)^{1/2}$ is the electron plasma frequency. This is the dispersion relation for the electrostatic waves in the presence of the electrons shear flow along the external magnetic field. Eq. (2.16) has the roots,

$$\left(\Omega_0\right)_{1,2} = \frac{1}{2g_2} \left[-g_1 \pm \left\{ g_1^2 + 4 g_0 g_2 \left(\frac{k_\parallel^2}{k_\perp^2} + \frac{k_\parallel}{k_\perp} A \right) \right\}^{\frac{1}{2}} \right] \tag{2.17}$$

where,

$$g_2 = \left(1 + \lambda_{De}^2 k_\perp^2\right) + \frac{k^2 \omega_{ce}^2}{k_\perp^2 \omega_{pe}^2}$$

$$g_1 = \frac{\left(\kappa_n + \kappa_B\right)\omega_{ce}}{k_\perp}$$

and,

$$g_0 = \left(1 + \lambda_{De}^2 k_\perp^2\right)\omega_{ce}^2$$

The instability condition from Eq. (2.17) is given by,

$$g_1^2 + 4 g_0 g_2 \left(\frac{k_\parallel^2}{k_\perp^2} + \frac{k_\parallel}{k_\perp} A \right) < 0 \tag{2.18}$$

2.3 Dipolar Vortices

In this section, We now present the stationary solutions of Eqs. (2.13) and (2.14) in a moving frame,

$$\xi = r_\perp + \alpha r_\parallel - ut$$

such that,

$$\phi\left(x, r_\perp, r_\parallel, t\right) = \phi(x, \xi)$$
$$v_{e\parallel}\left(x, r_\perp, r_\parallel, t\right) = v_{e\parallel}(x, \xi)$$

where α and u are constants. Then Eq. (2.14) in the new frame can be written as,

$$D_\xi \left[v_{e\parallel} - \Gamma_0 \phi\right] = 0 \tag{2.19}$$

where,

$$\Gamma_0 = \frac{e\left(\alpha + A\right)}{m_e\left(u - \alpha v_0\right)}\left[\left(\frac{T_e}{4\pi e^2 n_0}\right)\nabla^2 - 1\right]$$

and,

$$D_\xi = \partial_\xi - \frac{c}{B_0}\left(u - \alpha v_0\right)\left[\partial_x\phi\partial_\xi - \partial_\xi\phi\partial_x\right]$$

Let us choose the trivial solution of Eq. (2.19) given as

$$v_{e\parallel} = \Gamma_0 \phi \tag{2.20}$$

Similarly Eq. (2.13) can be expressed in ξ-frame, as

$$D_\xi\left[\frac{\nabla^2\phi}{4\pi e} + \frac{cn_0}{B_0\omega_{ce}}\nabla_\perp^2\phi\right] - \frac{cn_0}{B_0\left(u - \alpha v_0\right)}\left(\kappa_n + \kappa_B\right)\partial_\xi\phi - \frac{n_0\alpha}{\left(u - \alpha v_0\right)}\partial_\xi v_{e\parallel} = 0 \tag{2.21}$$

For weak dispersion, the term of the order of $\lambda_{De}^2 D_t \nabla_\perp^2 \nabla^2\phi$ is neglected in comparison with the polarization drift term. Assuming $\partial_\parallel << \boldsymbol{\nabla}_\perp$ and using Eq. (2.20) in Eq. (2.21) we obtain

$$D_\xi\left[\nabla_\perp^2\phi - F_1\phi\right] = 0 \tag{2.22}$$

where $F_1 = \beta_2/\beta_1$, and,

$$\beta_1 = \frac{\left(u-\alpha v_0\right)^2\left(\omega_{ce}^2+\omega_{pe}^2\right)-\alpha\left(\alpha+A\right)v_{Te}^2\omega_{ce}^2}{\omega_{ce}^2\left(u-\alpha v_0\right)^2} \tag{2.23}$$

$$\beta_2 = \frac{\left(u-\alpha v_0\right)\omega_{ce}\omega_{pe}^2\left(\kappa_n+\kappa_B\right)-\alpha\left(\alpha+A\right)\omega_{ce}^2\omega_{pe}^2}{\omega_{ce}^2\left(u-\alpha v_0\right)^2} \tag{2.24}$$

Eq. (2.22) is satisfied by the ansatz,

$$\nabla_\perp^2\phi = C_1\phi + C_2 x \tag{2.25}$$

where the constants C_1 and C_2 are related by,

$$C_1 = F_1 - \frac{c}{\left(u-\alpha v_0\right)B_0}C_2 \tag{2.26}$$

To obtain the dipolar vortex solution of Eq. (2.25), it is transformed into polar coordinates (r,θ) by substituting $x = r\cos\theta$, $\xi = r\sin\theta$, where $r = \left(x^2+\xi^2\right)^{1/2}$ and $\theta = \arctan\left(\xi/x\right)$. Then we divide the (r,θ) plane into inner region $(r < r_0)$ and outer region $(r > r_0)$ of a arbitrary circle of radius r_0. For bounded solution, in the outside region we must have $C_2 = 0$, so from (2.26) we obtain,

$$C_1 = F_1 = \lambda_1^2 \tag{2.27}$$

Thus Eq. (2.25) can be written as,

$$\frac{\partial^2\psi}{\partial r^2} + \frac{1}{r}\frac{\partial\psi}{\partial r} - \left(\lambda_1^2 + \frac{1}{r^2}\right)\psi = 0 \tag{2.28}$$

where we have used $\phi\left(r,\theta\right) = \psi\left(r\right)\cos\theta$. By solving Eq. (2.28) and using $\phi\left(r,\theta\right) = \psi\left(r\right)\cos\theta$, we obtain,

$$\phi^{out}\left(r,\theta\right) = Q^{out}K_1\left(\lambda_1 r\right)\cos\theta \tag{2.29}$$

where Q^{out} is a constant and K_1 is the first order modified Bessel function of the second kind. For bounded and localized solutions, we require,

$$\lambda_1^2 > 0 \tag{2.30}$$

For the inner solution of Eq. (2.25) for $r < r_0$, assuming $C_1 = -\lambda_2^2$ and $F_1 = \lambda_1^2$, Eq. (2.26) becomes,

$$C_2 = \frac{(u - \alpha v_0) B_0 \left(\lambda_1^2 + \lambda_2^2\right)}{c} \tag{2.31}$$

Thus to obtain the inner solution using (2.31), Eq. (2.25) can now be written as,

$$\frac{\partial^2 \psi}{\partial r^2} + \frac{1}{r}\frac{\partial \psi}{\partial r} + \left(\lambda_2^2 - \frac{1}{r^2}\right)\psi = C_2 r \tag{2.32}$$

Solving Eq. (2.32) and using back in $\phi(r, \theta) = \psi(r)\cos\theta$, we obtain,

$$\phi^{in}(r, \theta) = \left[Q^{in} J_1(\lambda_2 r) + \frac{C_2}{\lambda_2^2} r\right]\cos\theta \tag{2.33}$$

where Q^{in} and λ_2^2 are constants and J_1 is the first order ordinary Bessel function. The constants Q^{in} and Q^{out} are determined from the physically justified continuity conditions of ϕ and $\nabla_\perp^2 \phi$ at $r = r_0$.

$$Q^{in} = -\frac{(u - \alpha v_0) B_0 \lambda_1^2 r_0}{c\lambda_2^2 J_1(\lambda_2 r_0)} \tag{2.34}$$

$$Q^{out} = \frac{(u - \alpha v_0) B_0 r_0}{c K_1(\lambda_1 r_0)} \tag{2.35}$$

The continuity condition of $\nabla_\perp \phi$ at $r = r_0$ gives a relation between λ_1 and λ_2 and is given as follows,

$$\frac{K_2(\lambda_1 r_0)}{K_1(\lambda_1 r_0)} = -\frac{\lambda_1 J_2(\lambda_2 r_0)}{\lambda_2 J_1(\lambda_2 r_0)} \tag{2.36}$$

2.4 Solitons

In the preceding section we studied the possible dipolar vortex solutions of the non-linear equations under the condition $\mathbf{v}_E \cdot \boldsymbol{\nabla} \gg v_{e\|}\partial_\|$. Following Ref. [77], here we investigate the soliton solutions, which may exist for $\mathbf{v}_E \cdot \boldsymbol{\nabla} < v_{e\|}\partial_\|$. Thus under this condition, (2.13) becomes,

$$\lambda_{De}^2 \left(\partial_t + \mathbf{v}_0 \cdot \boldsymbol{\nabla} + v_{e\|}\partial_\|\right)\nabla^2 \Phi - D_e \left(\frac{d \ln n_0}{dx} - \frac{d \ln B_0}{dx}\right)\partial_\perp \Phi + \rho_e^2 D_t \nabla_\perp^2 \Phi + \partial_\| v_{e\|} = 0 \tag{2.37}$$

Similarly (2.14) can be written as,

$$\left(\partial_t + \mathbf{v}_0 \cdot \boldsymbol{\nabla} + v_{e\|}\partial_\|\right) v_{e\|} = v_{Te}^2 \left(\partial_\| \Phi + A\partial_\perp \Phi\right) - v_{Te}^2 \lambda_{De}^2 \left(\partial_\| \nabla^2 \Phi + A\partial_\perp \nabla^2 \Phi\right) \quad (2.38)$$

In order to obtain the stationary solution of our nonlinear equations, we consider the frame $\eta = r_\perp + \alpha r_\| - ut$, where u is the speed of the nonlinear structure, $\partial_\perp = d_\eta$, $\partial_\| = \alpha d_\eta$, $\partial_t = -u d_\eta$. Accordingly assuming $\alpha v_0 d_\eta \ll u d_\eta$, (2.38) can be expressed as,

$$d_\eta v_{e\|} - \frac{\alpha}{u} v_{e\|} d_\eta v_{e\|} = -\frac{v_{Te}^2}{u} (\alpha + A)\, d_\eta \Phi + \frac{v_{Te}^2 \lambda_{De}^2}{u} (\alpha + A) \left(1 + \alpha^2\right) d_\eta^3 \Phi \quad (2.39)$$

which can be written approximately as,

$$v_{e\|} = -\frac{v_{Te}^2}{u} (\alpha + A)\, \Phi + \frac{v_{Te}^2 \lambda_{De}^2}{u} (\alpha + A) \left(1 + \alpha^2\right) d_\eta^2 \Phi + \frac{\alpha}{2u} \left(\frac{v_{Te}^2}{u} (\alpha + A)\right)^2 \Phi^2 \quad (2.40)$$

where only the leading order nonlinear term is retained. Similarly, in this new frame, (2.37) becomes,

$$-u\lambda_{De}^2 (1 + \alpha^2) d_\eta^3 \Phi + D_e(\kappa_n + \kappa_B) d_\eta \Phi - u\rho_e^2 d_\eta^3 \Phi + \alpha d_\eta v_{e\|} = 0 \quad (2.41)$$

Eliminating $v_{e\|}$ from (2.41) by using (2.40), we obtain the nonlinear equation,

$$-d_\eta \Phi + \frac{1}{2} A_4 d_\eta \Phi^2 + B d_\eta^3 \Phi = 0 \quad (2.42)$$

where $A_4 = -A_3/A_2$ is the coefficient of the nonlinear term and $B = A_1/A_2$ is the coefficient of the dispersive term, where,

$$A_1 = \frac{u}{\omega_{pe}^2} \left(1 + \alpha^2\right) + \frac{u}{\omega_{ce}^2} - \frac{\lambda_{De}^2}{u} (\alpha + A) \left(1 + \alpha^2\right)$$

$$A_2 = \frac{1}{\omega_{ce}} (\kappa_n + \kappa_B) - \frac{\alpha}{u} (\alpha + A)$$

and

$$A_3 = \frac{\alpha^2}{u v_{Te}^2} \left(\frac{v_{Te}^2}{u} (\alpha + A)\right)^2$$

It is important to mention here that the nonlinear term in (2.42) comes from the parallel component of the equation of motion for electrons. We now present the drift soliton solution [39] of equation (2.42) by using the following boundary conditions $\Phi \to 0$, $d_\eta \Phi \to 0$ and $d_\eta^2 \Phi \to 0$ for $\eta \to \pm\infty$ for localized solutions. Thus the solution becomes,

$$\Phi = \Phi_m \, \mathrm{sech}^2 \left(\frac{\eta}{\delta} \right) \tag{2.43}$$

where $\Phi_m = 3/A_4$ is the amplitude and $\delta = \sqrt{4B}$ is the width of the soliton. Note that the solitary solution exist for $B > 0$, otherwise δ will become imaginary and there would be no solitary solution. For $A_4 < 0$, the solution (2.43) yields a refractive solitary pulse where as $A_4 > 0$ leads to the generation of compressive solitary pulse. Since $A_4 = -A_3/A_2$, and $A_3 > 0$, thus for refractive type pulse we need $A_2 > 0$. Since $B = A_1/A_2$, therefore when $A_2 < 0$ we also require $A_1 < 0$, so that the condition $B > 0$ for solitary solution remain valid as discussed before.

2.5 Numerical Results

As an illustration we apply our results to the parameters relevant to laboratory plasmas [36] to investigate the nonlinear structures which can be formed by the large amplitude electron parallel shear flow driven hybrid frequency waves. Therefore, we choose laboratory plasma parameters as, $n_0 = 10^9 \mathrm{cm}^{-3}$, $T_e = T_i = 3500$ K, and $B_0 = 20$ G, which gives $v_{Te} = 2.28 \times 10^7$ cm/s, $\omega_{pe} = 1.78 \times 10^9$ rad/s, $\omega_{ce} = 3.5 \times 10^8$ rad/s, $\lambda_{De} = 1.28 \times 10^{-2}$ cm, and $\rho_e = v_{Te}/\omega_{ce} = 0.065$ cm. Let us assume that the barium plasma is singly charged and hence $m_i = 2.3 \times 10^{-22}$ g, $v_{Ti} = (T_i/m_i)^{1/2} = 4 \times 10^4$ cm/s, $\omega_{pi} = 3.53 \times 10^6$ rad/s, and $\omega_{ci} = 1.38 \times 10^3$ rad/s. Assuming $\omega = \omega_r \pm i\omega_i$, we plot the linear dispersion relation showing ω_r vs $k_\perp$ and ω_i vs $k_\perp$ in Fig. (2-2) and Fig. (2-3), respectively, keeping in view that $\rho_e^2 k_\perp^2 < 1$ must remain valid to avoid Landau damping effects which require kinetic treatment. Let $\kappa_n = \kappa_B = 0.08$ cm^{-1}and $k_\perp = (0.8 \to 10)$ cm^{-1} so that the local approximation $\lambda_\perp = 2\pi/k_\perp << L_n = 1/\ \kappa_n$ remains applicable. Fig. (2-4) shows the nonlinear dipolar vortex for $u = 0.8 \times 10^8$ cm/s, $v_0 = 4.5 \times 10^8$ cm/s, $\lambda_1 = 2.3$, and $\alpha = 0.4$. It is clear that the dimensions of the vortex are several orders of magnitude larger than ρ_e. Fig. (2-5) shows the

dependence of the refractive solitary pulse on the velocity gradient.

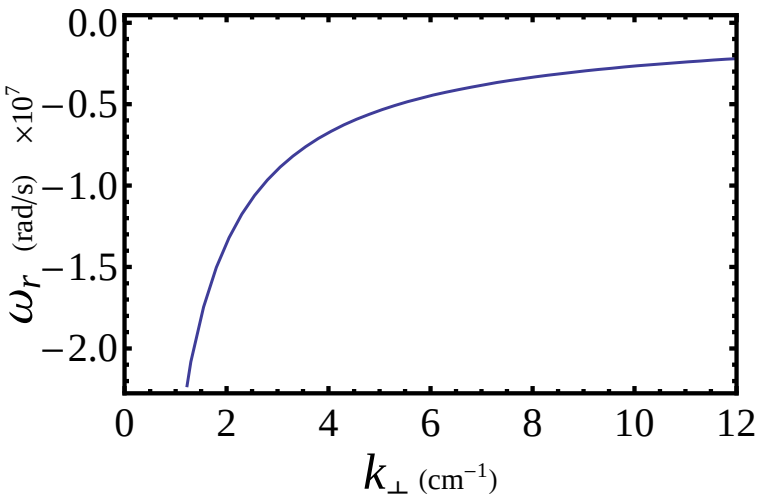

Figure 2-2: The real frequency ω_r of the linear dispersion relation is plotted against $k_\perp$.

2.6 Discussion

The nonlinear dynamics of an electrostatic perturbation driven by electron sheared flow in a magnetized plasma has been investigated. The perturbation has been studied keeping in view the potential experiments on Q-machine with heavier (barium) ion plasmas. In the presence of large sheared flows of electrons, this wave can become unstable. In the nonlinear regime, this electrostatic wave can give rise to dipolar vortices shown in Fig. (2-4), which can play an important role in plasma cross-field transport.

In addition, we have derived a nonlinear equation which admits solutions in the form of solitons. The nonlinear term in this case appears through the convective term in the parallel component of equation of motion. Unlike low frequency drift wave ($\omega < \omega_{ci}$), the electron drift soliton does not require the gradient in electron temperature to exist. The present investigation can be useful in the future theoretical and experimental studies on the heavier ion plasmas having sheared electron flows.

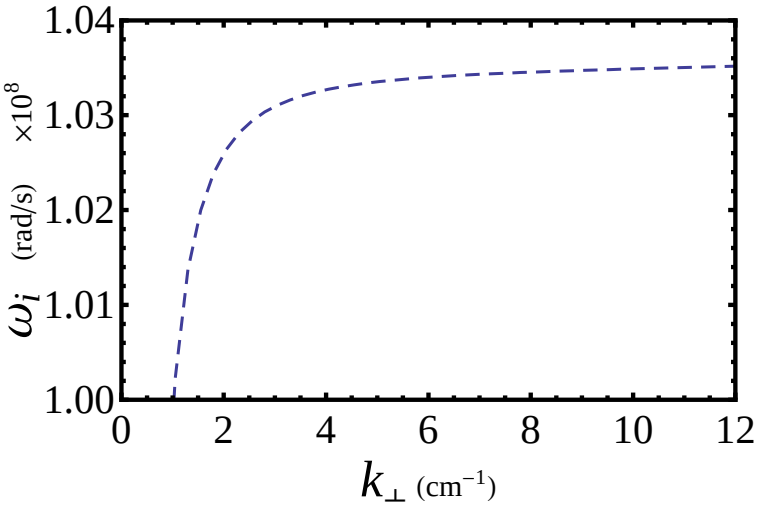

Figure 2-3: The growth rate ω_i of the electron shear flow instability is plotted against $k_\perp$.

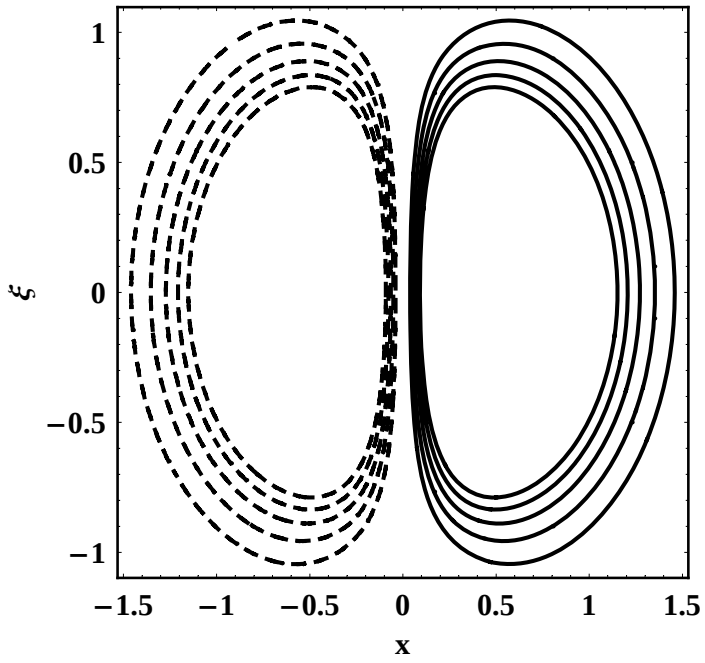

Figure 2-4: The dipolar vortices are plotted using equations (22) and (24) corresponding to our chosen plasma parameters.

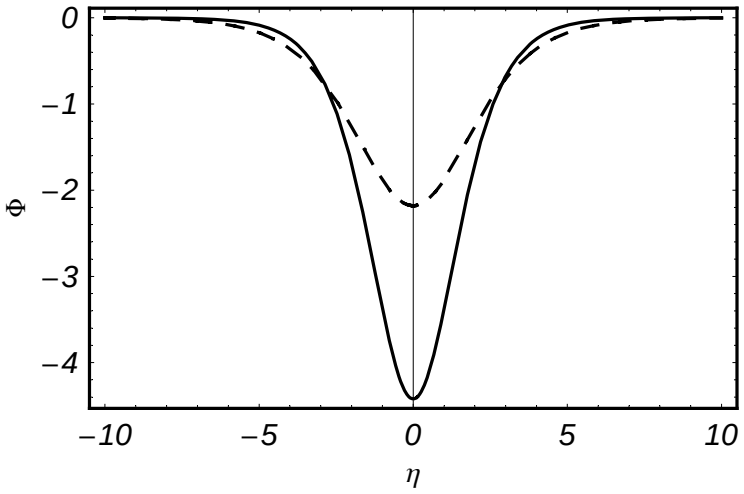

Figure 2-5: Amplitude variation of the refractive type soliton is shown corresponding to different values of $\kappa_v = \frac{1}{v_0}\frac{dv_0}{dx}$. The solid curve is for $\kappa_v \simeq 0.03$ cm^{-1} (dotted curve is for $\kappa_v \simeq 0.04$ cm^{-1}) while $u = 0.95 v_{Te}$ and $\alpha = 0.21$.

Chapter 3

Current-Driven Waves in Plasmas with Stationary Dust

It is well-known that the plasma density inhomogeneity gives rise to drift wave which has been theoretically predicted long ago [78–80]. A great deal of research work on the linear and nonlinear properties of this low frequency (compared to ion gyro-frequency) and long wavelength (compared to ion gyro-radius) electrostatic wave has appeared in literature [33, 40, 76, 81] and references therein. Moreover, this mode can couple with other low frequency waves as well like ion acoustic [31, 33] and Alfven [82–85] waves.

Many years ago, it was discovered that in the presence of stationary dust a very low frequency electrostatic Shukla-Varma [86] mode can appear in the plasma. The expression of local linear dispersion relation depends on the equilibrium number density which is space dependent. Thus the Fourier transformation does not seem to be appropriate in this case. However, this mode explains a physical picture in a broader sense with an approximate solution of the linear equations in a weakly inhomogeneous plasma. This mode propagate in the direction perpendicular to both external magnetic field $\mathbf{B}_0$ and density gradient $\boldsymbol{\nabla} n_{j0}$ where the subscript j stands for the plasma species.

Recently, it is proposed that a low frequency electrostatic wave can exist in plasmas in the presence of shear flow of electrons and ions while the dust is assumed stationary in equilibrium [26–28]. The main reason for the existence of this mode is the background current created by the flow of electrons and ions which gives rise to

shear in the magnetic field. Such a situation may occur at the boundary regions of some dusty planetary magnetospheres where the solar wind flows along the magnetic field lines and heavy dust remains stationary. It has been shown that the mode can become unstable under certain conditions due to the free energy stored in the shear flow of electrons and ions.

If the plasma has inhomogeneous density then the above mentioned mode [28] couples with the known drift waves as well as with ion acoustic wave. These modes can become unstable due to sheared flow of electrons and ions under certain conditions. In addition these waves can produce nonlinear structures, like vortices [27], solitons and shocks [69]. These linear instabilities and formation of nonlinear structures have been studied using multi-fluid plasma equations assuming Boltzmann density distribution for electrons along with weak shear flow gradient.

Space plasmas are often observed to have nonthermal electrons equilibrium distribution, such as, solar wind, planetary magnetospheres and auroral zone plasmas [56, 87, 88]. In such plasmas, the velocity distribution deviate from the usual Maxwellian equilibrium distribution, having nonthermal tails in the high energy region [89–91]. Such behavior is effectively modeled by a kappa or generalized Lorentzian distribution function [58, 91, 92], which appears to be more appropriate than a thermal Maxwellian distribution in a wide range of plasma situations. Noteworthy applications of the κ-distribution function include, e.g., an interpretation of observations in the Earth's foreshock [93] and solar wind models with coronal electrons [94, 95]. Recently, low frequency waves in inhomogeneous dusty plasmas and drift wave driven vortices with nonthermal distributions have been studied in Refs [96] and [97] respectively. "Superthermal" plasma behavior was also observed in various experimental plasmas [98]. The kappa distribution function is given by equation (1.18).

Here we study the low frequency mode proposed by Saleem [28] and its coupling with drift wave in a dusty plasma having excess of suprathermal electrons. Moreover, we investigate the nonlinear dynamics of these waves in the case of steeper gradient in sheared flow which has not been discussed in Refs. [26, 27]. Sheared-flow driven instability (D'Angelo's mode [19]) is also modified in the presence of suprathermal electrons. Further, it is investigated that the behavior and formation of nonlinear structures both dipolar and tripolar vortices modify due to current-driven mode and

excess of high energy electrons.

In the following, the plasma model is described and a set of nonlinear fluid equations is derived in a magnetized plasma. It is assumed that the electrons and ions have sheared flow velocity along the external magnetic field. The dust grains are assumed stationary in equilibrium. Then the linear dispersion relation is derived and instability conditions are discussed in different limits. The solutions of the nonlinear equations are also studied. For constant plasma flow or weaker gradient of flow, dipolar vortex solution is obtained. While for steeper velocity gradient, the solutions are obtained in the form of tripolar vortices.

3.1 Model and Basic Equations

We consider an inhomogeneous multi-component plasma containing electrons, ions and massive negatively charged dust grains. Let us assume that the initial external magnetic field is along the z-axis $B_0\hat{\mathbf{z}}$, where B_0 is the magnitude of the magnetic field and $\hat{\mathbf{z}}$ is a unit vector. We assume that electrons and ions flow with the same sheared velocity $\mathbf{v}_0 = v_0(x)\,\hat{\mathbf{z}}$ along the magnetic field while massive dust grains remain stationary. The equilibrium plasma density has a gradient perpendicular to the external magnetic field and is assumed to be along x-axis, where the density of each species decreases in the x direction. The steady state requires,

$$n_{i0}(x) = n_{e0}(x) + Z_d n_{d0}(x) \tag{3.1}$$

where $n_{i0}(x)$, $n_{e0}(x)$ and $n_{d0}(x)$ are the equilibrium number density of ions, electrons, and charged dust particles, respectively, and Z_d is the constant dust charge number. Since the equilibrium current, given as,

$$\mathbf{J}_0 = e\,(n_{i0} - n_{e0})\,v_0(x)\,\hat{\mathbf{z}} \neq \mathbf{0} \tag{3.2}$$

is non-zero, therefore it gives rise to an inhomogeneity in the static magnetic field. Thus the total magnetic field becomes inhomogeneous as defined through Eq. (2.1).

For cold ions, the continuity and momentum equations are given, respectively, as,

$$\left(\partial_t + \mathbf{v}_{i0}\cdot\boldsymbol{\nabla} + \mathbf{v}_i\cdot\boldsymbol{\nabla}\right) n_i + \boldsymbol{\nabla}\cdot\left(n_{i0}\mathbf{v}_i\right) = 0 \tag{3.3}$$

$$\left(\partial_t + \mathbf{v}_{i0}\cdot\boldsymbol{\nabla} + \mathbf{v}_i\cdot\boldsymbol{\nabla}\right)\mathbf{v}_i + \left(\mathbf{v}_i\cdot\boldsymbol{\nabla}\right)\mathbf{v}_{i0} = \frac{e}{m_i}\left(\mathbf{E} + \frac{1}{c}\mathbf{v}_i\times\mathbf{B}_0\right) \tag{3.4}$$

where m_i, n_i, $\mathbf{v}_i$, and e are, respectively, the mass, the number density, the fluid velocity, and the charge of the ions, c is the speed of light in vacuum and the subscript naught (0) denotes the equilibrium quantities. We assume $\mathbf{E} = -\boldsymbol{\nabla}\phi$ for electrostatic waves, where ϕ is the electrostatic potential.

From (3.4), the ion perpendicular motion is described by the recurrent formula,

$$\mathbf{v}_{i\perp} = \frac{c}{B_0}\hat{\mathbf{e}}_\parallel\times\boldsymbol{\nabla}_\perp\phi - \frac{1}{\omega_{ci}}\left(\partial_t + \mathbf{v}_{i0}\cdot\boldsymbol{\nabla} + \mathbf{v}_i\cdot\boldsymbol{\nabla}\right)\mathbf{v}_i\times\hat{\mathbf{e}}_\parallel = \mathbf{v}_E + \mathbf{v}_P \tag{3.5}$$

Here, $\mathbf{v}_E = \frac{c}{B_0}\hat{\mathbf{e}}_\parallel\times\boldsymbol{\nabla}_\perp\phi$ and $\mathbf{v}_P = -\frac{1}{\omega_{ci}}\left(\partial_t + \mathbf{v}_{i0}\cdot\boldsymbol{\nabla} + \mathbf{v}_i\cdot\boldsymbol{\nabla}\right)\mathbf{v}_i\times\hat{\mathbf{e}}_\parallel$ are the electric and polarization drifts, respectively, and $\omega_{ci} = eB_0/m_ic$ is the ion gyro frequency. Using (3.5) in (3.3) we get,

$$\begin{aligned}\left(\partial_t + \mathbf{v}_{i0}\cdot\boldsymbol{\nabla} + \mathbf{v}_i\cdot\boldsymbol{\nabla}\right) n_i - n_{i0}D_e\left(\frac{d\ln n_{i0}}{dx} - \frac{d\ln B_0}{dx}\right)\partial_\perp\Phi \\ -n_{i0}\rho_s^2\left(\partial_t + \mathbf{v}_{i0}\cdot\boldsymbol{\nabla} + \mathbf{v}_i\cdot\boldsymbol{\nabla}\right)\nabla^2\Phi + n_{i0}\partial_\parallel v_{i\parallel} = 0\end{aligned} \tag{3.6}$$

where $\Phi = e\phi/T_e$, $\rho_s = c_s/\omega_{ci}$, $c_s = (T_e/m_i)^{1/2}$ and $D_e = cT_e/eB_0$. The ion parallel dynamics is described as,

$$\left(\partial_t + \mathbf{v}_{i0}\cdot\boldsymbol{\nabla} + \mathbf{v}_i\cdot\boldsymbol{\nabla}\right) v_{i\parallel} + \left(\mathbf{v}_i\cdot\boldsymbol{\nabla}\right) v_{i0} = -c_s^2\partial_\parallel\Phi \tag{3.7}$$

Let us assume that the electrons obey the κ-type distribution. By integrating the distribution function given by Eq. (1.17) over the velocity space [58], we obtain,

$$n_e = n_{e0}\left(1 - \frac{e\phi}{T_e\left(\kappa - 3/2\right)}\right)^{-(\kappa-1/2)} \tag{3.8}$$

where the parameter κ measures the deviation from thermal equilibrium and T_e is the electron temperature for the corresponding Maxwellian plasma. It is important to

mention here that the series expansion of Eq. (3.8) for small electrostatic perturbation $e\phi < T_e$, is valid only for $\kappa \gtrsim 3$, because for smaller values of the parameter κ i.e., for $\kappa < 3$, higher order terms are comparable with lower order, and, therefore such terms can not be neglected [99]. Also, in the limit $\kappa \to \infty$, the Maxwellian distribution is recovered.

3.2 Dispersion Relation for Coupled Drift and Acoustic Modes

Linearizing the set of equations (3.6)-(3.8), we obtain respectively,

$$\left(\partial_t + \mathbf{v}_{i0}\cdot\boldsymbol{\nabla}\right) n_i - n_{i0} D_e \left(\frac{d\ln n_{i0}}{dx} - \frac{d\ln B_0}{dx}\right)\partial_\perp \Phi - n_{i0}\rho_s^2 \left(\partial_t + \mathbf{v}_{i0}\cdot\boldsymbol{\nabla}\right)\nabla^2\Phi + n_{i0}\partial_\parallel v_{i\parallel} = 0 \tag{3.9}$$

$$\left(\partial_t + \mathbf{v}_{i0}\cdot\boldsymbol{\nabla}\right) v_{i\parallel} = -c_s^2\partial_\parallel \Phi + \frac{c_s^2}{\omega_{ci}}\frac{dv_{i0}}{dx}\partial_\perp \Phi \tag{3.10}$$

and,

$$n_e = n_{e0}\left(\frac{\kappa - 1/2}{\kappa - 3/2}\right)\Phi \tag{3.11}$$

Let us operate $(\partial_t + \mathbf{v}_{i0}\cdot\boldsymbol{\nabla})$ on (3.9) and use equations (3.10, 3.11) with quasineutrality condition in perturbed state $n_i \approx n_e$ (not violating the equilibrium state $n_{i0}(x) = n_{e0}(x) + Z_d n_{d0}(x)$ and Eq. (3.2) which is essential for non-zero current) to obtain,

$$\left(\partial_t + \mathbf{v}_{i0}\cdot\boldsymbol{\nabla}\right)^2 \left[\left(\frac{\kappa - 1/2}{\kappa - 3/2}\right) n_{e0}\Phi - n_{i0}\rho_s^2\nabla^2\Phi\right] -$$
$$n_{i0} D_e \left(\frac{d\ln n_{i0}}{dx} - \frac{d\ln B_0}{dx}\right)\left(\partial_t + \mathbf{v}_{i0}\cdot\boldsymbol{\nabla}\right)\partial_\perp\Phi + n_{i0}c_s^2\partial_\parallel\left(-\partial_\parallel\Phi + A\partial_\perp\Phi\right) = 0 \tag{3.12}$$

where $A = (1/\omega_{ci})\,|dv_{i0}/dx|$. Let us Fourier transform (3.12) by assuming perturbations to be of the form $\sim \exp(-i\omega t + i\mathbf{k}_\perp\cdot\mathbf{r}_\perp + i\mathbf{k}_\parallel\cdot\mathbf{r}_\parallel)$ which gives the linear dispersion relation as,

$$\Omega_0^2\left[\left(\frac{\kappa - 1/2}{\kappa - 3/2}\right)\frac{n_{e0}}{n_{i0}} + \rho_s^2 k_\perp^2\right] - \left(\omega_{ni}^* + \omega_B^*\right)\Omega_0 - c_s^2 k_\parallel^2\left(1 - \frac{k_\perp}{k_\parallel}A\right) = 0 \tag{3.13}$$

where $\Omega_0 = \left(\omega - v_{i0}k_\parallel\right)$, $\omega^*_{ni} = -D_e k_\perp \left(d\ln n_{i0}/dx\right)$ and $\omega^*_B = D_e k_\perp \left(d\ln B_0/dx\right)$. Equation (3.13) is the dispersion relation for the coupled dispersive waves in an inhomogeneous plasma with stationary dust and Kappa distributed electrons. In the limit $\kappa \to \infty$, Eq. (3.13) reduces to Eq. (16) of Ref. [28]. For a homogeneous density plasma ω^*_{ni} vanishes, and (3.13) becomes,

$$\Omega_0^2\left[\left(\frac{\kappa-1/2}{\kappa-3/2}\right)\frac{n_{e0}}{n_{i0}} + \rho_s^2 k_\perp^2\right] - \omega^*_B\Omega_0 - c_s^2 k_\parallel^2\left(1 - \frac{k_\perp}{k_\parallel}A\right) = 0 \tag{3.14}$$

It is important to clarify here that for $n_{d0} = 0$, the equilibrium condition becomes $n_{i0}(x) = n_{e0}(x)$, as a result the background current, $\mathbf{J}_0 = e\left(n_{i0} - n_{e0}\right)v_0\left(x\right)\hat{\mathbf{z}}$ becomes zero. Hence the corresponding shear in the magnetic field vanishes, satisfying the Ampere's law. Thus the new drift mode ω^*_B disappears, because of $J_0 = 0$ (or $dB_0/dx = 0$) and the relation (3.13) becomes,

$$\Omega_0^2\left[\left(\frac{\kappa-1/2}{\kappa-3/2}\right) + \rho_s^2 k_\perp^2\right] - \omega^*_{ni}\Omega_0 - c_s^2 k_\parallel^2\left(1 - \frac{k_\perp}{k_\parallel}A\right) = 0 \tag{3.15}$$

which for a homogeneous density plasma $\omega^*_{ni} = 0$ yields modified D'Angelo's instability,

$$\Omega_0^2 = \frac{c_s^2 k_\parallel^2}{\left\{\left(\frac{\kappa-1/2}{\kappa-3/2}\right) + \rho_s^2 k_\perp^2\right\}}\left(1 - \frac{k_\perp}{k_\parallel}A\right) \tag{3.16}$$

for $k_\parallel/k_\perp < A$. The roots of Eq. (3.13) are,

$$\Omega_{0_{1,2}} = \frac{\omega^*_{ni} + \omega^*_B}{2\left(\frac{\kappa-1/2}{\kappa-3/2}\right)Q} \pm \frac{1}{2\left(\frac{\kappa-1/2}{\kappa-3/2}\right)Q}\left[\left(\omega^*_{ni} + \omega^*_B\right)^2 + 4\left(\frac{\kappa-1/2}{\kappa-3/2}\right)Qc_s^2k_\parallel^2\left(1 - \frac{k_\perp}{k_\parallel}A\right)\right]^{1/2} \tag{3.17}$$

where,

$$Q = \frac{n_{e0}}{n_{i0}} + \frac{\rho_s^2 k_\perp^2\left(\kappa - 3/2\right)}{\left(\kappa - 1/2\right)}$$

For $k_\parallel/k_\perp < A$, (3.17) gives an instability if following condition is satisfied,

$$\left(\omega^*_{ni} + \omega^*_B\right)^2 < 4\left(\frac{\kappa-1/2}{\kappa-3/2}\right)Qc_s^2k_\parallel^2\left|1 - \frac{k_\perp}{k_\parallel}A\right| \tag{3.18}$$

along with $k_\parallel/k_\perp < A$. For illustration, we choose the plasma parameters of the Saturn's rings at a radial distance 6.03×10^9cm [100] as $n_{e0} = 10^3\text{cm}^{-3}$, $n_{d0} = 10$

cm^{-3}, $Z_d = 3 \times 10^2$, $T_i = 10$ eV, $T_e = 10T_i$, $B_0 = 0.01$ G and $m_d = 1 \times 10^{-16}$ g, which gives $v_{Ti} = 3 \times 10^6$ cm/s, $\omega_{ci} = 95$ rad/s, and $\rho_s = 1 \times 10^5$ cm. Assuming $\omega = \omega_r \pm i\omega_i$, we plot the linear dispersion relations, Eq. (3.14) in Fig. (3-1), Eq. (3.13) in Figs. (3-2, 3-3) and Eq. (3.16) in Fig. (3-4) respectively, keeping in view that $\rho_s^2 k_\perp^2 < 1$ and $\partial_t << \omega_{ci}$ must remain valid to avoid Landau damping effects which require kinetic treatment and to remain in drift approximation. We choose $\kappa_n, \kappa_B < k_\perp$ so that the local approximation $\lambda_\perp = 2\pi/k_\perp << L_n = 1/\ \kappa_n$ also remains applicable.

3.3 Nonlinear Analysis

Equations (3.6), (3.7) and (3.8) are the set of nonlinear equations of the present dynamical plasma model. In order to find the nonlinear stationary solution, we have to transform these equations into moving frame (x, ξ) such that $\xi = r_\perp + \alpha r_\parallel - ut$, where u is the constant velocity of the moving frame and α is a constant angle of wavefront normal with $r_\parallel$-axis. In this new reference frame, Φ and $v_{i\parallel}$ are functions of x and ξ only and $\nabla_\perp \equiv (\partial_x, \partial_\xi)$. In order to elaborate the importance of shear flow we characterize it into two categories; weak and strong shear flows in comparison with $\mathbf{E} \times \mathbf{B}_0$ drift. Thus we will divide this section into two following subsections.

3.3.1 Weak Shear Limit

First we consider the case of weak shear flow by assuming $\mathbf{v}_E \cdot \boldsymbol{\nabla} >> \mathbf{v}_{i0} \cdot \boldsymbol{\nabla}_\parallel$, $\mathbf{v}_E \cdot \boldsymbol{\nabla} >> v_{i\parallel}\partial_\parallel$ and expand the kappa distributed electrons density expression (3.8) for small electrostatic perturbation $e\phi < T_e\,(\kappa - 3/2)$. Then Eq. (3.6) becomes,

$$d_t \left[a_1 - \rho_s^2 \nabla_\perp^2\right] \Phi + (v_{dn} + v_{dB})\, \partial_\perp \Phi + \partial_\parallel v_{i\parallel} = 0 \tag{3.19}$$

where,

$$a_1 = \frac{n_{e0}}{n_{i0}} \left[\frac{\kappa - 1/2}{\kappa - 3/2}\right]$$

here $d_t = (\partial_t + \mathbf{v}_E \cdot \boldsymbol{\nabla})$, $v_{dn} = -D_e\,(d\ln n_{i0}/dx)$, $v_{dB} = D_e\,(d\ln B_0/dx)$. Nonlinear ion parallel Eq. (3.7) can be written as,

$$d_t v_{i\parallel} = -c_s^2 \partial_\parallel \Phi + \frac{c_s^2}{\omega_{ci}} \frac{dv_{i0}}{dx} \partial_\perp \Phi \tag{3.20}$$

Equation (3.20) in the moving frame becomes,

$$\left[\partial_\xi - \frac{c_s^2}{u\omega_{ci}} \left(\partial_x \Phi \partial_\xi - \partial_\xi \Phi \partial_x\right)\right] v_{i\parallel} - \frac{\alpha c_s^2}{u} \partial_\xi \Phi + \frac{c_s^2}{u\omega_{ci}} \frac{dv_{i0}}{dx} \partial_\xi \Phi = 0 \tag{3.21}$$

A possible solution of Eq. (3.21) is,

$$v_{i\parallel} = \frac{c_s^2}{u} \left(\alpha - A\right) \Phi \tag{3.22}$$

where the quantity A is defined earlier in Eq. (3.12). Similarly Eq. (3.19) in (x, ξ)-frame can be expressed as,

$$\left[\partial_\xi - \frac{c_s^2}{u\omega_{ci}} \left(\partial_x \Phi \partial_\xi - \partial_\xi \Phi \partial_x\right)\right] \left(a_1 - \rho_s^2 \nabla_\perp^2 \Phi\right) - \frac{(v_{dn} + v_{dB})}{u} \partial_\xi \Phi - \frac{\alpha}{u} \partial_\xi v_{i\parallel} = 0 \tag{3.23}$$

Using (3.22) in (3.23), we obtain,

$$\left[\partial_\xi - \frac{c_s^2}{u\omega_{ci}} \left(\partial_x \Phi \partial_\xi - \partial_\xi \Phi \partial_x\right)\right] \left(\nabla_\perp^2 \Phi - F_1 \Phi\right) = 0 \tag{3.24}$$

where,

$$F_1 = \frac{1}{\rho_s^2} \left[a_1 - \frac{v_{dn} + v_{dB}}{u} - \frac{\alpha c_s^2 \left(\alpha - A\right)}{u^2}\right] \tag{3.25}$$

The solution of (3.24) can be written as,

$$\nabla_\perp^2 \Phi - F_1 \Phi = f_0 \left(\Phi - \frac{u\omega_{ci}}{c_s^2} x\right) \tag{3.26}$$

where the function f_0 can have any functional form. Following Ref. [44], we consider it as piecewise linear function such that,

$$f_0(\Phi - \frac{u\omega_{ci}}{c_s^2} x) = G_0(\Phi - \frac{u\omega_{ci}}{c_s^2} x) \tag{3.27}$$

where G_0 will have two different values in two regions. Thus Eq. (3.26) becomes,

$$\nabla_{\perp}^2 \Phi - F_1 \Phi = G_0 \left(\Phi - \frac{u\omega_{ci}}{c_s^2} x \right) \tag{3.28}$$

The vortex solution of (3.28) will be obtained after transforming it into polar coordinates (r, θ) by substituting $x = r\cos\theta$ and $\xi = r\sin\theta$, where $r = \left(x^2 + \xi^2\right)^{1/2}$ and $\theta = \arctan\left(\xi/x\right)$. Next we divide the (r, θ) plane into inner region $(r < r_0)$ and outer region $(r > r_0)$ of an arbitrary circle of radius r_0. For bounded solution, in the outer region, we assume $G_0 = 0$, so the solution of (3.28) for the this region $r > r_0$ becomes,

$$\Phi^{out}\left(r, \theta\right) = Q^{out} K_1\left(\lambda_1 r\right)\cos\theta \tag{3.29}$$

where $F_1 = \lambda_1^2$, Q^{out} is a constant and K_1 is the first order modified Bessel function of the second kind. For bounded and localized solutions, we require $\lambda_1 > 0$. The inner solution for $r < r_0$ is given by,

$$\Phi^{in}\left(r, \theta\right) = \left[Q^{in} J_1\left(\lambda_2 r\right) + \frac{u\omega_{ci}\left(\lambda_1^2 + \lambda_2^2\right)}{c_s^2 \lambda_2^2} r \right] \cos\theta \tag{3.30}$$

where $\lambda_1^2 + G_0 = -\lambda_2^2$, J_1 is the first order ordinary Bessel function of the first kind and Q^{in} and λ_2 are constants. The constants Q^{in} and Q^{out} are determined from the continuity of the solution at the boundary of the two regions $r = r_0$ in the following form,

$$Q^{in} = -\frac{u\omega_{ci}\lambda_1^2 r_0}{c_s^2 \lambda_2^2 J_1\left(\lambda_2 r_0\right)} \tag{3.31}$$

$$Q^{out} = \frac{u\omega_{ci} r_0}{c_s^2 K_1\left(\lambda_1 r_0\right)} \tag{3.32}$$

Note that λ_1 is known in terms of plasma parameters and λ_2 is related with λ_1 through (3.33). Then Q^{in} and Q^{out} become related through Eqs. (3.31) and (3.32) in terms of plasma parameters. The continuity condition of $\nabla_{\perp}\Phi$ at $r = r_0$ gives a relation between λ_1 and λ_2 as follows,

$$\frac{K_2\left(\lambda_1 r_0\right)}{\lambda_1 K_1\left(\lambda_1 r_0\right)} = -\frac{J_2\left(\lambda_2 r_0\right)}{\lambda_2 J_1\left(\lambda_2 r_0\right)} \tag{3.33}$$

The typical dipolar vortex solution from Eqs. (3.29) and (3.30) is drawn in Fig. (3-5) for data given in the linear section assuming $\omega_{ni}^{*} \neq 0$ and $\omega_{B}^{*} \neq 0$ whereas the constants are evaluated as $Q^{in} = 0.98$, $Q^{out} = 1.23$ and $\lambda_2 = 3.95$. The vortices are formed on ρ_s spatial scale and speed is evaluated form the data about as $u = 0.48 \times 10^6$ cm/sec.

It is worth mentioning here that these nonlinear structures (vortices) are different form the previous investigation. Firstly, these vortices can survive even if we ignore the density inhomogeneity and the acoustic wave. The reason is the presence of magnetic field shear due to equilibrium flow driven mode, which we call the new drift mode proposed in Refs. [27, 28]. Secondly the inclusion of the kappa factor due to high energy particles changes the behavior of the dipolar vortices. For bounded solution $F_1 > 1$ is required which modifies the speed limit of proposed vortices. Thirdly, the amplitude of these vortices will also be effected by the inclusion of the kappa factor. For demonstration the variation of the amplitude of Φ with x assuming $\xi \rightarrow 0$ is drawn in Fig. (3-6) for $\kappa = 3$ (dotted curve) and $\kappa = \infty$ (solid curve) corresponding to Boltzmann density distribution for electrons, which clearly shows that the amplitude is modified due to the superthermal electrons effect.

3.3.2 Strong Shear Limit

In this subsection, we will present the possible stationary vortex solutions assuming that $\mathbf{v}_E \cdot \boldsymbol{\nabla}$ and $\mathbf{v}_{i0} \cdot \boldsymbol{\nabla}_{\parallel}$ are the terms of the same order of magnitude i.e., the strong shear case. Then Eq. (3.7) becomes,

$$\left[\partial_\xi - \frac{\alpha v_{i0}}{u}\partial_\xi - \frac{c_s^2}{u\omega_{ci}}\left(\partial_x \Phi \partial_\xi - \partial_\xi \Phi \partial_x\right)\right]\left[v_{i\parallel} - \left(\alpha\omega_{ci}x - v_{i0}\right)\right] = 0 \tag{3.34}$$

The general solution of Eq. (3.34) can be written as,

$$v_{i\parallel} - \left(\alpha\omega_{ci}x - v_{i0}\right) = f_1\left(\Phi - \frac{u\omega_{ci}}{c_s^2}x + \frac{\alpha\omega_{ci}}{c_s^2}\psi_0\left(x\right)\right) \tag{3.35}$$

where f_1 is some arbitrary function of its argument and $\psi_0(x)$ is defined as $v_{i0} = d\psi_0/dx$. We choose f_1 for simplicity as a piecewise linear function of its argument and

write Eq. (3.35) as,

$$v_{i\|} - (\alpha\omega_{ci}x - v_{i0}) = C_1\left(\Phi - \frac{u\omega_{ci}}{c_s^2}x + \frac{\alpha\omega_{ci}}{c_s^2}\psi_0(x)\right) \tag{3.36}$$

Using Eq. (3.36), we eliminate $v_{i\|}$ from Eq. (3.6) and write it in the new frame as,

$$\left[\partial_\xi - \frac{\alpha v_{i0}}{u}\partial_\xi - \frac{c_s^2}{u\omega_{ci}}\left(\partial_x\Phi\partial_\xi - \partial_\xi\Phi\partial_x\right)\right] \times \left[\left\{a_1 - \rho_s^2\nabla_\perp^2\right\}\Phi - \frac{\alpha C_1\omega_{ci}\sigma}{c_s^2}x\right] = 0 \tag{3.37}$$

where,

$$\sigma = 1 + \frac{v_{dn} + v_{dB}}{\alpha C_1}$$

The solution of Eq. (3.37) can be written as,

$$\left\{a_1 - \rho_s^2\nabla_\perp^2\right\}\Phi - \frac{\alpha C_1\omega_{ci}\sigma}{c_s^2}x = f_2\left(\Phi - \frac{u\omega_{ci}}{c_s^2}x + \frac{\alpha\omega_{ci}}{c_s^2}\psi_0(x)\right) \tag{3.38}$$

We assume $v_{i0} = ax + b$, where a and b are constants and,

$$f_2(\eta) = C_0 + C_2(\eta)$$

Here η is the argument of the function and C_0, C_2 are constants and will have different values in two regions. Then equation (3.38) becomes,

$$\left\{a_1 - \rho_s^2\nabla_\perp^2\right\}\Phi - C_2\Phi - F_2x + 2F_3x^2 - C_0 = 0 \tag{3.39}$$

where we have also assumed,

$$\frac{\alpha\omega_{ci}\psi_0 - u\omega_{ci}x}{c_s^2} = \kappa_1 x^2$$

$$F_2 = \frac{\omega_{ci}\left[\alpha C_1\sigma - C_2u + C_2\alpha b\right]}{c_s^2}$$

and,

$$F_3 = -\frac{\omega_{ci}C_2\alpha a}{4c_s^2}$$

Equation (3.39) contains both x and x^2 terms which makes it difficult to be solved analytically. Under the condition $F_2 = 0$, Eq. (3.39) reduces to,

$$\nabla_{\perp}^2 \Phi - \frac{1}{\rho_s^2} \{a_1 - C_2\} \Phi - \frac{2F_3}{\rho_s^2} x^2 - \frac{C_0}{\rho_s^2} = 0 \tag{3.40}$$

In order to find out the solution of (3.40) we use similar procedure as in the case of dipolar vortices i.e., transferring it into polar coordinates as $x = r\cos\theta$, $\xi = r\sin\theta$, $x^2 = r^2(1 - \cos 2\theta)/2$. This will give us higher order vortices. The outer solution for $r > r_0$ becomes,

$$\Phi^{out}(r, \theta) = A_0 K_0(\lambda_3 r) + A_2 K_2(\lambda_3 r)\cos 2\theta \tag{3.41}$$

where K_0 and K_2 are modified Bessel functions of zeroth and second order, respectively. The inner solution for $r < r_0$ is given by,

$$\Phi^{in}(r, \theta) = Q_0 J_0(\lambda_4 r) - A\frac{r^2}{2} - Q + \left(Q_2 K_2(\lambda_4 r) - A\frac{r^2}{2}\right)\cos 2\theta \tag{3.42}$$

where $A = F_3/\lambda_4^2$, $Q = 2(A - C_{0,in}/\lambda_4^2)$, $\lambda_3^2 = a_1$ and constants $C_{0,out}$, $C_{2,out}$ have been assumed to be zero. This solution contains the monopolar and quadrupolar parts. The monopolar part can superimpose on the quadrupolar parts and in resultant give us the tripolar type vortices. The arbitrary constants A_0, A_2, Q_0, Q_2 and λ_4 will be found from the continuity of Φ, $\partial_r\Phi$ and $\nabla^2\Phi$ at the boundary of the circle $r = r_0$. For arbitrary choices of free parameters $C_{2,in}\kappa_1 = 3.5$, $r_0 = 2.6, C_{0,in} = -1.9, C_{0,out} = 0$, the constants have the values $\kappa = 3.0$, $\lambda_3 = 1.64$, $A = 1.6$, $Q = -7.0$, $A_0 = 26.8$, $Q_0 = -817.02$, $A_2 = -11.75$, $Q_2 = -276.1$ and $\lambda_4 = 2.18$, which has been calculated from the 1st zero of the Bessel function $J_2(\lambda_4 r_0)$ of the nonlinear relation,

$$\lambda_3 K_3(\lambda_3 r_0) J_2(\lambda_4 r_0) + \lambda_2 K_2(\lambda_3 r_0) J_3(\lambda_4 r_0) = 0$$

For illustration, we apply it to the Saturn's rings data given above and typical tripolar vortices are shown in Fig. (3-7), where space is normalized with gyroradius ρ_s. It is important to mention here that the behavior of the tripolar vortices will also depend upon the new drift type mode and kappa factor which makes it different from structures studied previously.

3.4 Summary

The low frequency current-driven electrostatic wave in a plasma having sheared flow of electrons and ions parallel to external magnetic field in the presence of stationary dust has been investigated using kappa distribution for electrons and the effects of steeper gradient of sheared flow on the nonlinear dynamics have been pointed out. This is a drift wave like mode which has been recently [27,28] proposed to be the normal mode of dusty plasmas and it can exist even if the density of the plasma is homogeneous. It has also been shown that the D'Angelo's purely growing instability is modified due to the presence of suprathermal electrons in the plasma.

In Fig. (3-1), the dispersion relation (3.14) of new stable current-driven electrostatic wave is plotted corresponding to two different limits. In Figs. (3-2) and (3-3), the real and imaginary frequencies of dispersion relation of the coupled modes of Eq. (3.13) are plotted. The instability criteria requires to satisfy the condition (3.18) along with $k_{\parallel}/k_{\perp} < A$. In Fig. (3-4), the effects of kappa distributed electrons on D'Angelo's instability in the absence of stationary dust are shown. In this case $J_0 = 0$ and $\omega_B^* = 0$. The dipolar vortex solution of nonlinear Eq. (3.28) is plotted in Fig. (3-5) in (x, ξ) plane and the variation of the electrostatic amplitude with x for $\xi = 0$ is shown in Fig. (3-6) for plasma parameters used in Fig. (3-2). In case of steeper gradient of sheared flow of electrons and ions, the nonlinear equation (3.40) gives tripolar vortex solution under certain condition as shown in Fig. (3-7).

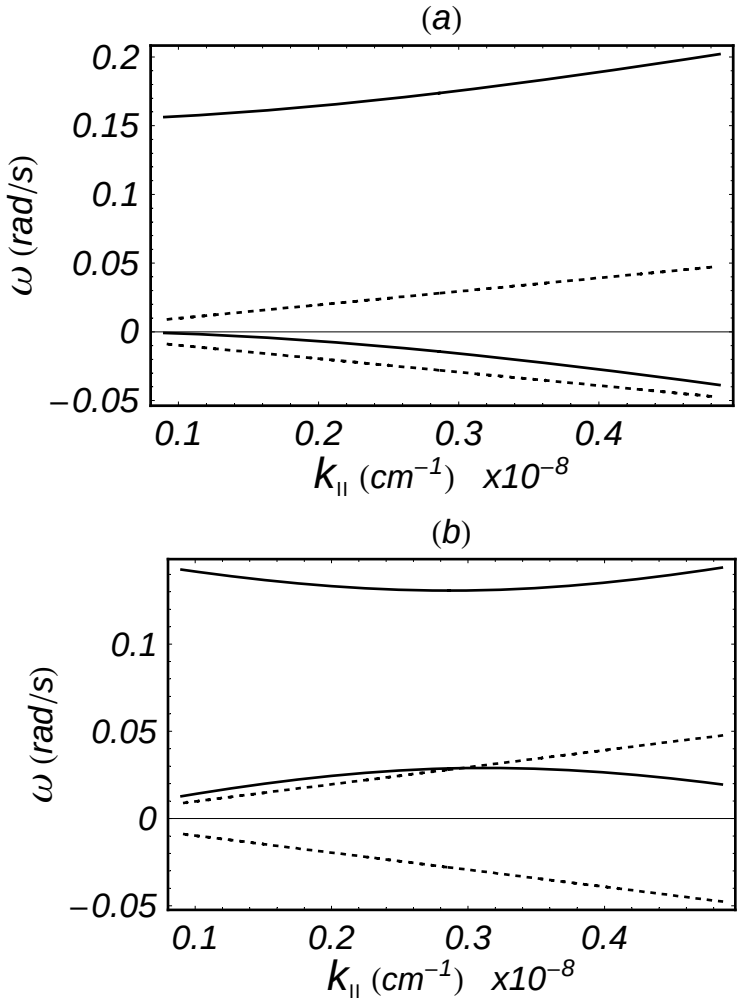

Figure 3-1: Real Frequency [Eq. (3.14)] is plotted against the parallel wave number $k_{\|}$ for the homogeneous density plasma (a) for $k_{\|}/k_{\perp} > A$ while $A = 6 \times 10^{-5}$ and (b) for $k_{\|}/k_{\perp} < A$ while $A = 6 \times 10^{-3}$. The other parameters are $\rho_s = 10^5$ cm, $k_{\perp} = 1 \times 10^{-6}$ cm^{-1}, $k_{\|} = 9 \times 10^{-4} k_{\perp}$, $k_B = k_{\perp}/25$ and $\kappa = \infty$. The perturbation remains stable corresponding to these parameters.

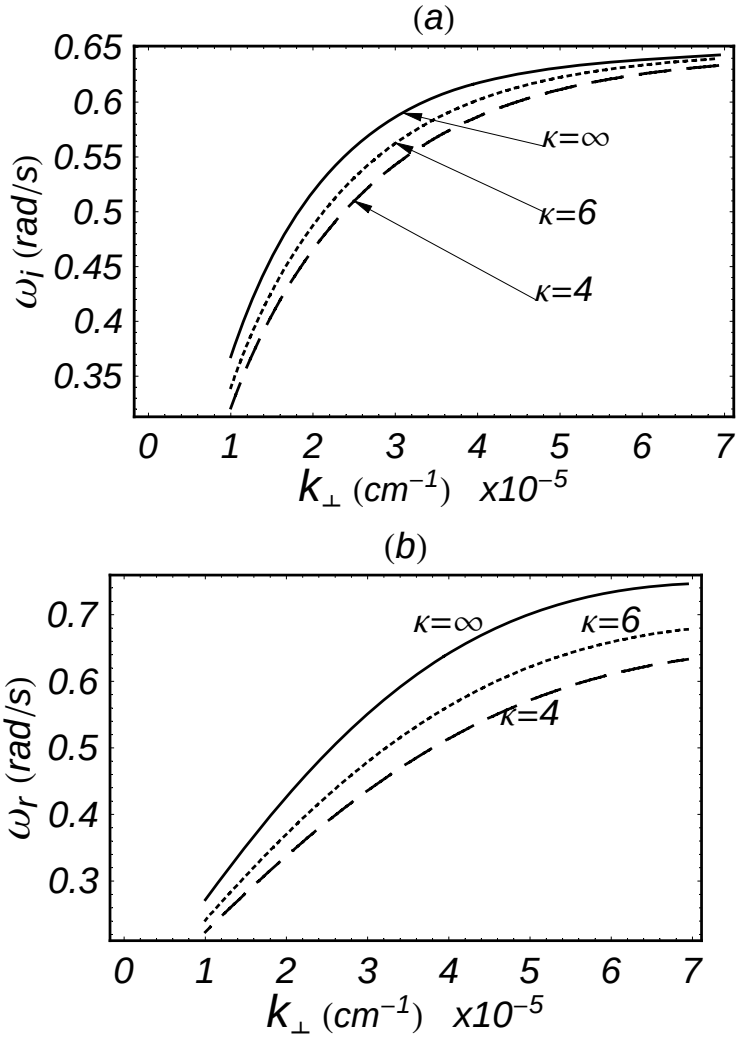

Figure 3-2: (a) Imaginary and (b) real, parts of the frequencies [Eq. (3.13)] are plotted against the perpendicular wave number $k_\perp$ for varying spectral index κ, taking $\rho_s = 10^4$ cm, $k_\perp = 10^{-5}$ cm^{-1}, $k_\parallel = 10^{-3}k_\perp$, $k_B = k_n = 0.1k_\perp$ and $A = 0.007$.

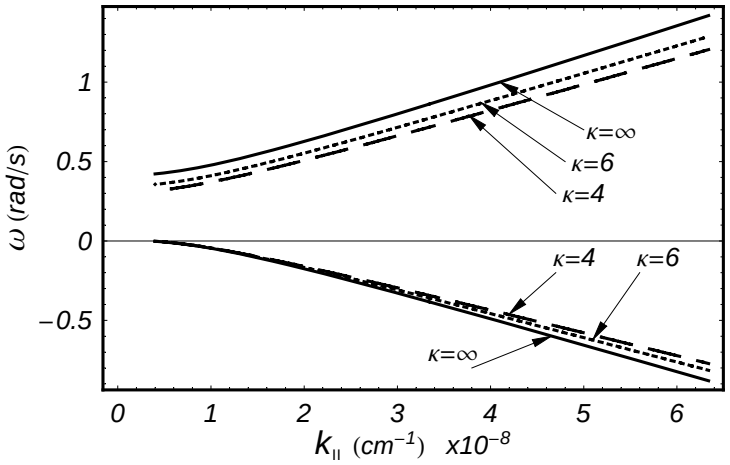

Figure 3-3: Frequency [Eq. (3.13)] is plotted for stable perturbation against the parallel wave number $k_{\|}$ for varying spectral index κ, taking $\rho_s = 10^5$ cm, $k_\perp = 2\times10^{-6}$ cm^{-1}, $k_{\|} = 2 \times 10^{-3} k_\perp$, $k_B = k_n = k_\perp/60$ and $A = 0.001$.

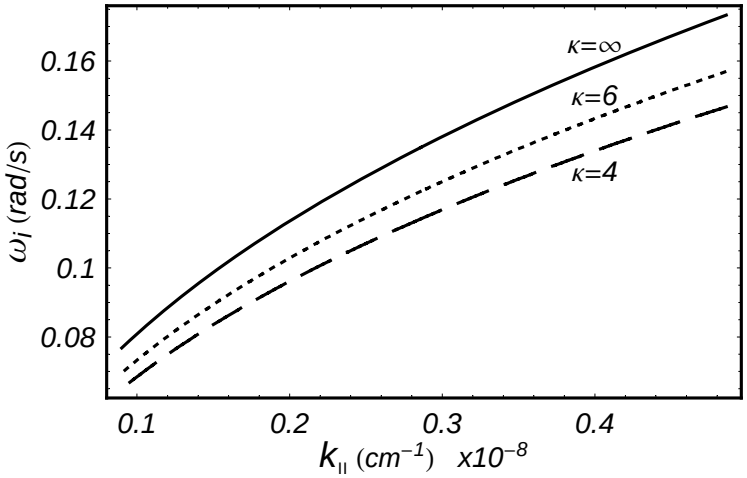

Figure 3-4: Doppler shifted growth rate ω_i [Eq. (3.16)] is plotted against the parallel wave number $k_{\|}$ for different values of κ, taking $A = 0.07$, $\rho_s = 10^5$ cm, $k_\perp = 1 \times 10^{-6}$ cm^{-1} and $k_{\|} = 9 \times 10^{-4} k_\perp$.

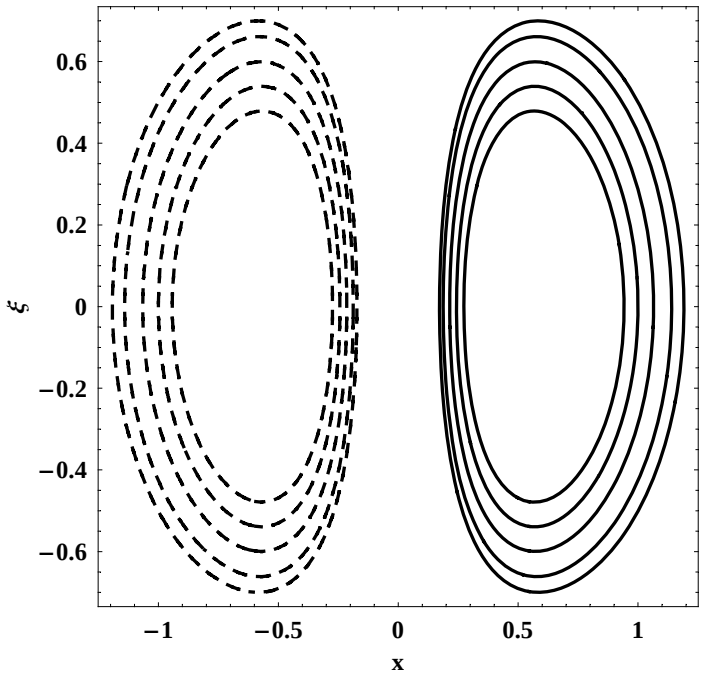

Figure 3-5: Contour plot of dipolar vortices is shown corresponding to the parameters of Fig. (3-2).

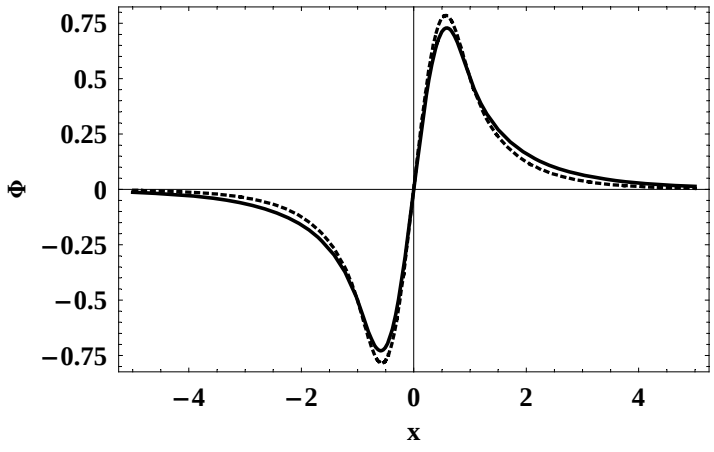

Figure 3-6: Variation of amplitude of vortices with x assuming $\xi \to 0$ corresponding to Fig. (3-5) for different values of κ. Dotted curve is for $\kappa = 3$, while solid curve is for $\kappa = \infty$.

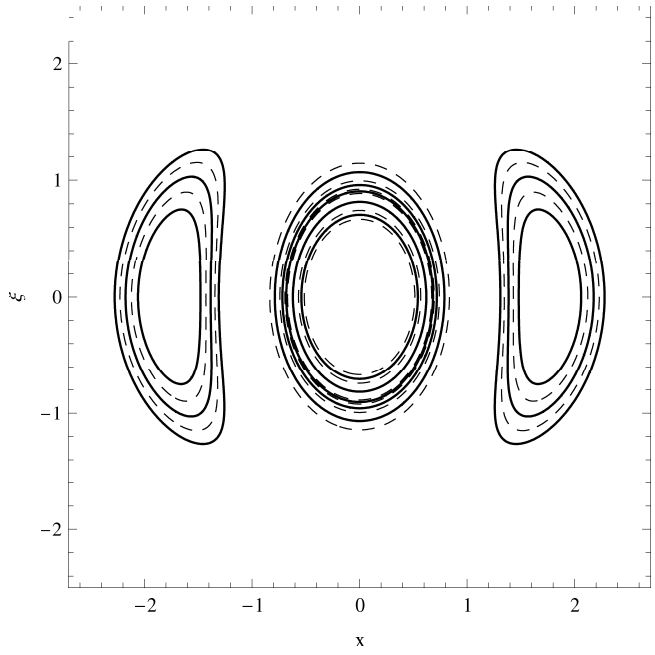

Figure 3-7: Contour plot of tripolar vortices of Eqs. (3.41, 3.42) is shown in the case of steeper gradient of sheared flow corresponding to the parameters of Fig. (3-2).

Chapter 4

Current-Driven Dust Waves

A few years ago [27,28] it has been proposed that the sheared flow of electrons and ions along the initial constant magnetic field in the presence of stationary dust can introduce low frequency electrostatic drift-type waves and instabilities even if the plasma density is homogeneous. The dynamics of cold ions has been considered while the electrons are treated to be inertia-less. It is assumed that the local steady state has been attained by the system with the same sheared flow of electrons and ions $\mathbf{v}_{e0} = \mathbf{v}_{i0} = v_0(x)\hat{\mathbf{z}}$ along the initial constant magnetic field $\mathbf{B}_0 = B_0\hat{\mathbf{z}}$. Due to the quasi-neutrality $n_{i0} - n_{e0} = Z_d n_{d0}$ a zero order current along z-axis is produced which twists the initial field and the total magnetic field $\mathbf{B}_0$ becomes sheared. The magnetic field gradient plays a similar role for producing this wave which the density gradient plays in the dynamics of usual drift wave. Such a wave can appear in electron-ion plasma as well if the magnitudes of the sheared flow velocities of electrons and ions are different.

Here, we suggest that the drift-wave like electrostatic perturbation can also take place at temporal and spatial scales of dust species if we consider their dynamics assuming electrons and ions to follow the Boltzmann density distributions. An unstable mode analogous to D'Angelo's mode may also appear if the effect of smaller flow velocity of dust fluid is taken into account.

The zero-order current can give rise to several kinds of waves and instabilities in dusty plasmas. The nonlinear dynamics of these current driven waves have also been considered by several authors [28, 67]. A great deal of literature exists on dust waves [101, 102]. We will, here, focus on the low frequency waves at dust time scales

due to nonzero equilibrium current.

The well-known electrostatic drift wave in electron-ion plasma was discovered long ago [34, 75, 78–80]. It has been shown that the current-driven low frequency wave [27] can couple with the usual drift wave if density gradient is taken into account. Both types of drift waves can become unstable due to sheared flow of electrons and ions. If the parallel propagation is ignored, then the dispersion relation gives two flute-like modes; one has been studied by Shukla and Varma [86] which exists due to density inhomogeneity and the other has been proposed by Saleem [27, 28] which exists due to the sheared current in the plasma. These waves exist at ion time scales with frequencies $\omega < \omega_{ci}$ and their perpendicular length scale is $k_\perp^{-1}$ where $\rho_s \leq k_\perp^{-1}$. The dust has been assumed to be stationary in these investigations.

A large number of very low frequency waves exist in dusty plasmas because dust particles are very heavy compared to ions. For example dust acoustic [103] and dust drift [104] waves are the low frequency modes of such plasmas.

In this chapter, we present several current-driven waves and instabilities which can take place if the dust dynamics is taken into account and both electrons and ions are assumed to be inertia-less. The nonlinear dynamics of these low frequency waves is also investigated. First the model is described and nonlinear equations are derived. Then the linear dispersion relation and its different limits are obtained. Moreover, the solutions of the nonlinear equations are obtained in the form of vortices and solitons. The results are applied to the boundary region of Saturn's dusty magnetosphere. Finally, the model and the results are summarized.

4.1 Theoretical Model

We consider a magnetized plasma consisting of electrons, ions and dust particles in the presence of original planetary constant magnetic field $\mathbf{B}_0 = B_0\hat{\mathbf{z}}$. The presence of the charged dust particles modify the equilibrium quasi-neutrality condition as given by Eq. (3.1). Due to the interaction of solar wind, the plasma can have a sheared flow and we assume it to be along the initial zero order magnetic field, $\mathbf{v}_{j0} = v_{j0}(x)\hat{\mathbf{z}}$ $(j = e, i, d)$ for simplicity. Two cases are discussed; in case a, it is assumed that $|v_{e0}| = |v_{i0}| = v_0(x)$, $v_{d0} = 0$ (dust is stationary) and in case b, it is assumed that

$v_{d0}(x) \neq 0$ but $|v_{d0}| < v_0$. The wave geometry indicating the sheared magnetic field due to the non-zero equilibrium current is shown in Fig. (2-1) and the inhomogeneous magnetic field is given by Eq. (2.1).

The dust dynamics is described by the equations of continuity,

$$\partial_t n_d + \boldsymbol{\nabla}_\perp \cdot (n_d \mathbf{v}_{d\perp}) + \partial_\parallel \left(n_d v_{d\parallel}\right) = 0 \tag{4.1}$$

and momentum,

$$(\partial_t + \mathbf{v}_d \cdot \boldsymbol{\nabla})\, \mathbf{v}_d = \frac{q_d}{m_d}(\mathbf{E} + \frac{1}{c}\mathbf{v}_d \times \mathbf{B}_0) \tag{4.2}$$

where m_d, n_d, $\mathbf{v}_d$, and q_d are, respectively, the mass, the number density, the fluid velocity, and the charge of the dust particles. For negatively charged dust particles, $q_d = -eZ_d$. The perpendicular velocity of cold dust fluid can be expressed as,

$$\mathbf{v}_{d\perp} \approx \frac{c}{B_0}\hat{\mathbf{e}}_\parallel \times \boldsymbol{\nabla}_\perp \phi + \frac{c}{B_0 \omega_{cd}} D_t \boldsymbol{\nabla}_\perp \phi = \mathbf{v}_E + \mathbf{v}_P \tag{4.3}$$

where $\omega_{cd} = Z_d e B_0 / m_d c$ is the dust cyclotron frequency and $D_t = (\partial_t + \mathbf{v}_{d0} \cdot \boldsymbol{\nabla} + \mathbf{v}_d \cdot \boldsymbol{\nabla})$. We consider only electrostatic waves for which we use $\mathbf{E} = -\boldsymbol{\nabla}\phi$, where ϕ is the electrostatic potential. The subscript naught (0) denotes the steady state quantities. Equation (4.1) can be expressed as,

$$D_t n_d + \mathbf{v}_E \cdot \boldsymbol{\nabla} n_{d0} + n_{d0} \boldsymbol{\nabla} \cdot \mathbf{v}_E + n_{d0} \boldsymbol{\nabla} \cdot \mathbf{v}_P + n_{d0} \partial_\parallel v_{d\parallel} = 0 \tag{4.4}$$

Using (4.3) in (4.4), we obtain,

$$D_t n_d - \frac{n_{d0} c}{B_0}\left(\frac{d \ln n_{d0}}{dx} - \frac{d \ln B_0}{dx}\right)\partial_\perp \phi + \frac{n_{d0} c}{B_0 \omega_{cd}} D_t \nabla_\perp^2 \phi + n_{d0} \partial_\parallel v_{d\parallel} = 0 \tag{4.5}$$

For parallel motion of dust particles, Eq. (4.2) gives,

$$D_t v_{d\parallel} = \frac{Z_d e}{m_d}\partial_\parallel \phi - (\mathbf{v}_d \cdot \boldsymbol{\nabla})\, \mathbf{v}_{d0} \tag{4.6}$$

For low frequency waves $\omega \ll k_\parallel v_{Te}, k_\parallel v_{Ti}$, the electrons and ions are assumed to obey

the Boltzmann distributions, respectively, as,

$$n_e = n_{e0}(x) \exp\left(\frac{e\phi}{T_e}\right) \tag{4.7}$$

$$n_i = n_{i0}(x) \exp\left(-\frac{e\phi}{T_i}\right) \tag{4.8}$$

where n_e, n_i, $T_e(x)$ and $T_i(x)$ are the electron and ion number densities and temperatures, respectively, and e is the magnitude of the electron charge. Assuming $e\phi < (T_e, T_i)$ and using (4.7) and (4.8) with the help of quasi-neutrality ($n_i = n_e + Z_d n_d$), we get,

$$n_d = -\frac{eZ_d n_{d0}}{T_{eff}}\phi \tag{4.9}$$

where $T_{eff} = Z_d^2 n_{d0}/\left(n_{i0}/T_i + n_{e0}/T_e\right)$. Using (4.9) in (4.5) we obtain,

$$D_t\phi + D_f\left(\frac{d\ln n_{d0}}{dx} - \frac{d\ln B_0}{dx}\right)\partial_\perp\phi - \rho_d^2 D_t \nabla_\perp^2\phi - \frac{T_{eff}}{Z_d e}\partial_\parallel v_{d\parallel} = 0 \tag{4.10}$$

where $D_f = cT_{eff}/Z_d eB_0$, $\rho_d = C_{DA}/\omega_{cd}$ and $C_{DA} = (T_{eff}/m_d)^{1/2}$ is the dust acoustic speed. Equations (4.6) and (4.10) are the coupled nonlinear differential equations for studying the low frequency electrostatic waves in a dusty plasma having zero-order current and density inhomogeneity. In deriving (4.6) and (4.10), the temperature of electrons and ions have been assumed to be constant.

4.2 Linear Analysis

We neglect the nonlinear terms in Eqs. (4.6) and (4.10) and use Fourier transform by assuming that the perturbed quantities are proportional to $\exp(-i\omega t + i\mathbf{k}_\perp\cdot\mathbf{r}_\perp + i\mathbf{k}_\parallel\cdot\mathbf{r}_\parallel)$. Then we obtain the local linear dispersion relation as,

$$\Omega_0^2\left(1+\rho_d^2 k_\perp^2\right) + \left(\omega_d^* + \omega_{Bd}^*\right)\Omega_0 - C_{DA}^2 k_\parallel^2\left(1 + A\frac{k_\perp}{k_\parallel}\right) = 0 \tag{4.11}$$

where $\Omega_0 = (\omega - \omega_0)$, $\omega_0 = v_{d0}k_\parallel$, $\omega_d^* = -D_f k_\perp\left(d\ln n_{d0}/dx\right)$, $\omega_{Bd}^* = D_f k_\perp\left(d\ln B_0/dx\right)$, $A = v_{d0}\kappa_{dv}/\omega_{cd}$ and $\kappa_{dv} = |d\ln v_{d0}/dx|$. If external current is neglected, then (4.11) reduces to equation (24) of Ref. [104], which is the coupled dispersion relation of dust

drift wave and dust acoustic wave. The dust drift mode is modified in (4.11) due to the sheared flow of the plasma species. The roots of (4.11) are,

$$(\Omega_0)_{1,2} = \frac{1}{2g_0}\left[-\left(\omega_d^* + \omega_{Bd}^*\right) \pm \left\{\left(\omega_d^* + \omega_{Bd}^*\right)^2 + 4g_0 C_{DA}^2 k_\parallel^2 \left(1 + A\frac{k_\perp}{k_\parallel}\right)\right\}^{\frac{1}{2}}\right] \quad (4.12)$$

where $g_0 = (1 + \rho_d^2 k_\perp^2)$. Equation (4.12) gives an instability for $A < 0$ if the following conditions are satisfied simultaneously,

$$\frac{k_\parallel}{k_\perp} < |A| \quad (4.13)$$

and

$$\left(\omega_d^* + \omega_{Bd}^*\right)^2 < 4g_0 C_{DA}^2 k_\parallel^2 \left|1 + A\frac{k_\perp}{k_\parallel}\right| \quad (4.14)$$

In the limit $v_{d0} \to 0$, (4.11) becomes,

$$\omega^2\left(1 + \rho_d^2 k_\perp^2\right) + \left(\omega_d^* + \omega_{Bd}^*\right)\omega - C_{DA}^2 k_\parallel^2 = 0 \quad (4.15)$$

which is the dispersion relation for stable drift modes. In the limit of a spatially uniform plasma the dust drift frequency ω_d^* which arises due to density gradient, vanishes, and we obtain from (4.15) the dispersion relation,

$$\omega^2\left(1 + \rho_d^2 k_\perp^2\right) + \omega_{Bd}^*\omega - C_{DA}^2 k_\parallel^2 = 0 \quad (4.16)$$

It may be noted here that this current-driven drift mode can exist in a homogeneous density plasma. Equation (4.16) describes the coupling between the current-driven dust and the usual dust acoustic wave.

If ω_d^* and ω_{Bd}^* are neglected, then (4.11) gives a purely growing instability,

$$\Omega_0^2 = \frac{C_{DA}^2 k_\parallel^2}{(1 + \rho_d^2 k_\perp^2)}\left(1 + A\frac{k_\perp}{k_\parallel}\right) \quad (4.17)$$

provided that $A < 0$ along with

$$\frac{k_\parallel}{k_\perp} < |A| \quad (4.18)$$

This is a dust time scale purely growing mode and has the structure similar to

D'Angelo's mode [19] which exists because of ion dynamics while the electrons obey Boltzmann density distribution. The purely growing dust instability can appear in a uniform density plasma if the current is small and $\omega^*_{Bd} \ll C_{DA}k_\parallel$ holds along with (4.18).

4.3 Nonlinear Analysis

4.3.1 Vortex Solutions

First we consider the nonlinear effects that arise through the convective part of the polarization drift in the equation of motion. Here, we look for a possible stationary solution of the nonlinear equations (4.6) and (4.10) in the form of vortices. Following a general procedure [44] we define a new frame (x, ξ), by choosing $\xi = r_\perp + \alpha r_\parallel - ut$, where u is the speed of the vortex and α is the angle of wavefront normal with $\hat{\mathbf{e}}_\parallel$-axis. In (x, ξ) frame, ϕ and $v_{d\parallel}$ are functions of x, ξ and $\nabla^2_\perp \phi = (\partial_{xx}\phi + \partial_{\xi\xi}\phi)$. Assuming, $|\partial_t + \mathbf{v}_E \cdot \boldsymbol{\nabla}| \gg \left|\mathbf{v}_{d0} \cdot \boldsymbol{\nabla} + v_{d\parallel}\partial_\parallel\right|$, we can write (4.6) in the (x, ξ) frame as,

$$\left[\partial_\xi - \frac{c}{uB_0}\left(\partial_x\phi\partial_\xi - \partial_\xi\phi\partial_x\right)\right] v_{d\parallel} + \frac{Z_d e\alpha}{um_d}\partial_\xi\phi + \frac{c}{uB_0}v'_{d0}\partial_\xi\phi = 0 \tag{4.19}$$

Equation (4.19) is satisfied for,

$$v_{d\parallel} = -\left(\frac{Z_d e\alpha}{um_d} + \frac{c}{uB_0}v'_{d0}\right)\phi \tag{4.20}$$

Equation (4.10) in (x, ξ) frame becomes,

$$\left[\partial_\xi - \frac{c}{uB_0}\left(\partial_x\phi\partial_\xi - \partial_\xi\phi\partial_x\right)\right]\left(\rho_d^2\nabla_\perp^2 - 1\right)\phi - \frac{(v_d + v_{Bd})}{u}\partial_\xi\phi - \frac{\alpha T_{eff}}{uZ_d e}\partial_\xi v_{d\parallel} = 0 \tag{4.21}$$

where $v_d = D_f(d\ln n_{d0}/dx)$ and $v_{Bd} = D_f(d\ln B_0/dx)$. Eliminating $v_{d\parallel}$ in (4.21) by using (4.20), we obtain,

$$\left[\partial_\xi - \frac{c}{uB_0}\left(\partial_x\phi\partial_\xi - \partial_\xi\phi\partial_x\right)\right]\left(\nabla_\perp^2\phi - F_1\phi\right) = 0 \tag{4.22}$$

where $F_1 = \left[1 + (v_d + v_{Bd})/u - \alpha C_{DA}^2 v_{d0}^{'}/\omega_{cd} u^2 - \alpha^2 C_{DA}^2/u^2\right]/\rho_d^2$. Equation (4.22) is satisfied by the ansatz,

$$\nabla_\perp^2 \phi = C_1 \phi + C_2 x \tag{4.23}$$

where C_1 and C_2 are constants related as $C_1 - F_1 + cC_2/uB_0 = 0$ through (4.22). The dipole vortex solution of (4.23) is obtained by following the standard method [44]. Accordingly, we transform (x, ξ) coordinates to polar coordinates (r, θ) by substituting $x = r\cos\theta$, $\xi = r\sin\theta$, where $r = \left(x^2 + \xi^2\right)^{1/2}$ and $\theta = \arctan(\xi/x)$. Then the (r, θ) plane is divided into an inner circular region $r < r_0$ and outer region $r > r_0$ corresponding to a typical vortex of size r_0. For bounded solution in the outer region, we must have $C_2 = 0$, and obtain the outer region solution of (4.23) as,

$$\phi^{out}(r, \theta) = Q^{out} K_1(\lambda_1 r)\cos\theta \tag{4.24}$$

where $\lambda_1^2 = F_1$, Q^{out} is a constant to be determined and K_1 is the first order modified Bessel function of the second kind. The Bessel equation requires $0 < \lambda_1^2$ that is $0 < F_1$ in the region $r_0 < r$. The inner region $(r < r_0)$ solution of (4.23) is given by,

$$\phi^{in}(r, \theta) = \left[Q^{in} J_1(\lambda_2 r) + \frac{C_2^{in}}{\lambda_2^2} r\right]\cos\theta \tag{4.25}$$

where $C_1^{in} = -\lambda_2^2$, $C_2^{in} = uB_0\left(\lambda_1^2 + \lambda_2^2\right)/c$ and Q^{in} are constants to be determined and J_1 is the first order ordinary Bessel function. The constants Q^{in}, Q^{out} and λ_2 are determined from the continuity of ϕ, $\nabla_\perp^2\phi$ and $\nabla_\perp\phi$ at the boundary of the circle $r = r_0$, and given, respectively, as,

$$Q^{in} = -\frac{uB_0\lambda_1^2 r_0}{c\lambda_2^2 J_1(\lambda_2 r_0)}, Q^{out} = \frac{uB_0 r_0}{cK_1(\lambda_1 r_0)} \tag{4.26}$$

and

$$\frac{K_2(\lambda_1 r_0)}{K_1(\lambda_1 r_0)} + \frac{\lambda_1 J_2(\lambda_2 r_0)}{\lambda_2 J_1(\lambda_2 r_0)} = 0 \tag{4.27}$$

It is important to mention here that, for localized solutions, the condition $0 < F_1$ implies,

$$0 < \left[1 + \frac{v_d + v_{Bd}}{u} - \frac{\alpha C_{DA}^2 v_{d0}^{'}}{\omega_{cd} u^2} - \frac{\alpha^2 C_{DA}^2}{u^2}\right] \tag{4.28}$$

For the case of $v_{d0} = 0$ (stationary dust), the relation (4.28) becomes

$$0 < \left[1 + \frac{v_d + v_{Bd}}{u} - \frac{\alpha^2 C_{DA}^2}{u^2}\right] \tag{4.29}$$

4.3.2 Soliton Solutions

Here we study the nonlinear effects that arise due to the temperature inhomogeneities of the electrons and ions. Assuming, $\partial_x \ll \partial_\perp$, $v_{d0}\partial_\parallel \ll \partial_t$, and using (4.9) in (4.5) we obtain,

$$\partial_t \Phi + v_T^* \Phi \partial_\perp \Phi - D_f \left(\kappa_{nd} + \kappa_B\right) \partial_\perp \Phi - \rho_d^2 \partial_t \nabla_\perp^2 \Phi - \partial_\parallel v_{d\parallel} = 0 \tag{4.30}$$

where $\Phi = eZ_d\phi/T_{eff}$ $\kappa_{nd} = |d \ln n_{d0}/dx|$, $\kappa_B = |d \ln B_0/dx|$, $\kappa_T = |d \ln T_{i,e}/dx|$ and $v_T^* = D_f \kappa_T$. It is assumed here that $\kappa_{nj} << \kappa_T$ and vector nonlinearity is ignored following Ref. [32]. Equation (4.6) can be expressed as,

$$\partial_t v_{d\parallel} = C_{DA}^2 \left(\partial_\parallel + A\partial_\perp\right) \Phi \tag{4.31}$$

In order to obtain the travelling wave solution in the form of a soliton from equations (4.30) and (4.31), we define a new coordinate η,such that $\eta = r_\perp + \alpha r_\parallel - ut$, where u is the velocity of the nonlinear structure. Then (4.31) becomes,

$$v_{d\parallel} = -\frac{C_{DA}^2}{u} \left(\alpha + A\right) \Phi \tag{4.32}$$

Similarly writing (4.30) in η frame and using (4.32), we obtain,

$$d_\eta \Phi + A_0 \Phi d_\eta \Phi + B d_\eta^3 \Phi = 0 \tag{4.33}$$

where,

$$A_0 = \frac{u v_T^*}{-u^2 - u D_f \left(\kappa_{nd} + \kappa_B\right) + \alpha C_{DA}^2 \left(\alpha + A\right)} \tag{4.34}$$

and

$$B = \frac{u^2 \rho_d^2}{-u^2 - u D_f \left(\kappa_{nd} + \kappa_B\right) + \alpha C_{DA}^2 \left(\alpha + A\right)} \tag{4.35}$$

We now obtain the pulse like solution [39] of (4.33) for a balance between the nonlinear and dispersion terms and using the following boundary conditions $\Phi \to 0$, $d_\eta \Phi \to 0$

and $d_\eta^2\Phi \to 0$ for $\eta \to \pm\infty$. Therefore (4.33) has a solution,

$$\Phi = \Phi_m \, \mathrm{sech}^2\left(\frac{\eta}{\sqrt{4B}}\right) \tag{4.36}$$

where $\Phi_m = 3/A_0$ is the amplitude and $\delta = \sqrt{4B}$ is the width of the pulse.

4.4 Applications

The present model is applied to Saturn's magnetosphere at the boundary region which contains negative dust. We choose the typical parameters representative of plasmas in Saturn environment [100] as $B_0 \simeq 0.1$ G, $n_{e0} \simeq 10^3$ cm^{-3}, $Z_d \simeq 10^2 - 10^3$, $n_{d0} \simeq 10$ cm^{-3}, $m_d = 10^{-16}$ g, $T_e \simeq 5 \times 10^4$ K and $T_i \simeq 5 \times 10^3$ K. Accordingly, we obtain $\omega_{cd} \simeq 0.016$ rad/s, $\rho_d = 136812$ cm and assume $\kappa_{nd} < k_y$ to satisfy local approximation. We choose $v_0 \simeq 10^7$cm/s (closer to solar wind velocity), $v_{d0}(\ll v_0) \simeq 2.5 \times 10^4$cm/s and assume $\kappa_{dv} \approx \kappa_{nd}$ which yields $|A| \simeq 0.2$. Corresponding to these parameters, the Ampere's law determines the scale length of magnetic field gradient $L_B = |d \ln B_0/dx|^{-1}$ where $\kappa_B \simeq 3 \times 10^{-7}$cm^{-1}.

For small $k_\parallel$,we may have $C_{DA}k_\parallel < \omega_{Bd}^*$ and in this case (4.16) gives

$$\omega = -\omega_{Bd}^* = -D_f k_\perp \frac{d}{dx}\left(\ln B_0\right) \tag{4.37}$$

Note that this is the dispersion relation of the low frequency current-driven dust drift wave which exists due to the zero-order current produced by the electrons and ions.

It seems important to present a comparison of (4.11) and equation (17) of Ref. [69] which is re-written here as,

$$\left(\frac{n_{e0}}{n_{i0}} + \rho_s^2 k_\perp^2\right)\Omega_0^2 - \left(\omega_{ni}^* + \omega_{Bi}^*\right)\Omega_0 - c_s^2 k_\parallel^2\left(1 - \frac{k_\perp}{k_\parallel}S\right) = 0 \tag{4.38}$$

Here $S = 1/\omega_{ci}\,|dv_{i0}/dx|$, $\rho_s = c_s/\omega_{ci}$, $\omega_{ci} = eB_0/m_i c$, $\omega_{Bi}^* = D_e\kappa_B k_\perp$, $D_e = \frac{cT_e}{eB_0}$ and $c_s = (T_e/m_i)^{1/2}$ is the ion acoustic speed. Note that D_f contains T_{eff} and D_e contains T_e, therefore ω_{Bd}^* is current-driven dust wave and ω_{Bi}^* is current-driven ion wave. The dispersion relation (4.38) is valid when dust is assumed to be stationary and electrons

and ions are flowing with the same velocity $\mathbf{v}_0(x)$ along z-axis. In a pure electron-ion plasma $n_{e0}/n_{i0} = 1$, the relation (4.38) will be valid if zero order velocities of ions and electrons are different $\mathbf{v}_{i0} < \mathbf{v}_{e0}$. If density is homogeneous in electron-ion plasma, and $v_{i0} \simeq 0$ is assumed then (4.38) reduce to,

$$\left(1 + \rho_s^2 k_\perp^2\right) \Omega_0^2 - \omega_{Bi}^* \Omega_0 - c_s^2 k_\parallel^2 = 0 \tag{4.39}$$

The current is only due to the sheared flow of electrons in this case. The different magnitude of the current will give different scale length L_B of the magnetic field gradient.

In Fig. (4-1), the stable frequency of coupled dispersion relation (4.15) is plotted against $k_\parallel$ and $\omega_r \simeq \omega_{Bd}^*$ is the frequency of the current-driven dust wave. The frequency increases for the case of inhomogeneous plasma $(\omega_d^* \neq 0)$. In Fig. (4-2), the growth rate of the dispersion relation (4.11) is plotted against perpendicular wave number $k_\perp$ for both cases $\omega_d^* = 0$ and $\omega_d^* \neq 0$. The waves having periods and e-folding times of the order of an hour or lesser are more relevant in Saturn's magnetosphere since the day at this planet is about 10 hrs long, and the boundary region at night side (where the planet's magnetic field has parallel flow of electrons and ions) should face solar wind for sufficient time to give rise to these electrostatic waves and instabilities.

The dispersion relation (4.11) for $\omega_d^* = 0$ reduces to,

$$\Omega_0^2 \left(1 + \rho_d^2 k_\perp^2\right) + \omega_{Bd}^* \Omega_0 - C_{DA}^2 k_\parallel^2 \left(1 + A \frac{k_\perp}{k_\parallel}\right) = 0 \tag{4.40}$$

The dipolar vortices for dust modes are shown in Fig. (4-3). The solitons of electrostatic potential Φ are plotted in Fig. (4-4) taking into account the effects of both the background current and the density inhomogeneity in the presence of temperature gradients of electrons and ions. The effects of variation of the scale lengths of temperature gradients are pointed out keeping other parameters to be the same. In Fig. (4-5), the effect of the change in shear flow scale length is shown keeping other parameters the same as in Fig. (4-4). The amplitude of the solitons increases corresponding to smaller value of A. The forms of solitary pulses in homogeneous density $(\boldsymbol{\nabla} n_{j0} = 0)$ plasma are shown in Figs. (4-6) and (4-7).

4.5 Summary

Several waves and instabilities have been investigated in the presence of field-aligned current in dusty plasmas. The previous investigations [27, 28] considered only the ion waves assuming dust to be stationary. We have demonstrated that in dusty plasmas new type of low frequency and long wavelength perturbations are introduced when the plasma species have sheared flows. The initial ambient magnetic field is assumed to be along z-axis $\mathbf{B}_0 = B_0\hat{\mathbf{z}} \equiv$ constant which is modified as $\mathbf{B}_0 = B_0\hat{\mathbf{e}}_{\|}$ due to the zero-order current $\mathbf{J}_0 \neq \mathbf{0}$. In the homogeneous density plasma, if the velocities of electrons, ions and dust are small then the effects of the current $\mathbf{J}_0$ can be neglected. In this case equation (4.12) predicts a purely growing instability (4.17) if the condition (4.18) holds. This instability is similar to the purely growing instability discovered long ago [19] in pure electron-ion plasmas. In equation (4.11)(for $v_{d0} \neq 0$) the current-driven dust drift like wave $\omega_r \simeq \omega^*_{Bd}$ couples with the purely growing mode of dusty plasma (Eq. 4.17). The nonlinear dynamics has also been investigated and it is proposed that these very low frequency electrostatic waves can produce stationary structures like vortices and solitons.

Since the solar wind is structured and narrow streams have sheared flows, therefore it is expected that in the boundary regions of dusty magnetospheres where these flows are almost parallel to the planet's magnetic field, the above mentioned waves and instabilities appear. We have assumed that a local steady state has reached and therefore the complex atomic processes are not considered here. Moreover, to highlight the basic physical model the variations in grain sizes and masses have not been discussed. The theoretical model presented here is general and it has been applied to Saturn's magnetosphere for illustration.

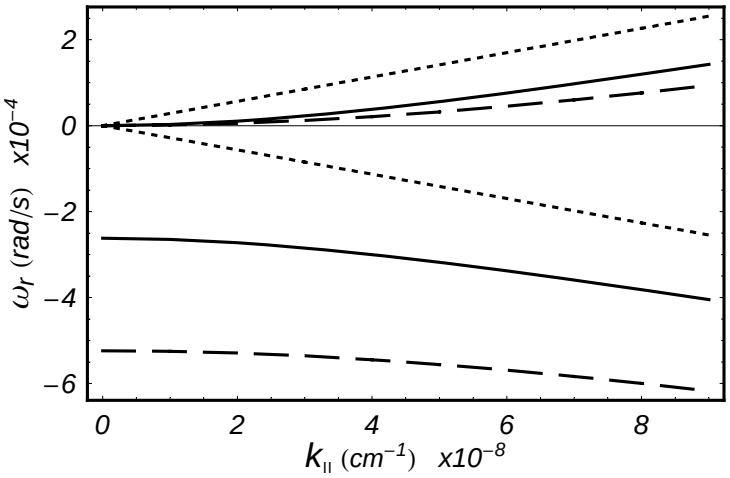

Figure 4-1: Real frequency ω_r of stable waves (for $A = 0$) [Eq. (4.15)] is plotted against the parallel wave number $k_{\|}$ for the homogeneous density plasma with $\omega_d^* = 0$ (solid line) and inhomogeneous density plasma with $\omega_d^* \neq 0$ (dashed line), whereas the dotted lines represent dust acoustic mode.

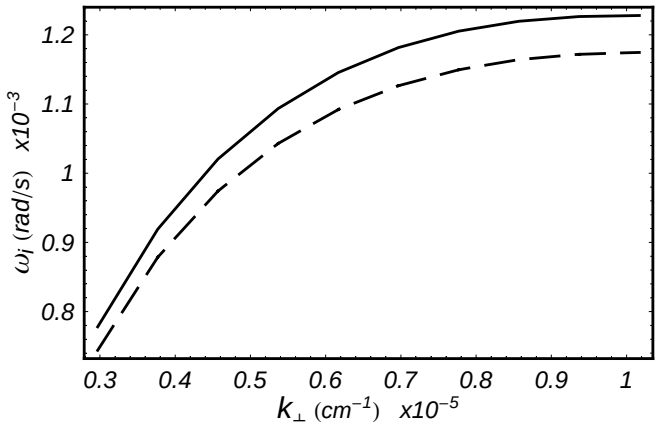

Figure 4-2: Growth rate ω_i (of unstable wave for $k_{\|}/k_{\perp} < |A|$) [Eq. (4.11)] is plotted against the perpendicular wave number $k_{\perp}$ for the homogeneous density plasma with $\omega_d^* = 0$ (solid line) and inhomogeneous density plasma with $\omega_d^* \neq 0$ (dashed line) for $|A| \simeq 0.2$. The other parameters are same as in Fig. (4-1).

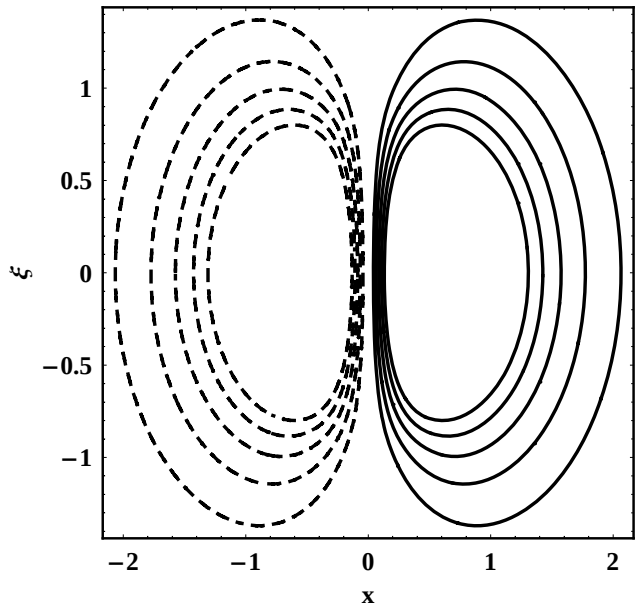

Figure 4-3: Contour plot of dipolar vortices is shown corresponding to the parameters of Fig. (4-1).

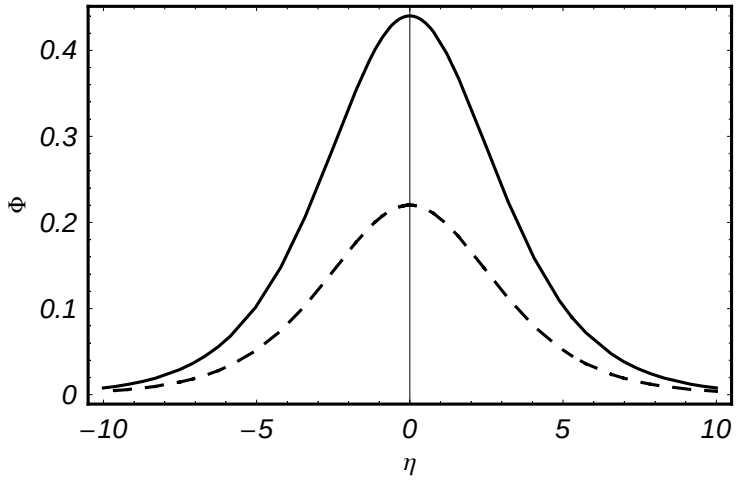

Figure 4-4: The solitary wave potential Φ is plotted against η (normalised with ρ_d) for $\boldsymbol{\nabla} n_{j0} \neq 0$ corresponding to parameters given in Fig. (4-1) for $|A| \simeq 0.2$, $u = 0.15 C_{DA}$, $\alpha = 0.3$, $k_T = 100 k_{nd}$ (solid curve) and $k_T = 200 k_{nd}$ (dashed curve).

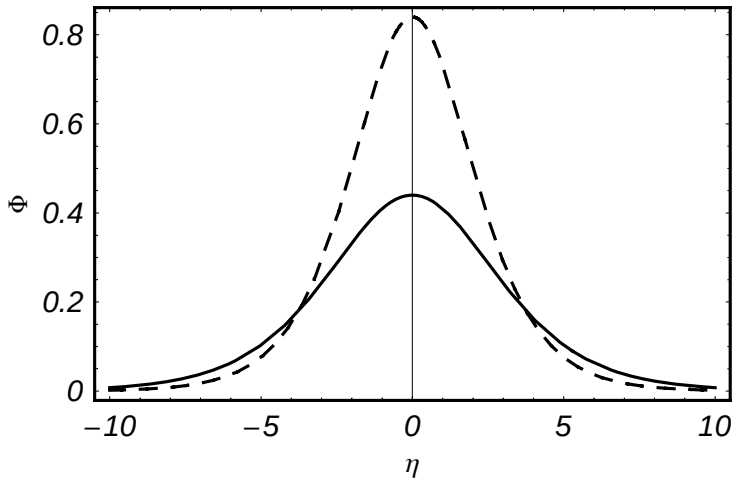

Figure 4-5: The solitary wave potential Φ is plotted against η (normalised with ρ_d) for $\boldsymbol{\nabla} n_{j0} \neq 0$ corresponding to parameters given in Fig. (4-1) for $k_T = 100 k_{nd}$, $u = 0.1 C_{DA}$, $\alpha = 0.3$, $|A| \simeq 0.2$ (solid curve) and $|A| \simeq 0.18$ (dashed curve).

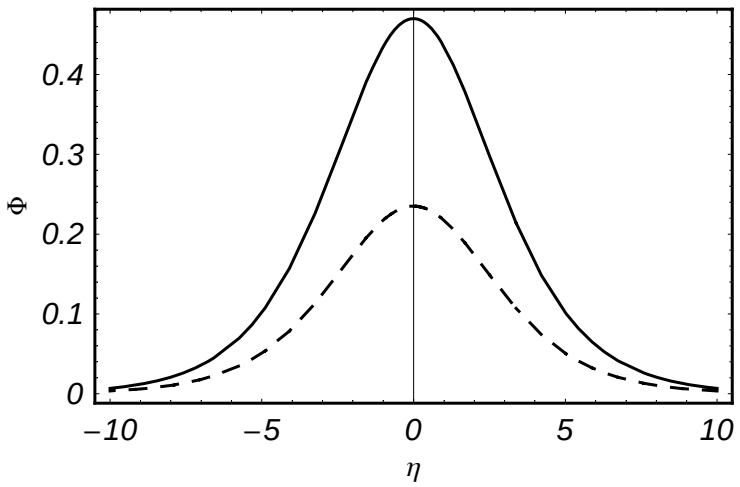

Figure 4-6: The soliton is plotted for a homogeneous density plasma ($\nabla n_{j0} = 0$) corresponding to parameters in Fig. (4-4).

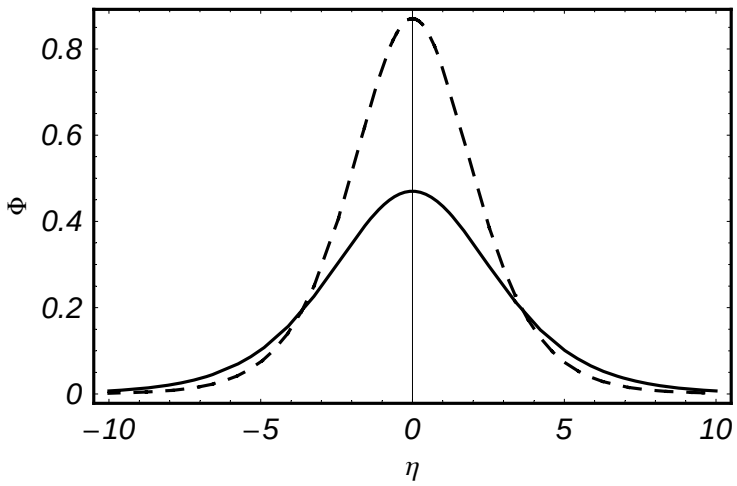

Figure 4-7: The soliton is plotted for a homogeneous density plasma ($\nabla n_{j0} = 0$) corresponding to parameters in Fig. (4-5).

Chapter 5

Drift Modes in Bounded Bi-ion Plasmas

The drift wave is a low frequency mode of inhomogeneous plasma and is very important because its resistive and reactive instabilities contribute to particle and energy transport in plasmas [31]. It has been noticed that even for small amplitudes $e\phi/T_e \simeq \rho_s/L_n$ the nonlinear effects can not be ignored in drift wave theory particularly corresponding to smaller wavelengths $k_\perp \rho_s \simeq 1$ [105]. Here ρ_s is the ion Larmor radius at electron temperature T_e, L_n is the scale length of the nonuniformity of density and subscript $\perp$ represents the direction perpendicular to the magnetic field. The robust long living structures associated with this mode have been observed experimentally [106–108]. The solar wind interaction with dusty plasmas of planetary and cometary environments can also give rise to nonlinear drift wave structures [26].

It is interesting to point out here a controversy appeared in literature about the electrostatic drift wave in the presence of shear flow. Long ago [19], it was pointed out that the plasma shear flow (without current) can give rise to a purely growing linear instability in the low frequency regime $\partial_t \ll \omega_{ci}$ in a slab geometry with constant external magnetic field. The plasma density was assumed to be nonuniform, but the drift wave frequency did not appear as a real part in the linear dispersion relation (Eq. (18)) of Ref. [19]. Arguments and counterarguments about the role of equilibrium density gradient in this work have been presented [37, 109]. Recently [29] it has been pointed out that the drift wave contribution in the linear dispersion relation of Ref. [31]

is canceled due to the use of Eq. (10) of this reference which is not needed. However, it is now well known that the plasma shear flows in the direction parallel to the external magnetic field can produce finite amplitude drift waves even in the absence of collisions. Such an instability can play a role in the dynamics of solar spicules as well [110]. The pioneering work of D'Angelo [19] on shear flow instability has also been reconsidered as an eigenvalue problem in a sheared slab geometry [111].

More than two decades ago [112], the eigenvalue equation for drift waves in a cylindrical geometry was solved numerically in a collisional plasma neglecting the ion parallel motion. A few years ago [113], it has been shown that the analytical solutions of the drift wave eigenvalue problem in a cylinder can be obtained. The drift wave coupled with ion cyclotron waves in a bounded cylindrical electron-ion plasma was studied neglecting the collisions. Then this work was also extended for the case of electron-positron-ion plasmas [114].

The electron temperature gradient mode (η_e mode) has been investigated in toroidal geometry [115, 116]. The eigenvalue problem for toroidal drift waves has also been studied in several different limits [117, 118]. A detailed discussion on this topic can be found for instance in Ref. [119]. The drift wave eigenvalue problem in a slab geometry with sheared magnetic field was studied long ago [120] for the case of an electron-ion plasma. These authors obtained a solution for the drift eigenvalue equation and showed that the mode can behave as a standing wave in the interior and it propagates outwards as an outgoing wave. Similar studies in the high frequency regime were also done [121].

In many cases, the plasma contains two ion species like the case of Hydrogen-Helium plasma of solar corona, Neon-Argon plasma of pinch devices and also the Deuterium-Tritium fusion plasmas. The Earth foreshock region is characterized by the existence of two proton populations, the protons coming from solar wind and protons reflected at bow shock [122]. SO_2^+ ions near Io flowing around Jupiter's moon provides another example of the bi-ion plasmas [123]. The addition of the second ion species into the ordinary electron-ion plasma modifies the dispersion properties of the low frequency modes [124].

Here, we investigate the behavior of global drift mode in a bounded cylindrical plasma containing two ion species. In the global mode analysis, instead of deriving

the dispersion relation using Fourier transform, we here derive the eigenvalue value equation for drift waves in cylindrical geometry along with appropriate boundary conditions. The system of equations is not closed when we use multi fluid theory for two ion species (having different masses) in the plasma and take into account the ion cyclotron wave dynamics. We focus our attention on the drift mode which is modified significantly in such plasma systems. Since $\partial_t \ll \omega_{ci}$ is generally true for the drift wave regime, therefore, we investigate the dynamics of this mode in a bounded plasma having two ion species and ignore the ion cyclotron modes. The effect of magnetic shear on the eigenvalue solutions of the drift wave equation in a slab geometry is also investigated on the lines of Ref. [120] for the case of two-ion component plasma.

5.1 Basic Equations

We consider a plasma embedded in a constant external magnetic field ($\mathbf{B_0} = B_0\hat{\mathbf{z}}$) directed along z-axis and having density gradient in radial direction $\boldsymbol{\nabla} n_{j0} = \mathbf{e_r} dn_{j0}/dr$. In the presence of two ion species, the steady state requires,

$$n_{a0} + n_{b0} = n_{e0}$$

For cold ions, the equation of motion can be written as,

$$m_j n_j \left(\partial_t + \mathbf{v}_j \cdot \boldsymbol{\nabla}\right) \mathbf{v}_j = n_j q_j \left(\mathbf{E} + \frac{\mathbf{v}_j}{c} \times B_0 \hat{\mathbf{z}}\right) \tag{5.1}$$

where the subscript j represents the two ion species a and b of different masses. For electrostatic perturbations we use $\mathbf{E} = -\nabla\phi$, where ϕ is the electrostatic potential. In the linear limit, from equation (5.1), we obtain,

$$(\partial_t^2 + \omega_{cj}^2)\mathbf{v}_{\perp j1} = -\frac{\omega_{cj}}{B_0}\boldsymbol{\nabla}_\perp \partial_t \phi_1 + \frac{\omega_{cj}^2}{B_0}\hat{\mathbf{z}} \times \boldsymbol{\nabla}_\perp \phi_1 \tag{5.2}$$

where $\omega_{cj} = eB_0/m_j c$ is the gyrofrequency of the ions. Using Equation (5.2) in the linearized ion continuity equation,

$$\partial_t n_{j1} + n_{j0}\boldsymbol{\nabla}_\perp \cdot \mathbf{v}_{\perp j1} + \boldsymbol{\nabla} n_{j0} \cdot \mathbf{v}_{\perp j1} = 0 \tag{5.3}$$

we obtain,

$$(\partial_t^2+\omega_{cj}^2)\partial_t n_{j1}-n_{j0}\frac{\omega_{cj}}{B_0}\nabla_\perp^2\partial_t\phi_1+\boldsymbol{\nabla}n_{j0}\cdot\left[-\frac{\omega_{cj}}{B_0}\boldsymbol{\nabla}_\perp\partial_t\phi_1+\frac{\omega_{cj}^2}{B_0}\hat{\mathbf{z}}\times\boldsymbol{\nabla}_\perp\phi_1\right]=0 \quad (5.4)$$

Note that the subscripts naught (0) and one (1) denote the background and perturbed quantities, respectively. The subscript (1) is dropped in the subsequent calculations. Assuming $\partial_t^2 << \omega_{cj}^2$ and writing Eq. (5.4) for $j = a, b$, and then adding these equations, we get,

$$\partial_t(n_a+n_b)-\left(\frac{n_{a0}}{\omega_{ca}}+\frac{n_{b0}}{\omega_{cb}}\right)\frac{1}{B_0}\nabla_\perp^2\partial_t\phi+\boldsymbol{\nabla}n_{e0}\cdot\frac{1}{B_0}\hat{\mathbf{z}}\times\boldsymbol{\nabla}_\perp\phi-\frac{1}{B_0}\left(\frac{\boldsymbol{\nabla}n_{a0}}{\omega_{ca}}+\frac{\boldsymbol{\nabla}n_{b0}}{\omega_{cb}}\right)\cdot\boldsymbol{\nabla}_\perp\partial_t\phi=0 \quad (5.5)$$

where $\omega_{ca}=eB_0/m_ac$ and $\omega_{cb}=eB_0/m_bc$. For small electrostatic perturbations, the perturbed electron density n_e can be expressed as,

$$n_e=n_{e0}\left(\frac{e\phi}{T_e}\right) \quad (5.6)$$

The Poisson equation can be written as,

$$\nabla^2\phi=4\pi e(n_e-n_a-n_b) \quad (5.7)$$

Using Eqs. (5.5) and (5.6) in Eq. (5.7) we obtain,

$$\lambda_{De}^2\nabla^2\partial_t\Phi-\partial_t\Phi+\left(\frac{n_{a0}}{\omega_{ca}}+\frac{n_{b0}}{\omega_{cb}}\right)\frac{cT_e}{en_{e0}B_0}\nabla_\perp^2\partial_t\Phi-\frac{cT_e}{eB_0}\frac{\boldsymbol{\nabla}n_{e0}}{n_{e0}}\cdot\hat{\mathbf{z}}\times\boldsymbol{\nabla}_\perp\Phi+$$

$$\frac{cT_e}{en_{e0}B_0}\left(\frac{\boldsymbol{\nabla}n_{a0}}{\omega_{ca}}+\frac{\boldsymbol{\nabla}n_{b0}}{\omega_{cb}}\right)\cdot\boldsymbol{\nabla}_\perp\partial_t\Phi=0 \quad (5.8)$$

where $\Phi=e\phi/T_e$ and $\lambda_{De}=\left(T_e/4\pi e^2n_{e0}\right)^{1/2}$ is the Debye length.

5.2 Local Dispersion Relation

In Cartesian geometry, assuming exponential density profiles for $j = a, b$ with constant gradient scale lengths, the ion continuity equation yields,

$$(1 - g\frac{n_{a0}}{n_{e0}}\rho_{sa}^2\nabla_\perp^2)\partial_t\Phi + D_e\boldsymbol{\nabla}\ln n_{e0}\times\hat{\mathbf{z}}\cdot\boldsymbol{\nabla}_\perp\Phi = 0 \tag{5.9}$$

where $g = (1+n_{b0}m_b/n_{a0}z_bm_a)$, $D_e = cT_e/eB_0$ and $\nabla n_{j0} = -\hat{\mathbf{x}}dn_{j0}/dx$ has been used. Assuming the perturbations of the form $\exp[i\,(k_\perp y - \omega t)]$, the dispersion relation for drift waves can be written as,

$$\omega = \frac{\omega_{*e}}{1 + g\frac{n_{a0}}{n_{e0}}\rho_{sa}^2k_\perp^2} \tag{5.10}$$

where $\omega_{*e} = \mathbf{v}_{De}\cdot\mathbf{k}_\perp$ is the drift frequency, $\mathbf{v}_{De} = D_e\boldsymbol{\nabla}\ln n_{e0}\times\hat{\mathbf{z}} = (D_e\kappa_{en})\hat{\mathbf{y}}$ is the diamagnetic velocity and $\kappa_{en} = |1/n_{e0}\;dn_{e0}/dx| =$ constant, is the inverse density gradient scale length. Note that in the limit $n_{b0} = 0$, the relation (5.10) reduces to (ei) case $\omega = \omega_{*e}/\left(1+\rho_s^2k_\perp^2\right)$ where $\rho_s^2 = c_s^2/\Omega_i^2$ and $c_s^2 = T_e/m_i$. If the contribution of vector nonlinearity is taken into account in drift wave theory then one obtains Hasegawa-Mima (HM) equation [40] which also admits vortex solutions. Hence one can notice that the Eqs. (5.8) and (5.9) are the linearized forms of HM equation.

5.3 Global Drift Mode in a Cylinder

Assuming the perturbations in a cylindrical plasma to be of the form $\Phi = \Phi(r)\exp[-i\omega t + im\theta]$ (where m is the poloidal mode number), and ignoring the first term in Eq. (5.8), we obtain,

$$\left[\frac{\partial^2}{\partial r^2} + \frac{1}{r}\frac{\partial}{\partial r} - \frac{2r}{a_0^2}\frac{\partial}{\partial r} - \frac{m^2}{r^2} + b_0^2\right]\Phi(r) = 0 \tag{5.11}$$

where,

$$b_0^2 = \left(\frac{2m}{\omega a_0^2} - \frac{r_0^2}{\rho_{sa}^2}\right)\frac{1}{N_m} \tag{5.12}$$

Here we have assumed $n_{j0}(r) = N_{j0}\exp(-r^2/a_0^2)$ where a_0 is the characteristic inhomogeneity scale length and r_0 is the radius of the cylinder, also N_m is defined as,

$$N_m = \frac{N_{a0}}{N_{e0}} + \frac{N_{b0}}{N_{e0}}\frac{\omega_{ca}}{\omega_{cb}}$$

where $\rho_{sa}^2 = c_{sa}^2/\omega_{ca}^2$ and $c_{sa}^2 = T_e/m_a$ is the ion acoustic speed. The global drift mode in a cylindrically bounded partially ionized plasma was studied long ago [112]. The linear equation was solved numerically to find out the wave potential structure corresponding to three different density profiles. Recently, it has been shown that a similar equation can be solved analytically [113]. In this study, the limit $\partial_t << \omega_{ci}$ has been relaxed and the coupled global ion cyclotron wave and the drift wave have been investigated assuming the plasma to be fully ionized whereas electron-ion collisions have been neglected. In the presence of two types of ions a and b, the system of equations is not closed if the ion cyclotron waves are also investigated along with the drift wave. Therefore, we are considering the electrostatic global perturbation only in the limit $\partial_t << \omega_{ca}, \omega_{cb}$ because drift wave is an important low frequency mode of inhomogeneous plasma. The general solution of Eq. (5.11) can be written similar to the case of Ref. [110] as,

$$\Phi(r) = C_1 r^{-m} F_1(r) + C_2 r^m F_2(r) \tag{5.13}$$

where,

$$F_1(r) = {}_1F_1[a_1, b_1, \alpha r^2] \equiv {}_1F_1\left[-\frac{a_0^2 b_0^2}{4} - \frac{m}{2}, 1-m, \frac{r^2}{a_0^2}\right] \tag{5.14}$$

and,

$$F_2(r) = {}_1G_1[a_2, b_2, \alpha r^2] \equiv {}_1G_1\left[-\frac{a_0^2 b_0^2}{4} + \frac{m}{2}, 1+m, \frac{r^2}{a_0^2}\right] \tag{5.15}$$

The first term on the right hand side of Eq. (5.13) diverges as $r \to 0$. Therefore the constant C_1 is assumed to be zero. To obtain physically acceptable solutions of Φ we assume the boundary condition $\Phi(r) \to 0$ as $r \to r_0$. These solutions are found by varying b_0 for a given equilibrium density profile (and a given constant a_0). If $a_0^2 = 0.5$ is chosen similar to Ref. [113], in a D-T plasma with $m_a = 2$ and $m_b = 3$, then we obtain $b_0^2 = 15, 30, 48$ corresponding to $m = 1, 2, 3$ respectively. Note that

here $m = 2, 3$ do not denote the ion cyclotron waves as in Ref. [113]. Rather, the azimuthal mode number m is varied for the global drift wave similar to Ref. [112] to investigate the variations in the potential profiles corresponding to different poloidal wave lengths. The plots of $\Phi(r)$ versus r are shown in Fig. (5-1) where, $n_{a0} = 0.5$, $n_{b0} = 0.5$ and $N_m = 1.25$ have been used. The locus of pairs (a_0^2, b_0^2) corresponding to three different values of N_m has been plotted in Fig. (5-2) while we choose $m = 1$ just for a comparison with Fig. (2) of Ref. [113]. The frequency of the global mode ω is plotted against a_0^2 in Fig. (5-3) corresponding to $m = 1$. The frequency ω varies if the ratio of the concentration of D and T varies. Similar plot of ω versus a_0^2 for a Neon-Argon plasma is shown in Fig. (5-4). The dispersion equation (5.12) for eigen frequencies of the drift wave can be written as,

$$(\frac{r_0^2}{\rho_{sa}^2} + N_m b_0^2)\omega = \frac{2m}{a_0^2} \tag{5.16}$$

The frequency of the drift mode becomes a little larger when it is decoupled from ion cyclotron wave. This decoupling is justified in the limit $\partial_t^2 << \omega_{ci}^2$. It may be mentioned here that $Q(r)$ of Ref. [112] becomes equal to b_0^2 for single ion plasma case in the limit $\nu_i = 0$ and $\nu_e = 0$.

5.4 Effect of Magnetic Shear in Slab Geometry

It is important to investigate the effects of magnetic shear on the drift mode. In a Tokamak the magnetic field has both a toroidal and a poloidal component and hence each field line has a rotational transform and it does not closes on itself in one toroidal rotation [125]. Sheared magnetic field can be expressed as,

$$\mathbf{B_0} = B_0(\hat{\mathbf{z}} + \frac{x}{L_s}\hat{\mathbf{y}})$$

where L_s is the characteristic length for the magnetic field shear and B_0 is constant. The Eq. (5.8) is modified due to magnetic field shear and it becomes,

$$\lambda_{De}^2 \nabla^2 \partial_t^2 \Phi - \partial_t^2 \Phi + \left(\frac{n_{a0}}{\omega_{ca}} + \frac{n_{b0}}{\omega_{cb}}\right) \frac{cT_e}{en_{e0}B_0} \nabla_\perp^2 \partial_t^2 \Phi - \frac{cT_e}{eB_0} \frac{\boldsymbol{\nabla} n_{e0}}{n_{e0}} \cdot \hat{\mathbf{z}} \times \boldsymbol{\nabla}_\perp \partial_t \Phi$$

$$+\frac{cT_e}{en_{e0}B_0}\left(\frac{\boldsymbol{\nabla} n_{a0}}{\omega_{ca}}+\frac{\boldsymbol{\nabla} n_{b0}}{\omega_{cb}}\right)\cdot\boldsymbol{\nabla}_\perp\partial_t^2\Phi+\left(\frac{n_{a0}\omega_{ca}+n_{b0}\omega_{cb}}{n_{e0}B_0}\right)(\hat{\mathbf{z}}\cdot\boldsymbol{\nabla})^2\frac{cT_e}{e}\Phi=0 \quad (5.17)$$

Assuming the perturbation of the form $\Phi=\Phi(x)\exp[-i\omega t+ik_y y+ik_z z]$, using,

$$\boldsymbol{\nabla}_\perp=\hat{\mathbf{x}}\frac{\partial}{\partial x}+\hat{\mathbf{y}}\frac{\partial}{\partial y}$$

and ignoring first term in Eq. (5.17) we obtain,

$$N_1\rho_{sa}^2\left(\frac{\partial^2}{\partial x^2}-k_y^2\right)\Phi+\frac{\omega_{*e}}{\omega}\Phi-\Phi-\left(\frac{v_{*a}}{\omega_{ca}}+\frac{v_{*b}}{\omega_{cb}}\right)\frac{\partial\Phi}{\partial x}+N_2\frac{c_{sa}^2}{v_*^2}\frac{x^2}{L_s^2}\Phi=0 \quad (5.18)$$

where,

$$N_1=(\frac{n_{a0}}{n_{e0}}+\frac{n_{b0}}{n_{e0}}\frac{\omega_{ca}}{\omega_{cb}})$$

$$N_2=(\frac{n_{a0}}{n_{e0}}+\frac{n_{b0}}{n_{e0}}\frac{\omega_{cb}}{\omega_{ca}})$$

$$v_*=\frac{cT_e}{eB_0}|\frac{1}{n_{e0}}\frac{dn_{e0}}{dx}|$$

and,

$$v_{*j}=\frac{cT_e}{eB_0}|\frac{1}{n_{j0}}\frac{dn_{j0}}{dx}|$$

In the above equation for small magnetic shear we have assumed $(\hat{\mathbf{z}}\cdot\boldsymbol{\nabla})^2=-x^2k_y^2/L_s^2$ and in the drift wave limit, ω^2 has been replaced by $v_*^2k_y^2$ and $\omega_{*e}=v_*k_y$ has been used [31].

The general solution of Eq. (5.17) can be written as,

$$\Phi(x)=C_0exp(i\beta x^2+\gamma x) \quad (5.19)$$

Using Eq. (5.19), we obtain from Eq. (5.18),

$$N_1\rho_{sa}^2(2i\beta+\gamma^2+4i\beta\gamma x-4\beta^2x^2)-N_1\rho_{sa}^2k_y^2+\frac{\omega_{*e}}{\omega}-1+N_2\frac{c_{sa}^2}{v_*^2}\frac{x^2}{L_s^2}-\left(\frac{v_{*a}}{\omega_{ca}}+\frac{v_{*b}}{\omega_{cb}}\right)(2i\beta x+\gamma)=0 \quad (5.20)$$

Comparing coefficients of x^2, x and x^0 we get, respectively,

$$4\beta^2N_1\rho_{sa}^2-\frac{c_{sa}^2}{v_*^2}\frac{N_2}{L_s^2}=0 \quad (5.21)$$

$$2\gamma N_1\rho_{sa}^2 - \left(\frac{v_{*a}}{\omega_{ca}} + \frac{v_{*b}}{\omega_{cb}}\right) = 0 \tag{5.22}$$

and,

$$2i\beta N_1\rho_{sa}^2 + \gamma^2 N_1\rho_{sa}^2 - N_1\rho_{sa}^2 k_y^2 - \gamma\left(\frac{v_{*a}}{\omega_{ca}} + \frac{v_{*b}}{\omega_{cb}}\right) + \frac{\omega_{*e}}{\omega} - 1 = 0 \tag{5.23}$$

Using the values of β, γ from Eqs. (5.21) and (5.22) in Eq. (5.19) we obtain,

$$\Phi(x) = C_0 exp\left[\frac{(\frac{v_{*a}}{\omega_{ca}} + \frac{v_{*b}}{\omega_{cb}})x}{2N_1\rho_{sa}^2}\right] exp\left[-\frac{ix^2 c_{sa}}{2\rho_{sa}v_* L_s}\sqrt{\frac{N_2}{N_1}}\right] \tag{5.24}$$

It is well-known that the drift wave has the stronger tendency to become unstable where $k_\parallel$ is small and hence the electron shielding is less efficient. We are using Cartesian geometry for simplicity to understand the basic physics of drift mode in a two-ion component plasma. Due to shear in the field, the $k_\parallel$ increases as the wave moves towards plasma walls. When $k_\parallel$ has grown such that $k_\parallel v_{ti} = \omega$, the ion Landau damping sets in and the wave is absorbed. Keeping this fact in view, we use the absorbing boundary conditions [31,120,121]. The magnetic shear twists the field lines in a tokamak. A toroidal eigen mode is also twisted according to it's poloidal mode number k_θ which is equivalent to $k_y = k_\theta/r$ (r is the radial position along minor radius in tokamak). Since $k_\parallel \simeq xk_y/L_s$, therefore we expect that the drift waves generated near $k_\parallel \simeq 0$, propagate towards larger x. The wave is absorbed where $k_\parallel$ has grown so that $\omega \simeq k_\parallel v_{ti}$ and ion Landau damping becomes operative [31]. It may also be mentioned here that if,

$$(\frac{1}{n_0}\frac{dn_0}{dx})\frac{d\phi}{dx} << \frac{d^2\phi}{dx^2}$$

is assumed similar to Ref. [121], then the first derivative term in Eq. (5.18) can be omitted and hence it becomes Weber equation.

Fig. (5-5) shows the increasing amplitude of $\Phi(x)$ with increasing x corresponding to $n_{a0} = n_{b0}$ for a D-T plasma. It shows that the amplitude of the wave is reduced in case of two-ion species present in equal concentration $n_{a0} = n_{b0}$. The increasing electrostatic wave potential will be slowly absorbed by resonant ions at the resonant layer where $\omega \sim k_\parallel v_{ti}$. In the limit $n_{b0} = 0$, Eq. (5.24) becomes Eq. (38) of Ref. [113] which is the (ei) case. The solution (5.24) is valid for different concentration ratios of

the two ion species and for different ions like Neon-Argon plasma.

5.5 Discussion

The behavior of electrostatic drift wave in a two-ion component plasma has been investigated in several different cases including the eigenvalue problem in a cylinder, the local dispersion relation and the magnetic shear effects in a Cartesian geometry. It is not straightforward to study the coupled ion cyclotron and drift modes in case of a two-ion component plasma in the presence of electrons. In principle, the frequencies of ion cyclotron and drift modes are different. The frequency of low frequency global drift mode is very small compared to Ω_i. We notice that when it is investigated without taking into account it's coupling with ion cyclotron waves, the frequency of drift wave becomes a little larger as can be seen by comparing plots of our Fig. (5-3) with the drift wave plot of Fig. (3) of Ref. [113].

It has been pointed out that the plasma shear flow along the external magnetic field can give rise to electrostatic waves in a Cartesian geometry [29] and references therein. The local drift wave instability appears to exist due to the free energy source available in the form of shear flow as is shown in Eq. (26) of Ref. [29]. If the flow is constant, then the instability disappears. But in a tokamak the toroidal shear flows are usually accompanied by the poloidal sheared flow and they can not be developed because the field lines are twisted. In tokamak geometry, it has been shown that the shear flows tend to suppress drift waves [126]. In the present work only the effects of shear flow parallel to the constant external magnetic field is investigated in a two-ion component plasma.

Long ago [112] the drift wave was studied in a partially ionized plasma bounded by a cylinder and the eigenvalue equation was solved numerically corresponding to different poloidal mode numbers $m = 1, 2, 3$ and corresponding to different background density profiles. Recently [113], it has been shown that the similar eigenvalue equation has the exact analytical solution. In this investigation the dynamics of coupled ion cyclotron and drift waves has been studied and the poloidal mode number $m = 1, 2, 3$ denote the drift wave and the two branches of ion cyclotron wave, respectively.

We have analyzed the behavior of drift wave with different poloidal wavenumbers

$m = 1, 2, 3$. The behavior of drift wave has also been investigated taking into account the effect of magnetic shear. For this purpose we have used Cartesian geometry for simplicity. Moreover, the absorbing boundary condition has been assumed. As shown in Fig. (5-5), the amplitude of the oscillatory drift wave is reduced in the presence of two-ion species with the same concentration $n_{a0} = n_{b0}$.

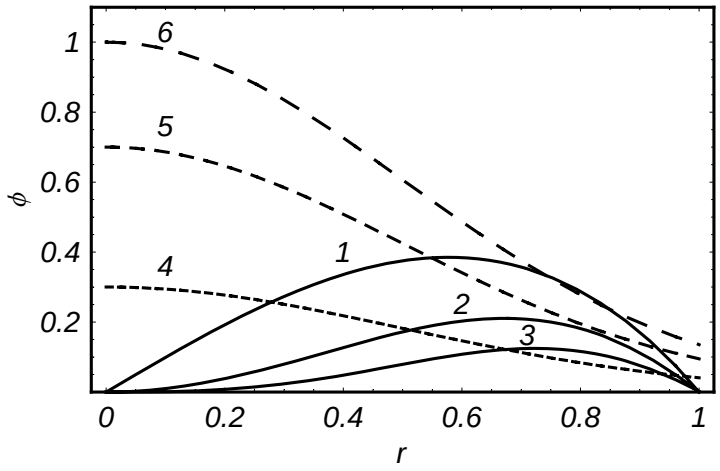

Figure 5-1: Amplitudes ϕ of the waves as eigen functions of Eq. (5.11) (curves 1-3) are shown whereas curves 4-6 represent the density profiles for species a, b and e, respectively.

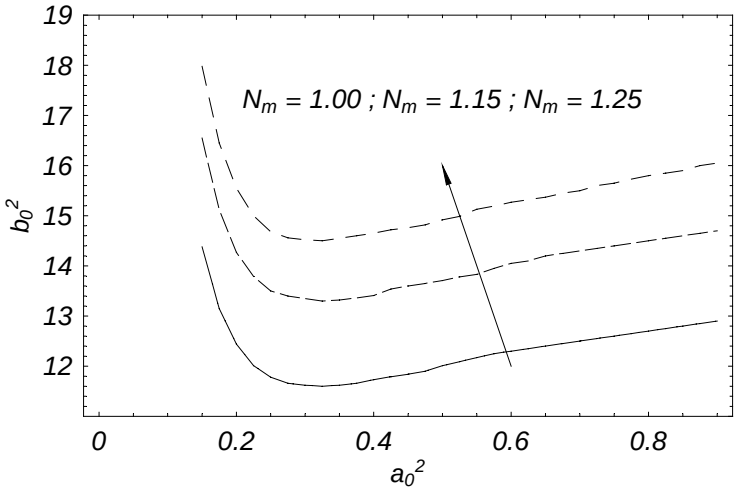

Figure 5-2: The locus of pairs (a_0^2, b_0^2) for different concentrations of the two-ion species.

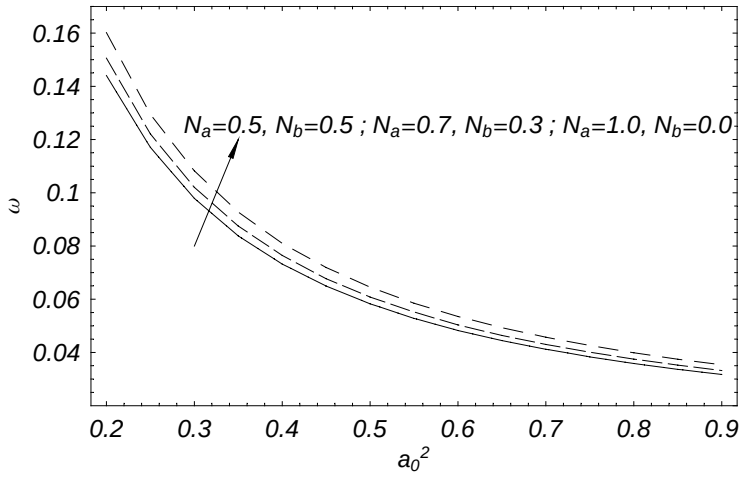

Figure 5-3: The frequency of the drift waves for Deuterium-Tritium plasma for locus of pairs (a_0^2, b_0^2) taken from Fig. (5-2).

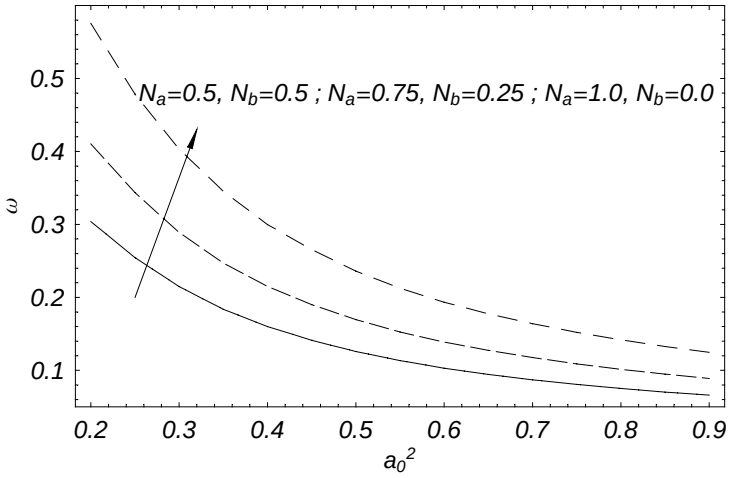

Figure 5-4: The frequency of the drift waves for Neon-Argon for locus of pairs (a_0^2, b_0^2) taken from Fig. (5-2).

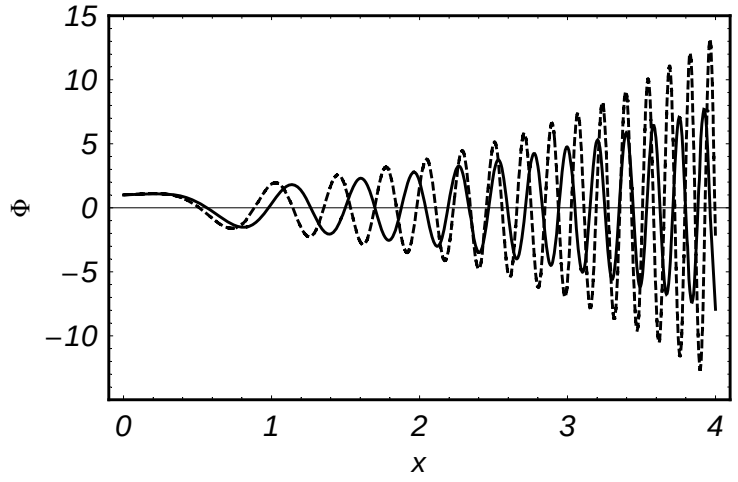

Figure 5-5: The sketch of potential (the solid curve) obtained by using Eq. (5.24) is for two-ion species whereas the dotted curve correspond to the single ion plasma.

Chapter 6

Summary and Conclusions

In chapter 2, we have studied the linear and nonlinear electrostatic waves driven by electron shear flow velocity in heavier ion (barium) magnetized plasmas. In the linear limit, we have derived the dispersion relation for the drift-type mode in the frequency range $\omega_{ci} \ll \omega_r \ll \omega_{ce}$, which exists only due to the zero-order current $\mathbf{J}_0(x)$. In the absence of the current the mode disappears. Since the frequency of the mode is much greater than the barium ion gyrofrequency, the ions are assumed to be stationary. It is shown that such a mode can exist even in uniform density plasma in the presence of an inhomogeneous magnetic field. It is also shown that the wave can become unstable due to the steady state sheared electron current under certain conditions. The growth rate corresponding to laboratory plasma parameters is analyzed. In the nonlinear regime, the short wavelength current-driven electrostatic wave can form stationary structures. It is shown that instability gives rise to vortex structures and solitons, which can play an important role in particle and energy transport.

In chapter 3, we have studied the linear and nonlinear dynamics of current-driven ion modes in magnetized dusty plasmas. It is shown that an electrostatic drift-type mode can appear due to the equilibrium sheared flow of electrons and ions along the constant external magnetic field. The electron and ion flow velocities are assumed to be equal, while the dust is considered as stationary fluid. Later on, the electrons are assumed to obey the kappa distribution. In the linear limit, a dispersion relation for drift-type waves is derived with frequency $\omega_r \ll \omega_{ci}$. The dust dynamics is again not considered in this study. Due to the zero-order current the mode can exist even

in a homogeneous density plasma. However, the presence of dust has been shown to be essential for the mode to exist. It is due to the fact that in the absence of dust i.e., $n_{d0} = 0$, the ion and electron densities become equal and the zero-order current vanishes. For the sake of generality, the density inhomogeneity effects are also included. Moreover, it is shown that the mode becomes unstable under certain conditions. We have applied the model to Saturn's rings and the various limiting cases are discussed. The effects of the kappa distributed electrons on the instability are also shown in figures. By increasing the value of the spectral index κ, the mode frequency is reduced. In the limit $\kappa \to \infty$, the electron response becomes adiabatic. Furthermore, the nonlinear coherent structures in the form of vortices have also been investigated. Depending upon the strength of the shear flow, different vortex structures are shown to be formed. It is shown that in the weak shear limit, the dipolar vortex structures are formed. As opposed to the previous investigations on dipolar vortices in inhomogeneous density plasmas, we have investigated the vortex formation even in homogeneous density plasma with zero-order current. In addition the kappa distributed electrons changes the behavior of the vortex structure. On the other hand in the strong shear limit, with steep flow gradient the nonlinear equations are shown to admit tripolar vortices under certain conditions.

In chapter 4, we have studied the waves and instabilities on the dust time scale in the presence of zero-order current produced by the sheared flow of electrons and ions directed along the initial constant magnetic field. The dispersion relation for coupled dust drift and dust acoustic waves is derived in the linear limit. For low frequency waves the electrons and ions are assumed to follow Boltzmann distribution. Here, we have studied the drift mode under two different situations for shear flow. In the first case the ions and electrons are assumed to have equal shear flow velocity with stationary dust, while in the second case dust shear flow velocity is also taken into account, but it is assumed smaller than ion and electron shear flow velocities, in order to assure non-zero current. In the first case with no dust shear flow velocity, we obtained a stable drift mode, whereas in the presence of dust shear flow, the mode might become unstable, provided certain conditions are satisfied. For weak shear limit, the nonlinear equations are shown to admit dipolar vortices. Moreover, due to the temperature inhomogeneities of electrons and ions, a KdV like equation is derived

that admits pulse like solutions.

In chapter 5, we have studied the electrostatic drift waves in a bi-ion inhomogeneous magnetized plasma. The local dispersion relation is derived in the presence of two ion species. The global mode is investigated using a cylindrical geometry. The solution of the linear equations for the global mode is obtained analytically. The effects of the magnetic field shear on the behavior of drift wave are also studied. It is shown that the amplitude of the oscillatory drift wave is reduced due to the two ion species with the same concentration $n_{a0} = n_{b0}$ as opposed to ordinary electron-ion plasma.

Bibliography

[1] F. F. Chen, *Introduction to Plasma Physics and Controlled Fusion*, Second edition, volume 1, Plenum Press, (1984).

[2] J. A. Bittencourt, *Fundamentals of Plasma Physics*, Third edition, Springer-Verlag, New York, (2004).

[3] L. Meitner and O. R. Frisch, Nature **143**, 239 (1939).

[4] S. Glasstone and U. Lovberg, *Controlled Thermonuclear Reactions*, van Nostrond, Princeton Univ. Press, (1960).

[5] P. M. Bellan and M. Porkolab, Phys. Fluids **17**, 1592 (1974).

[6] M. Y. Yu, P. K. Shukla, and K. H. Spatschek, J. Plasma Phys. **20**, 189 (1978).

[7] T. H. Stix, *Waves in Plasmas*, AIP, New York, (1992).

[8] P. K. Shukla, Phys. Plasmas **8**, 1791 (2001).

[9] V. E. Fortov, A. V. Ivlev, S. A. Khrapak, A. G. Khrapak, and G. E. Morfill, Phys. Rep. **421**, 1 (2005).

[10] C. K. Goertz, Rev. Geophys. **27**, 271 (1989).

[11] P. Bliokh, V. Sinitsin, and V. Yaroshenko, *Dusty and Self-Gravitational Plasmas in Space*, Kluwer Academic, Dordrecht, (1995).

[12] F. Verheest, *Waves in Dusty Space Plasmas*, Kluwer Academic, Dordrecht, (2000).

[13] W. E. Amatucci, J. Geophys. Res. **104**, 14481 (1999).

[14] K. Ida, Plasma Phys. Control. Fusion **40**, 1429 (1998).

[15] E. Agrimson, N. D'Angelo, and R. L. Merlino, Phys. Rev. Lett. **86**, 5282 (2001).

[16] C. Teodorescu, E. W. Reynolds, and M. E. Koepke, Phys. Rev. Let. **88**, 185003 (2002).

[17] M. Koepke, Phys. Scr. **T107**, 182 (2004).

[18] M. Koepke and E. W. Reynolds, Plasma Phys. Control. Fusion **49**, A145 (2007).

[19] N. D'Angelo, Phys. Fluids **8**, 1748 (1965).

[20] N. D'Angelo and S. V. Goeler, Phys. Fluids **9**, 309 (1966).

[21] G. Ganguli, M. J. Keskinen, H. Romero, R. Heelis, T. Moore, and C. Pollock, J. Geophys. Res. **99**, 8873 (1994).

[22] V. V. Gavrishchaka, S. B. Ganguli, and G. I. Ganguli, Phys. Rev. Lett. **80**, 728 (1998); J. Geophys. Res. **104**, 12 683 (1999).

[23] V. V. Gavrishchaka, G. I. Ganguli, W. A. Scales, S. P. Slinker, C. C. Chaston, J. P. McFadden, R. E. Ergun, and C. W. Carlson, Phys. Rev. Lett. **85**, 4285 (2000).

[24] M. V. Goldman, D. L. Newman, A. Mangeney, and F. Califano, Transp. Theory Stat. Phys. **34**, 225 (2005).

[25] S. Ali Shan, H. Saleem, and M. Sajid, Phys. Plasmas **15**, 072904 (2008).

[26] H. Saleem, Phys. Plasmas **13**, 012903 (2006).

[27] H. Saleem, Phys. Plasmas **18**, 049903 (2011).

[28] H. Saleem, Phys. Lett. A **375**, 3877 (2011).

[29] H. Saleem, J. Vranjes, and S. Poedts, Phys. Plasmas **14**, 072104 (2007).

[30] W. Horton, Rev. Mod. Phys. **71**, 735 (1999).

[31] J. Weiland, *Collective Modes in Inhomogeneous plasma,* IOP, Bristol, (2000).

[32] H. Tasso, Phys. Lett. **24A**, 618 (1967).

[33] B. B. Kadomtsev, *Plasma Turbulence*, Academic, New York, (1965).

[34] F. F. Chen, Phys. Fluids **8**, 1323 (1965).

[35] B. Eliasson, P. K. Shukla, and J. O. Hall, Phys. Plasmas **13**, 024502 (2006).

[36] H. Saleem and B. Eliasson, Phys. Plasmas **18**, 052103 (2011).

[37] P. K. Shukla, B. Eliasson, and M. Koepke, Phys. Plasmas **13**, 052115 (2006).

[38] Laboratory experiments on the parallel electron velocity shear are planned to be conducted with the WVU Q-machine at West Virginia University.

[39] A. Hasegawa, *Plasma instabilities and nonlinear effects*, Springer, Berlin, (1975).

[40] A. Hasegawa and K. Mima, Phys. Fluids **21**, 87 (1978).

[41] A. Hasegawa and M. Wakatani, Phys. Rev. Lett. **59** 1581 (1987).

[42] J. G. Charney, Pub. Kosjones Nors. Videnshap. Akad Oslo **17**, 3 (1948).

[43] A. Hasegawa, C. G. Maclennan, and Y. Kodama Phys. Fluids **22**, 2122 (1979).

[44] V. D. Larichev and G. M. Reznik, Dokl. Akad. Nauk SSSR **231**, 1077 (1976).

[45] J. S. Russell, *Report on Waves*, 14th meeting of the British Association for the Advancement of Science, London: BAAS, (1844).

[46] A. C. Newell, *Solitons in Mathematics and Physics*, SIAM, (1985).

[47] D. J. Korteweg and G. de Vries, Phil. Mag. **39**, 422 (1895).

[48] C. S. Gardner and G. K. Morikawa, Rep. NYC-9082. Courant Inst. of Math. Sci., New York Univ. New York, (1960).

[49] M. D. Kruskal and N. J. Zabusky, Annu. Rep. MATTQ-21. Plasma Phys. Lab., Princeton Univ., Princeton, New Jersey, (1963).

[50] H. Washimi and T. Taniuti, Phys. Rev. Lett. **17**, 996 (1966).

[51] N. J. Zabusky and M. D. Kruskal, Phys. Rev. Lett., **15**, 240 (1965).

[52] W. C. Feldman, J. R. Asbridge, S. J. Bame and M. D. Montgomery, J. Geophys. Res. **78**, 2017 (1973).

[53] V. Formisano, G. Moreno, and F. J. Palmiotto, Geophys. Res. **78**, 3714 (1973).

[54] J. D. Scudder, E. C. Sittler, and H. S. Bridge, J. Geophys. Res. **86,** 8157 (1981).

[55] E. Marsch, K. H. Muhlhauser, R. Schwen, H. Rosenbauer, W. Pilipp, and F. M.Neubauer, J. Geophys. Res. **87**, 52 (1982).

[56] V. M. Vasyliunas, J. Geophys. Res. **73**, 2839 (1968).

[57] V. Pierrard and M. Lazar, Sol. Phys. **267**, 153 (2010).

[58] T. K. Baluku and M. A. Hellberg, Phys. Plasmas **15**, 123705 (2008).

[59] E. E. Antonova and N. O. Ermakova, Adv. Space Res. **42**, 987 (2008).

[60] M. A. Hellberg, R. L. Mace, T. K. Baluku, I. Kourakis, and N. S. Saini, Phys. Plasmas **16** 094701, (2009).

[61] D. Summers and R. M. Thorne, Phys. Fluids B **3**, 1835 (1991).

[62] M. A. Hellberg and R. L. Mace, Phys. Plasmas **9**, 1495 (2002).

[63] C. R. Choi, K. W. Min, and T. N. Rhee, Phys. Plasmas **18**, 092901 (2011).

[64] M. N. Kadijani, H. Abbasi, and H. Hakimi Pajouh, Plasma Phys. Control. Fusion **53**, 025004 (2011).

[65] Ali Ahmad and H. Saleem, Phys. Plasmas **19**, 042107 (2012).

[66] Ali Ahmad and H. Saleem, Phys. Lett. A **377**, 3128 (2013).

[67] Ali Ahmad, S Ali Shan, Q. Haque, and H. Saleem, Phys. Plasmas **19**, 092115 (2012).

[68] Ali Ahmad, M. Sajid, and H. Saleem, Phys. Plasmas **15**, 012105 (2008).

[69] H. Saleem, W. M. Moslem, and P. K. Shukla, J. Geophys. Res. **117**, A08220 (2012).

[70] H. Romero, G. Ganguli, Y. C. Lee, and P. J. Palmadesso, Phys. Fluids **4**, 1708 (1992).

[71] S. Ishiguro, T. Sato, and H. Takamaru, Phys. Rev. Lett. **78**, 4761 (1997).

[72] G. Ganguli, S. Slinker, V. Gavrishchaka, and W. Scales, Phys. Plasmas **9**, 2321 (2002).

[73] M. E. Koepke, W. E. Amatucci, J. J. Carroll III, V. Gavrishchaka, and G. Ganguli, Phys. Plasmas **2**, 2523 (1995).

[74] W. E. Amatucci, D. N. Walker, G. Ganguli, J. A. Antoniades D. Duncan, J. H. Bowles, V. Gavrishchaka, and M. E. Koepke, Phys. Rev. Lett. **77**, 1978 (1996).

[75] B. B. Kadomtsev and A. V. Timofeev, Sov. Phys. Doklady **7**, 826 (1963).

[76] W. Horton, Phys. Rep. **192**, 1 (1990).

[77] G. D. Aburdzhaniya, F. F. Kamenets, V. P. Lakhin, A. B. Mikhailovskii, and O. G. Onishchenko, Phys. Lett. **105A**, 48 (1984).

[78] L. I. Rudakov and R. Z. Sagdeev, Sov. Phys. Dokl. **6**, 415 (1961); B. B. Kadomtsev and A. V. Timofeev, *ibid.* **7**, 826 (1963).

[79] N. A. Krall and M. N. Rosenbluth, Phys. Fluids **6**, 254 (1963).

[80] F. F. Chen, Phys. Fluids **7**, 949 (1964); **8**, 912 (1965).

[81] F. W. Perkins and D. L. Jassby, Phys. Fluids **14**, 102 (1971); E. Marden Marshall, R. F. Ellis, and J. E. Walsh, Plasma Phys. Controlled Fusion **28**, 1461 (1986); L. Zang, *ibid.* **34**, 501 (1992).

[82] A. B. Mikhailovskii, *Electromagnetic Instabilities in an Inhomogeneous Plasma,* IOP, Bristol, (1992).

[83] B. N. Kuvshinov and A. B. Mikhailovskii, Plasma Phys. Rep. **22**, 529 (1996).

[84] O. A. Pokhotelov, O. G. Onishchenko, P. K. Shukla, and L. Stenflo, J. Geophys. Res. **104**, 19797 (1999).

[85] Q. Haque and H. Saleem, J. Geophys. Res. **108**, (A12), 1433 (2003).

[86] P. K. Shukla and R. K. Varma, Phys. Fluids B **5**, 236 (1993).

[87] M. P. Leubner, J. Geophys. Res. **87**, 6335 (1982).

[88] T. P. Armstrong, M. T. Paonessa, E. V. Bell, and S. M. Krimigis, Geophys. Res. **88**, 8893 (1983).

[89] M. P. Leubner, Phys. Plasmas **11**, 1308 (2004).

[90] P. Schippers, M. Blanc, N. André, I. Dandouras, G. R. Lewis, L. K. Gilbert, A. M. Persoon, N. Krupp, D. A. Gurnett, A. J. Coates, S. M. Krimigis, D. T. Young, and M. K. Dougherty, J. Geophys. Res. **113**, A07208 (2008).

[91] M. A. Hellberg, R. L. Mace, R. J. Armstrong, and G. Karlstad, J. Plasma Phys. **64**, 433 (2000).

[92] A. Hasegawa, K. Mima, and M. Duong-van, Phys. Rev. Lett. **54**, 2608 (1985).

[93] W. C. Feldman, R. C. Anderson, J. R. Asbridge, S. J. Bame, J. T. Gosling, and R. D. Zwickl, J. Geophys. Res. **87**, 632 (1982).

[94] V. Pierrard and J. F. Lemaire, J. Geophys. Res. **101**, 7923 (1996).

[95] M. Maksimovic, V. Pierrard, and J. F. Lemaire, Astron. Astrophys. **324**, 725 (1997).

[96] W. Masood and Ali Ahmad, Astrophys. Space Sci. **340**, 367 (2012).

[97] S. Ali Shan and Q. Haque, Phys. Plasmas **19**, 084503 (2012).

[98] S. Magni, H. E. Roman, R. Barni, C. Riccardi, Th. Pierre, and D. Guyomarc'h, Phys. Rev. E **72**, 026403 (2005).

[99] T. K. Baluku and M. A. Hellberg, Phys. Plasmas **19**, 012106 (2012).

[100] P. K. Shukla and A. A. Mamun, Phys. Lett. A **315**, 258 (2003).

[101] O. Havnes, T. Aslaksen, T. W. Hartquist, F. Li, F. Melandsø, G. E. Morfill, and T. Nitter, J. Geophys. Res. **100**, 1731 (1995).

[102] P. K. Shukla and A. A. Mamun, *Introduction to Dusty Plasma Physics*, Bristol, Institute of Physics, (2002).

[103] N. N. Rao, P. K. Shukla, and M. Y. Yu, Planet. Space Sci. **38**, 543 (1990).

[104] P. K. Shukla, M. Y. Yu, and R. Bharuthram, J. Geophys. Res. **96**, 21343 (1991).

[105] A. Hasegawa and T. Sato, *Space Plasma Physics*, Springer, Berlin, (1989).

[106] J. Vranjes, A. Okamoto, S. Yoshimura, S. Poedts, M. Kono, and M. Y. Tanaka, Phys. Rev. Lett. **89**, 265002 (2002).

[107] A. Okamoto, K. Hara, K. Nagaoka, S. Yoshimura, J. Vranjes, M. Kono, and M. Y. Tanaka, Phys. Plasmas **10**, 2211 (2003).

[108] K. Nagaoka, A. Okamoto, S. Yoshimura, M. Kono, and M. Y. Tanaka, Phys. Rev. Lett. **89**, 075001 (2002).

[109] N. D'Angelo, Phys. Plasmas **13**, 094701 (2006).

[110] H. Saleem, J. Vranjes, and S. Poedts, Astron. Astrophys. **471**, 289 (2007).

[111] S. Sen, R. A. Cairns, R. G. Storer, and D. R. McCarthy, Phys. Plasmas **7**, 1192 (2000).

[112] R. F. Ellis and E. Marden-Marshall, Phys. Fluids **22**, 2137 (1979).

[113] J. Vranjes and S. Poedts, Phys. Plasmas **11**, 891 (2004).

[114] Ali Ahmad, H. Saleem, J. Vranjes, and S. Poedts, Phys. Lett. A **366**, 466 (2007).

[115] W. Horton, B. G. Hong, and W. M. Tang, Phys. Fluids **31**, 2971 (1988).

[116] P. K. Shukla and J. Weiland, Phys. Lett. A **137**, 132 (1989).

[117] W. J. Connor, R. J. Hastie, and J. B. Taylor, Phys. Rev. Lett. **40**, 396 (1978).

[118] S. C. Guo and J. Weiland, Nucl. Fusion **37**, 1095 (1997).

[119] W. Horton, Rev. Mod. Phys. **71(3)**, 735 (2006).

[120] L. D. Pearlstein and H. L. Berk, Phys. Rev. Lett. **23**, 22 (1969).

[121] H. L. Berk, L. D. Pearlstein, J. D. Callen, C. W. Horton, and M. N. Rosenbluth, Phys. Rev. Lett. **22**, 876 (1969).

[122] E. W. Greenstadt, G. Le, and R. J. Strangeway, Adv. Space Res. **15**, 71 (1995).

[123] M. G. Kivelson, K. K. Khurana, R. J. Walker, J. Warnecke, C. T. Russell, J. A. Linker, D. J. Southwood and C. Polanskey, Science **274**, 396 (1996).

[124] G. Mann, P. Hackenberg, and E. Marsch, J. Plasma Phys. **58**, 205 (1997).

[125] J. Wesson, *Tokamaks*, Clarendon Press-Oxford (2004).

[126] H. Biglari, P. H. Diamond, and P. W. Terry, Phys. Fluids B **2**, 1 (1990).